

# Active Receive Antennas as Sensors for Radars

Shalini Sodagam



University of Kansas  
2335 Irving Hill Road  
Lawrence, KS 66045-7612  
<http://crexis.ku.edu>

Technical Report  
CReSIS TR 107

August 17, 2006

*This work was supported by grants from the  
National Science Foundation  
(#OPP-0122520 and #ANT-0424589).*

Recent developments in RF field have made possible miniaturization of many RF systems such that they fit into places where space is premium. One such example is the Uninhabited Air Vehicle being developed by Center for Remote Sensing of Ice Sheets to house the radar system and antennas used for measuring ice sheet thickness in places like Greenland, Alaska and Antarctica. While the radar size can be miniaturized using the latest development in chip manufacturing technology, integrating the current large sized antenna with the UAV is an issue. To resolve this, electrically small antennas followed by high impedance amplifiers were developed and characterized to be used with radar systems that work within 100 MHz to 300 MHz bandwidth to achieve performance comparable to the larger antennas.

The active antenna was tested in the lab and its specifications include a bandwidth of 436 MHz, i.e. from 20 MHz to 456 MHz with an electronic gain of 7.5 dB and overall gain comparable to that of the horn antenna. The noise figure of the active antenna is below 3 dB and has a dynamic range of 103 dB without a jammer signal and 92 dB in presence of a -20 dBm jammer signal.

# Table of Contents

<i>Title Page:</i> .....	1
<i>Acceptance Page:</i> .....	2
<i>Abstract:</i> .....	3
<i>Acknowledgements:</i> .....	5
<i>Chapter 1: Introduction</i> .....	15
<i>1.1 Motivation:</i> .....	15
<i>1.2 Organization of Thesis</i> .....	17
<i>Chapter 2: Theory and Background of Active Antennas</i> .....	19
<i>2.1 Brief overview of Antenna Theory:</i> .....	19
2.1.1. Defining an antenna.....	19
2.1.2. Bandwidth Issues and Broadband Antenna Design: .....	20
2.1.3. Antenna size issues.....	21
<i>2.2 Electrically Small Antennas</i> .....	22
2.2.1. Hertzian Dipole Antenna: .....	22
2.2.2. Active Antennas .....	23
<i>2.3 Development of Active Antennas:</i> .....	26

<b><i>Chapter 3: Design and Simulations of Active Antenna</i></b> .....	31
<b><i>3.1 Design:</i></b> .....	31
<b>3.1.1 Requirements</b> .....	31
<b>3.1.2 Basis of Design:</b> .....	32
<b>3.1.3 Design Evolution:</b> .....	33
<b>3.1.4 Circuit Description:</b> .....	35
<b>3.1.5 Antenna Element Description:</b> .....	38
<b><i>3.2 Simulations:</i></b> .....	39
<b>3.2.2 Amplifier Simulations</b> .....	42
<b>3.2.3 Antenna Simulations</b> .....	62
<b><i>Chapter 4 Implementation and Measurement</i></b> .....	65
<b><i>4.1 Implementation</i></b> .....	65
<b>4.1.1 Implementation of Active antenna amplifier</b> .....	65
<b>4.1.2 Implementation of monopole antenna</b> .....	68
<b><i>4.2 Measurements</i></b> .....	69
<b>4.2.1 DC Probing:</b> .....	69
<b>4.2.2 Stability</b> .....	70
<b>4.2.3 Gain and Bandwidth:</b> .....	72
<b>4.2.4 Input impedance and Output impedance:</b> .....	74

4.2.5 Noise Figure:.....	76
4.2.6 Saturation and Minimum Detectable Signal (MDS): .....	80
4.2.7 Free – Space Experiment: .....	90
<i>Chapter 5: Conclusion and Future Work</i> .....	99
5.1 Conclusion: .....	99
5.2 Future Work.....	101
<i>References</i> .....	103
<i>Appendix</i> .....	106

## List of Figures

Figure 2.1: Broadband antennas .....	20
Figure 2.2: Log periodic antenna .....	21
Figure 3.1: Circuit of active antenna amplifier designed by Sainati and Fessenden [3]33	
Figure 3.2: Circuit Schematic of our active antenna.....	35
Figure 3.3: Capacitively loaded 4.5” monopole antenna.....	39
Figure 3.4: Equivalent circuit of a monopole antenna.....	40
Figure 3.5: (a) ADS TOM model.....	41
Figure 3.5: (b) PSpice Model.....	41
Figure 3.6: Equivalent model for DC path of the bias-tee.....	42
Figure 3.7: Equivalent model for limiter diode. ....	42
Figure 3.8: DC annotation of active antenna amplifier from all software packages ...	43
Figure 3.9: Simulated Gain of active antenna amplifier from Pspice.....	45
Figure 3.10: Simulated gain of active antenna amplifier w/o transmission lines from ADS.....	45

Figure 3.11: Simulated gain of active antenna amplifier with transmission lines from ADS.....	45
Figure 3.12: Simulated gain of active antenna amplifier with transmission lines from MWO .....	46
Figure 3.13: Input Impedance of active antenna amplifier from ADS .....	49
Figure 3.14: Stability factor K of active antenna amplifier from ADS .....	50
Figure 3.15: Stability factor $ \Delta $ of active antenna amplifier from ADS .....	50
Figure 3.16 (a) Load stability circles for frequencies 10 to 150 MHz .....	51
Figure 3.16 (b) Source stability circles for frequencies 10 to 150 MHz.....	51
Figure 3.17: Simulated noise figure Pspice .....	52
Figure 3.18: Simulated noise figure of active antenna amplifier from ADS.....	53
Figure 3.19: Simulated noise figure of active antenna amplifier from MWO.....	53
Figure 3.20: (a) ADS saturation simulation Input signal: -60 dBm.....	55
Figure 3.20: (b) ADS saturation simulation Input signal: -40 dBm.....	55
Figure 3.20: (c) ADS saturation simulation Input signal: -20 dBm .....	55
Figure 3.21: (a) ADS saturation simulation with jammer at -60 dBm.....	59

Figure 3.21 (b) ADS saturation simulation with jammer at -40 dBm .....	59
Figure 3.21 (c) ADS saturation simulation with jammer at -20 dBm .....	59
Figure 3.22: Dimensions of the monopole to be used with active antenna .....	63
Figure 3.23 (a): Input Impedance (real, imaginary) of the monopole .....	63
Figure 3.23 (b): Input Impedance (magnitude) of the monopole.....	64
Fig 4.1: Layer stack up.....	65
Figure 4.2: PCB layout for active antenna amplifier.....	66
Figure 4.3: populated board of active antenna amplifier .....	66
Figure 4.4 (a): layout of monopole antenna with capacitive patch;.....	67
Figure 4.4 (b): final antenna after milling.....	67
Figure 4.5: Setup for oscillation test .....	70
Figure: 4.6 Measured spectral output from oscillation test.....	71
Figure: 4.7 Test setup for S-parameter measurements.....	72
Figure 4.8: Measured gain of active antenna amplifier .....	73
Figure 4.9: S11 measured from Network Analyzer .....	74

Figure 4.10 (a): Input impedance with limiter diode .....	75
Figure 4.10 (b): Input impedance without limiter diode.....	75
Figure: 4.11 S22 measured in network analyzer.....	76
Figure 4.12 (a):Setup 1: Noise floor measurement with 50 dB amplifier .....	77
Figure 4.12 (b):Setup 2: Noise floor measurement with the active antenna amplifier	77
Figure 4.13: Noise floor measurement with setup 1 and setup 2.....	78
Figure 4.14 Noise figure of active antenna amplifier .....	79
Figure 4.15: Setup 1 - MDS and Saturation without jammer signal.....	80
Figure 4.16: Setup 2 - MDS and Saturation with jammer signal.....	81
Figure: 4.17 (a) Radar test setup without active antenna.....	85
Figure: 4.17 (b) Radar test setup with active antenna.....	85
Figure 4.18: Radar results for MDS (a) with 60 dB attenuation,.....	86
Figure 4.18: Radar results for MDS (b) with 80 dB attenuation.....	86
Figure 4.18: Radar results for MDS (c) with 100 dB attenuation .....	86
Figure 4.18: Radar results for MDS (d) with 110 dB attenuation.....	86

Figure 4.19: Radar setup-1 results with jammer signal (a) jammer at -60 dB.....	87
Figure 4.19: Radar setup-1 results with jammer signal (b) jammer at -30 dBm.....	87
Figure 4.19: Radar setup-1 results with jammer signal (c) jammer at -20 dBm.....	87
Figure 4.20: Radar setup-2 results with jammer signal (a) jammer at -60 dB.....	88
Figure 4.20: Radar setup-2 results with jammer signal (b) jammer at -30 dB.....	88
Figure 4.20: Radar setup-2 results with jammer signal (c) jammer at -20 dBm.....	88
Figure 4.21 (a) SNR versus attenuation comparison for setup without jammer.....	89
Figure 4.22 (b) SNR with desired signal with 60 dB attenuation;.....	89
Figure 4.22 (c) SNR with desired signal with 80 dB attenuation.....	90
Figure 4.23 (a): Free space experiment setup for reference antenna .....	92
Figure 4.23 (b): Setup for free space experiment with active antenna .....	92
Figure 4.24: Gain curves comparison of active antennas with different monopoles with the horn antenna.....	94
Figure 4.25: Free space experiment with spectrum analyzer (reference).....	96
Figure 4.25: Free space experiment with spectrum analyzer (active antenna).....	96
Figure 4.26: Received signal spectrum by horn antenna and active antenna .....	97

## List of Tables

Table 3.1: Summary of DC Simulation of active antenna amplifier results .....	44
Table 3.2: Summary of results of gain simulation.....	47
Table 3.3: Summary of Results from noise simulation.....	54
Table 3.4 (a) Summary of results saturation simulation without jammer.....	57
Table 3.4 (b) Summary of reusults saturation simualtion with jammer.....	60
Table 4.1 DC analysis measured results.....	70
Table 4.2 (a) Measured minimum detectable signal without jammer.....	81
Table 4.2 (b) Measured saturation point without jammer.....	82
Table 4.3 (a) Measured minimum detectable signal with jammer.....	83
Table 4.3 (b) Measured saturation point without jammer .....	83

***1.1 Motivation:***

Global sea level rise due to climatic changes and melting of polar ice sheets has been of great concern in the recent times, especially considering the fact that more than 60% of the world's population resides in the coastal areas. To quantify the contribution of ice sheets and outlet glaciers in the sea level rise remote sensing techniques have been developed to improve our understanding of ice parameters and their dynamics by mapping the internal layers and the bed of the ice sheets.

Center for Remote Sensing of Ice Sheets (CReSIS) established in 2005 is dedicated to development of new technologies and better computer models to measure and predict the response of ice sheets to climate change [19]. The technological development at CReSIS includes, but is not limited to, development of advanced radar systems that can measure ice sheet thickness, basal conditions, accumulation rates, etc. that support the requirements of the polar research community. Effort now is being focused on making these radars small, lightweight and with low power consumption.

For the field missions taken by CReSIS, the radar systems are run on autonomous platforms. These platforms can be divided into two categories: land-based and airborne. The land-based operations are done using the platform called a rover [21].

The airborne radars were originally operated on a P3 aircraft, and now are being operated on a Twin Otter aircraft. The latest addition to this list is the UAV (uninhabited air vehicle), currently under development, that will enable airborne remote sensing in places that are not accessible by conventional means and also provide smaller grid spacing in flight lines while mapping ice sheets.

It is evident from the above information that the focus in development is shifting slowly towards miniaturization, be it platforms or radars. It is now essential that the antenna systems integrated with the UAV should be small and light weight in order to have the optimal performance aerodynamically. The current antenna – half wave dipoles used with the airborne radars are nearly 1 m in length hence pose some problems in UAV design. At the same time the smaller antennas should have the comparable or superior performance as their larger counterparts in gain and bandwidth.

Drastically reducing the size of antennas without any compensation compromises the performance of the antenna. This thesis presents a sub-optimal antenna design using the concept of active antennas that has both the small size and broadband performance that is suitable for UAV's

## *1.2 Organization of Thesis*

Chapter 1 gives the motivation of the thesis, starting with emphasis on climate change and melting of ice sheets and effect on global community and then moving on to the next generation radar and autonomous platform development and the requirement for smaller size yet broadband antennas.

The rest of the thesis is divided into three main categories – theory, design and simulation, implementation and testing.

Chapter 2 starts with a brief overview of antenna theory, antenna design issues focusing mainly on antenna size and bandwidth, then goes into the theory of electrically-small antennas. Theory of active antennas follows and then a literature review of active antenna development is provided with a historical perspective.

Chapter 3 goes through the design basis of the active antenna presented in this thesis and the modifications made to the base design in order to suit our application starting with the high-impedance, low-noise amplifier design followed by antenna element design, then the combination of the two which forms the active antenna. The rest of the chapter goes through the simulations done to theoretically characterize the active antenna.

The first half of chapter 4 deals with the realization of the amplifier circuit and the monopole element, and the second describes in detail the experimental setups used to characterize the active antenna and the final measurement results with analysis of each of the results obtained.

Finally chapter 5 concludes the design of active antennas as a sensor for airborne radar, and the future work includes more testing techniques that can be done to understand the performance of the active antenna better and some design advancements that would enhance the performance of the active antenna.

***2.1 Brief overview of Antenna Theory:***

**2.1.1. Defining an antenna**

According to *Balanis* [1] an antenna can be termed as a transitional structure between free space and guiding devices such as coaxial lines or wave guides. They can radiate, or receive electromagnetic waves or more popularly known as radio waves, into or from free-space. There are several ways of describing an antenna based on its applications. An antenna can be seen as an energy converter or a transducer. In other words as it converts the E-fields present in free space to certain terminal voltage, or vice versa. An antenna serves the purpose of a spatial filter, through its radiation pattern and directive nature. That is it can transmit or receive in only the desired direction and reject the signals from any other direction. The propagation mode of the signal in free space is different from the propagation mode in the guiding device, so the antenna actually acts a propagation mode adapter for the two environments.

Apart from being a transducer, spatial filter and a propagation mode adapter, an antenna acts as an impedance matching device, as it is designed to transform the free space intrinsic impedance to the characteristic impedance of the guiding device or transmission line attached to it. The nature of this transformation decides the bandwidth of an antenna. An antenna can be completely described by its gain,

directivity, radiation pattern that includes the side lobe levels, polarization, efficiency and input impedance which is frequency dependent and which has to be matched characteristic impedance of the transmission line that follows it.

### 2.1.2. Bandwidth Issues and Broadband Antenna Design:

According to Andrew Alford [2], if the transformation from free space impedance to transmission line impedance is a gradual, like a tapered line then the overall reflection is not critically dependent on the length of the antenna, or the wavelength of the received signal. If not then the electrical length and the input impedance are the main factors to consider as they are both frequency dependent. Therefore matching network built to transform antenna impedance to transmission line impedance is perfect only at the design frequency and varies considerably with change in frequency. However as mentioned before, there exist antennas that follow the tapered impedance structure, flared out at the end that faces free-space and tapers down as it reaches the coaxial cable, examples of such antennas are the TEM horn antennas, Vivaldi antennas and bow tie antennas are wide band devices.

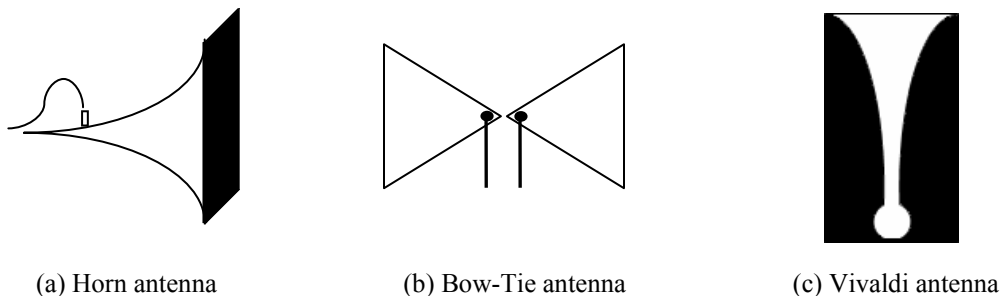


Figure 2.1: Broadband antennas

There are other classes broadband antennas like the spiral antennas which depend on their angular structure for wideband performance [1] or antenna arrays like the log periodic which have periodic structure and characteristics. More can be read about these broadband antennas in ref [1].

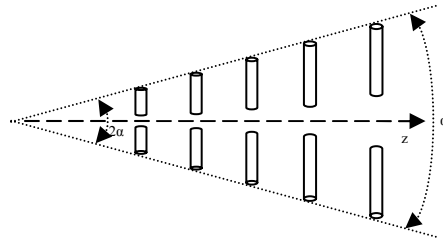


Figure 2.2: Log periodic antenna

With the exception of the above mentioned antennas, most of the other ones are restricted in their bandwidth.

### 2.1.3. Antenna size issues

Antennas are designed mostly based on the wavelength of the frequencies of operations. It can then be said that the physical size of the antenna is driven by the lowest frequency in the range of frequencies that the antenna operates. Suppose the lowest frequency of operation is 150 MHz, then a half-wave dipole antenna has to be at least 1 m in length as the wave length at that frequency is 2 m. However this is somewhat a problem when the application needs an antenna with smaller size. For example, underneath the wing of a small aircraft as a sensor for a radar system as is

our case or if the antenna needs to fit into automobiles (cars) as a sensor for collision prevention. The other antennas that are broadband, like the horn antenna and the log periodic array also have large dimensions and hence are not suitable for such application where space is limited. However there are antennas that can be made small but with a price, which is discussed in the next section

## ***2.2. Electrically Small Antennas***

It is a well known fact that when the length of a transmission line is reduced to less than  $1/8^{\text{th}}$  of a wavelength, the transmission line can be approximated to a frequency independent line. The same concept can be applied to antennas. Electrically small antennas are those that have very small length, typically less  $1/8^{\text{th}}$  of a wavelength. These antennas however have a higher impedance and Q factor. As Q factor increases the bandwidth in which there is a good impedance match decreases. This causes the efficiency to decrease. However there are cases wherein the antenna is small and has very high impedance, but good operating bandwidth. This antenna is called the Hertzian dipole antenna.

### **2.2.1. Hertzian Dipole Antenna:**

The Hertzian dipole is in form of a linear antenna, i.e. a straight wire antenna with a length much less than a wavelength of the frequency of operation. This makes the antenna seem frequency independent as long as the condition of electrically small

antenna is maintained. Thus the antenna works over a considerable range of frequencies as the current distribution over the length of the antenna is uniform. However the input impedance of the antenna is huge. A typical electrically small antenna has in its input impedance the following - radiation resistance, loss resistance, capacitive reactance and inductive reactance. Of these components, the loss resistance and inductive reactance are small while *capacitive reactance* is the one that is dominant. This makes the design of wideband matching networks all the more complicated. Also the directivity of this electrically small antenna is just 1.5. However if the reduction in length is compensated by an impedance converting network that is not band limited, and if the power received or radiated can be amplified then that overcomes the limitations of the Hertzian dipole. There is a certain class of electrically small antennas that use active elements for this kind of compensation. These are called *active antennas*.

### 2.2.2. Active Antennas

Active antennas are electrically small antennas that have an active element at its terminal in order to compensate the huge impedance leap caused by reducing the length of a conventional antenna. In conventional antennas, the matching of high antenna impedance is done using wideband matching networks which also give maximum power transfer. These type of matching networks are generally made of inductors and capacitors either lumped or transmission lines that are designed to give such reactive impedances. The latter is preferred as the high frequency performance is

better than that of the lumped components and also transmission lines have a higher Q factor and accuracy than lumped components. However despite the advantages, the matching networks are band limited as their electrical length varies as the frequency changes. Therefore it is essential that the compensation for shortening the antenna should be provided by something other than just passive components. This is where the active antennas concept derives its motivation from.

The active element, generally an amplifier is built with high input impedance that provides a huge frequency independent mismatch at the antenna terminals. This effectively doubles the terminal because of the large reflection coefficient at the input of the amplifier, contrary to the conventional matching networks that use matching for maximum power transfer. In this way the active antenna functions more as an E-field probe than as a power transformer. As long as the input impedance of the amplifier is much greater than the impedance of the antenna, the characteristics of the active antenna remain independent of frequency.

Active antennas overcome several of the shortcomings of traditional antennas. They are almost frequency independent, in the sense that their bandwidth is dependent on the amplifier rather than the radiating element. Most often a careful design of amplifier can ensure a very broadband performance of the antenna. Same is the case with the gain of the antenna which is also synthesized by the amplifier. Also since the antenna is electrically small, the overall length is much lesser than the conventional

antennas, and thus can be used in places where there is constraint on space. Another added advantage is that radiating element need not be complex, a simple monopole/dipole is enough to cover the entire frequency band required.

However the amplifier design is not simple, the main challenge being how to make the amplifier with as low noise as possible since the presence of noise degrades the system sensitivity. Also there exists a constant interference from jamming signals operating in the same environment as the active antenna. This jamming signal, if very strong, can saturate the amplifier and create undesirable non linear effects in the system. Amplifiers generally have a natural propensity to oscillate, and to design an amplifier that is stable at all frequencies is a non trivial task. However with if designed with care the above problems can be solved effectively.

There are certain disadvantages of active antennas that one has to bear with, for example: they need a dc power supply to operate. Also since they have an active device at the antenna terminals, they are not reciprocal. That is they can either transmit or receive, but not both as in conventional antennas.

### ***2.3. Development of Active Antennas:***

Active antennas have been in existence since the 1960's and have been improved over the ages to a large extent. Some of the significant work towards the development of active antennas was done by H.H Meinke and co-workers [4]. The motivation behind their work was to design electrically small antenna elements and arrays which have minimal mutual coupling and also have a broadband performance. The first class of active antennas were integrated with the antenna itself, like using bipolar transistor to obtain more capacitance and less impedance at the top end of a monopole, as added capacitance increases effective length of the antenna. But this did not help the bandwidth of the antennas so the effort shifted to having amplifiers at the feed of the antenna, so as to amplify the signal without any RF losses. However it was found that the sensitivity of the active antenna thus formed was less than its passive counterpart as the amplifier increased the noise along with the signal [3]. This made way for an improved amplifier design, which had acceptable bandwidth and noise figures. Also most of the work done in this period was in the high frequency band which is mostly limited by atmospheric noise so the amplifier noise figure was not as important. The drawback of these investigations was that they were mostly experimental and there were no predictions as such of the behavior of the active antennas.

In 1974 Wong gave a complete and thorough analysis of an active antenna involving loop monopole analysis coupled with circuit analysis and noise equivalents of both the monopole and the electronic circuit [5]. Then in 1978 Sainati et al [3] developed an active antenna with a two stage amplifier that had FET in the first stage and a low noise BJT in the second stage and analyzed the circuit in a less complicated fashion than Wong, but used the same concepts and analyzed the noise performance of the system and experimentally verified it. The emphases in these designs were less noise and more bandwidth even at the cost of transistor efficiency. The 1980's saw a marked improvement in the amplifier design part of active antennas while the radiating elements were still the simple monopole linear wire or loop. The focus was shifted to having a linear, noise-free antenna that can reproduce the received signal with minimal distortion and contamination from intermodulation products. Multi-stage design with overall negative feedback approach was used by Nordholt et al. [6] for frequencies below 30 MHz. It was also suggested that with proper feedback at the input and with a combination of series and shunt feedback at the output would provide much more gain that can overcome the output losses, and minimize distortion, thus making it useful even in areas that have strong interferers although high gain causes stability problems in amplifiers.

The early 1990's saw improvements the radiator element too with more planar antenna designs like microstrip slotted antennas integrated with FET amplifiers [7]. At this point applications in the UHF, VHF and microwave regions also started

applying active antennas for various automotive and wireless type applications. The JFET amplifiers were being replaced by the more wideband and low noise counterparts in GaAs FETs [8]. Grabherr et al. [17] used a GaAs FET amplifier integrated with an aperture coupled microstrip antenna to obtain a bandwidth of 1.6 GHz with 10 GHz center frequency with a gain of 10 dB and noise figure of 3 dB. Also Pantou et al [9] proved that active antenna arrays are as good as passive arrays in terms of gain and noise performance and also that they are more suitable for beam steering type applications, as the active antennas have enough gain (variable too) to overcome the losses caused by the insertion of phase shifters etc. in between the elements for steering purposes

By the end of 90's active antennas found more applications in the microwave/wireless technology region, and researcher sought out more stable transistors than the GaAs FETs, so SiGe HBT's which have the same noise performance as GaAs FETs were used instead [10]. Alternately, since FETs have a potential to oscillate due to parasitics at UHF frequencies and above, Skahill et al [11] used negative impedance components, popularly known as non-foster elements to achieve impedance compensation for length reduction. However they talk about compensation in the lower frequency range, which is not explicitly discussed.

By this point, there was a change of trend in the design of active antennas. The emphasis was no longer on proof of concept but on optimizing the existing designs to

suit a particular application. In the past few years, there have been many variations of the active antennas and some of them have even been marketed for commercial use such as TV antennas GPS receivers etc. Tan et al [16] developed low frequency radar (LOFAR) that works from 10 MHz to 150 MHz and is used for radio astronomy that employs active antenna arrays with beam steering as sensors for the radar. Fredrick et al [12] describe the use of active antennas concept to lower the noise figure of a transmitting system and also the antenna, a circular patch with a class F amplifier integrated in it, helped in suppressing the harmonics of the system. Other unique radiating elements such as the Quasi-yagi antenna was combined with two integrated LNAs as a sensor for a monopulsed radar designed to operate at 5.5 GHz. The authors add that this antenna could be used as two monopoles or a single dipole by making minor modifications in the feed structure. Al Khatib et al [13] used meandered lines on microstrip integrated with a small signal bipolar transistor amplifier that operated at 315 MHz with 100 MHz bandwidth and noise figure of 2 dB for automotive applications. Circularly polarized short circuited ring antenna with class E, 60 % efficient amplifier [14], stacked patch antennas with a broad band amplifier for 1.6 to 2 GHz range [15] were amongst some of the designs that were studied recently.

Whatever the application or design be, there are a set of standard performance criteria that have to be followed like - low noise figure, sufficient gain so as to overcome the system losses, oscillation free over all frequencies, linearity over the required

frequency band, output compatibility, i.e. low output reflectivity, wide dynamic range and lastly overload and static DC protection.

It was noted that the designs mentioned in the literature that operated within the frequency range of our interest (UHF-VHF) used JFETs and had a noise figure above 3 dB. Other designs that had low noise figures used GaAs FETs and were designed for operation in the microwave frequency range. It is also a well known fact that GaAs FETs generally tend to oscillate when used in the lower frequency range of their operation. Hence the main challenge in designing our active antennas was to use GaAs FETs in the VHF-UHF range for good gain, bandwidth and noise figures and at the same time maintain the stability of the amplifier through out the spectrum.

### **3.1 Design:**

#### 3.1.1 Requirements

As mentioned in chapter 1, the radar system for which this active antenna is being designed for works from 100 MHz to 300 MHz. So to optimize the use of active antennas as sensors for this radar system, the following performance criteria and design parameters were chosen.

1) Oscillation free operation

Since the GaAs FETs are susceptible to oscillations. It is necessary that our amplifier must be designed to be oscillation free over the entire spectrum.

2) Low noise figure (< 3 dB)

Noise of the active antenna places a constraint on the minimum level of the signal that can be detected [3]; hence the overall noise figure of the active antenna should be as small as possible.

3) Good power gain

Gain bandwidth of an amplifier specifies the maximum possible value for the product of gain and bandwidth. The quantity is a constant from which the highest gain for a given bandwidth can be inferred. High gains thus have reduced bandwidth, so that the gain bandwidth product is a constant. Also high gains lead

to oscillations. Thus a nominal gain that can overcome system losses and ensures oscillation free performance has to be chosen.

4) Low distortion level even in presence of strong jammers/interferers

There exist other transmitters operating in the same environment and same frequency band. The amplifier design should consider saturation from these transmitters (jammers) as this leads to signal distortion. The amplifier should be able to take at least -20 dBm of jammer signal without degrading the system sensitivity. The active antenna amplifier should have a wide dynamic range.

Apart from the above, there are some general specifications that have to be followed like high input impedance with low input capacitance (at least less than the antenna element capacitance) and output impedance of 50  $\Omega$ .

3.1.2 Basis of Design:

The design of our active antenna was based on the work done by Sainati and Fessenden [3]. Their design was, in turn, based on the work done by H.H. Meinke [4] and analysis done by Wong [5]. Their active antenna worked from 10 kHz to 500 MHz with 4 dB gain and over 10 dB of noise figure above 100 MHz and above 30 dB at lower frequencies [3]. Figure 3.1 shows their circuit reproduced by us in ADS. They used a JFET transistor in the first stage and a low noise RF amplifier (GPD-462) in the second stage. High noise figure at lower frequencies was perhaps acceptable due to the high atmospheric noise, and gain was low despite the two

stages. Our design follows the same basic circuitry but with GaAs FET in place of the JFET for low noise figure, better gain and bandwidth.

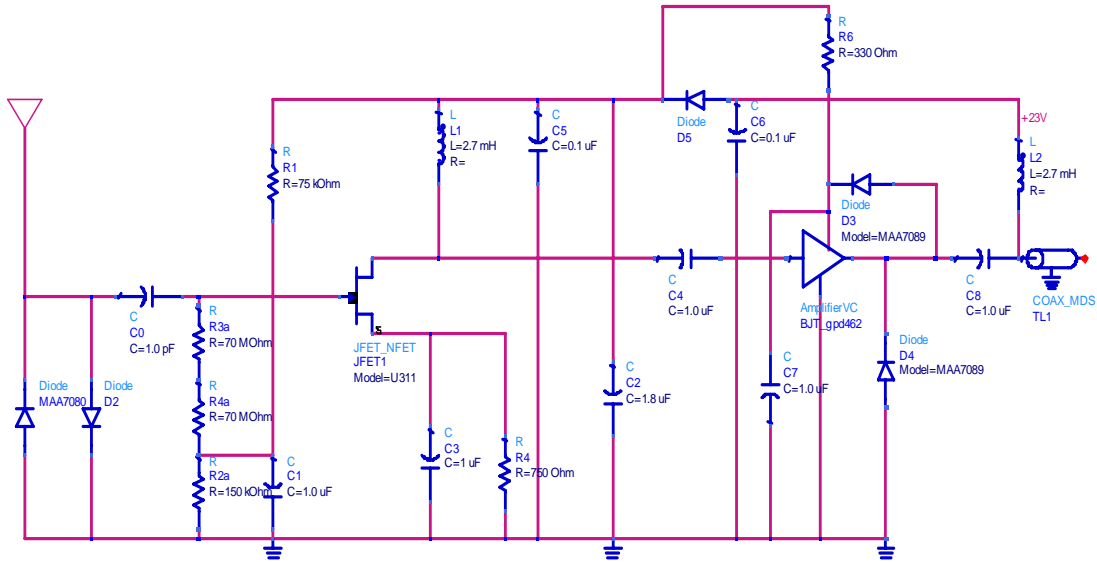


Figure 3.1: Circuit of active antenna amplifier designed by Sainati and Fessenden [3].

### 3.1.3 Design Evolution:

The active antenna design, while based on the above circuit, went through a number of refinements and modifications before being finalized for use outside the lab. This section will walk through the description of each version briefly and specify the drawbacks of each of them and why a newer version was built.

The first version was a very basic version which had used a GaAs FET in place of Sainati's U311 and had a low noise op-amp instead of the GPD-462. Bias resistor

values were changed accordingly. This circuit however turned out to be a highly unstable design and showed oscillations at 5 GHz frequency.

The next version used a JFET, a more stable component than GaAs FET, in the first stage and an op-amp in the next. Also discrete components like combination of inductors and capacitors at the output of the second stage and at the drain of the FET were replaced by bias-tees. This resulted in very good gain but just 100 MHz of bandwidth. Through lab experiments, it was found that the ferrite core in the bias-tee was behaving resistively beyond 150 MHz, so was not suitable to replace the inductor at the drain of the FET. Also using a JFET resulted in the noise figure above 10 dB.

The third version went back to the GaAs FET and through lab experiments it was found that by inserting a small capacitance between the drain and source, oscillations can be reduced. However there was still a limitation in bandwidth and this was because of the feedback capacitor at the op-amp that was used to suppress the spurious peak generated by the biasing network of the op-amp. So a minor modification was made to the board and a voltage divider from the drain was used to give the required bias voltage to the op-amp instead of inductors and resistors. This however drew a lot of current, 110 mA to be precise. Also simulations revealed that the op-amp saturates before the FET, so the final version, has just a single stage GaAs FET amplifier with a voltage divider on the output side that makes it compatible with

any 50 Ω system that follows it. Detailed description of this version, the components used in it and the analysis of its performance is discussed in the following sections.

### 3.1.4 Circuit Description:

The final version of the active antenna amplifier is shown in the figure 3.2 below. The amplifier has a GaAs FET (NE34018) that works from 0.1 GHz to 6 GHz, in a common source configuration.

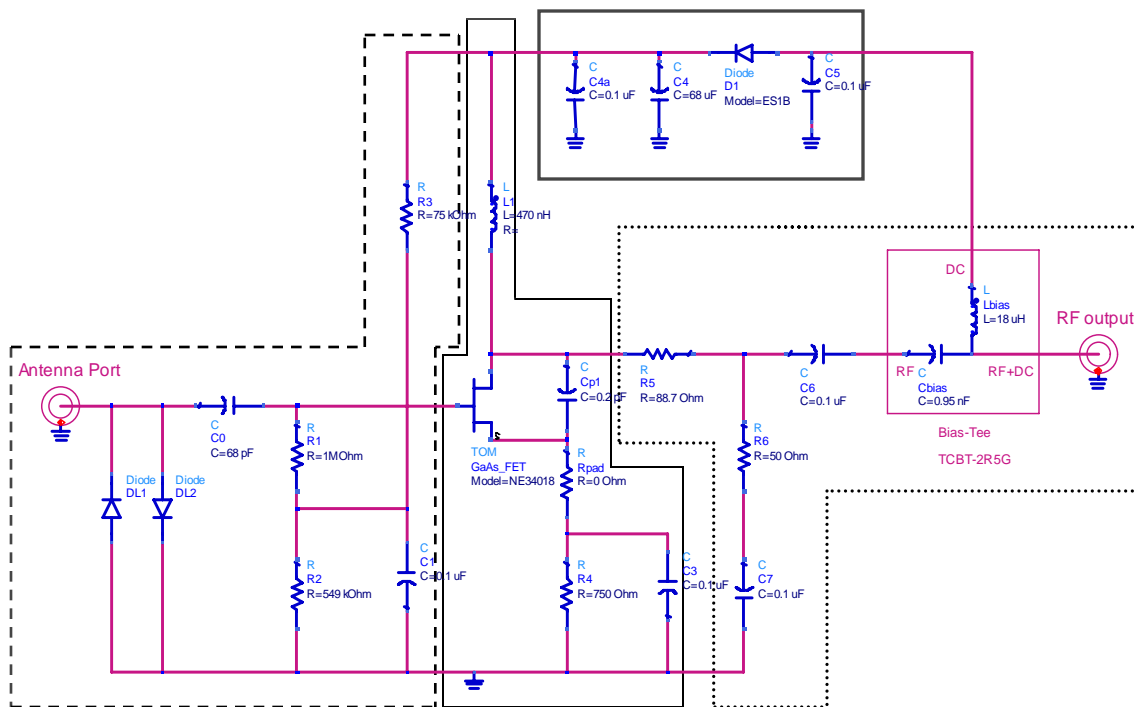


Figure 3.2 : Circuit Schematic of our active antenna

Legend:

----- - Input Section

————— - Main Section

..... - Output section

————— - Power Filtering Section

The circuit has two ports, the antenna port and the RF output port. DC power is brought in through an external bias-tee that is connected to the RF port. It is then passed through the DC path of the internal bias tee and through the power filtering section that consists of a diode and a set of capacitors that form a low pass filter. The capacitors used on the board need to have a self resonant frequency (SRF) greater than the upper limit of the desired frequency band. Since it is difficult to obtain capacitors of high SRF and high capacitance, a high SRF small capacitance (0.1  $\mu\text{F}$ , 40 GHz) was placed in parallel with the low SRF (47  $\mu\text{F}$ , 10 MHz) ones make the combination a high SRF capacitor.

The filtered DC is then passed to two points - the resistor  $R_3$  (75  $\text{k}\Omega$ ) in the input section and the inductor in the main section. Resistor  $R_2$  (549  $\text{k}\Omega$ ) along with  $R_3$  forms a voltage divider bias for the FET. There are two criteria for selecting the value of  $R_2$ . The primary being operation of FET close to saturation so that maximum gain can be obtained while maintaining the FET in reverse bias mode. The second being stability of the amplifier. It was found experimentally that the value of resistor  $R_2$  either adds or reduces the input stability of the amplifier. Based on this, a value of 549  $\text{k}\Omega$  was chosen. The RF signal received from the antenna connected to the antenna port, travels past the limiter diode through capacitor  $C_0$  the former is for protecting the FET against any static DC entering through input port. The latter is also for blocking DC. Since limiter diode, the input capacitance of the FET and the 1-M $\Omega$  resistor determines the input impedance, it is essential the limiter diode and the

FET have very low inherent capacitance. HSMP-3822 diode has a capacitance of 0.8 pF and the FET has 2.2 pF.

The main section consists of the FET itself with a capacitor  $C_{p1}$  connecting the source to the drain to provide stability. Value of the capacitor 0.2 pF was determined experimentally and this capacitor works up to 8 GHz. Since the FET is in a common source configuration, the source is connected to ground through a parallel combination of a 750  $\Omega$  resistor and a 0.1  $\mu$ F bypass capacitor, as was in Sainati's design. The only extra part included was a provision for a source feedback resistor in case of instability.

The drain of the FET is connected to DC supply through an inductor that isolates the RF signals from seeing the DC power section, but has also one other purpose – it determines the lower frequency limit of the amplifier. Increasing the inductor value increases the lower operating frequency limit. A value of 470 nH was chosen to give a lower limit frequency response of 30 MHz. The SRF of this inductor is 550 MHz which is higher than the maximum frequency of interest. The load section of the amplifier has a voltage divider formed by  $R_5$  (88.7  $\Omega$ ) and  $R_6$  (50  $\Omega$ ). This ensures that the FET sees a total of 138.7  $\Omega$ , but still has output compatibility to a 50  $\Omega$  system. Resistor  $R_6$  is fixed to 50  $\Omega$  but  $R_5$  can be varied depending on the gain needed decreasing the value of  $R_5$  increases the gain of the amplifier. However the stability of that amplifier has to be considered, while altering the resistor value high

gain value tends to make the amplifier unstable. An optimum value of  $88.7 \Omega$  was chosen that gives a gain of over 7 dB and also maintains stability over the entire spectrum. The signals are finally taken out through the RF path of both the internal and external bias tees into the rest of the receiver section.

#### 3.1.5 Antenna Element Description:

The requirements of the antenna element were not as stringent as on the amplifier. The antenna element that Sainati and Fessenden [3] used for their amplifier was a monopole wire antenna - the most tried and tested element, next being the dipole. So the only choice of radiating elements was between monopole and dipole. The monopole was chosen over dipole because the amplifier design was much more complicated for a dipole as it had to be in a push-pull type configuration, or a cascode double stage. But given the constraint of stability, double stage designs were more complex to implement and debug, so our design adopted the monopole as the radiating element.

There was however a small variation made in the structure. The monopole was loaded capacitively as indicated by figure 3.3 by including a rectangular patch at the end. The monopole had to be electrically small in length so a value of 4.5", which is  $< \lambda/8$  at 300 MHz, was chosen. Another variation was the antenna was made a PCB antenna unlike the wire that Sainati and Fessenden [3] used.

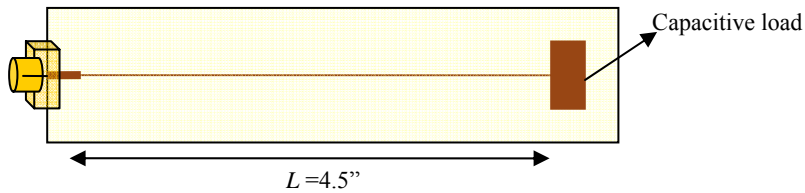


**Figure 3.3: Capacitively loaded 4.5" monopole antenna**

### **3.2 Simulations:**

To get a more definite idea of what the gain, bandwidth, noise figure and saturation levels of the amplifier are, the circuit design was simulated using various CAD tools including Cadence's Pspice, Agilent's Advanced Design System (ADS) and Applied Wave Research's Microwave Office (MWO). Components are modeled in different ways in each of the software packages. Model Accuracy depends on their complexity. Pspice uses spice model for the FET which is based on the non linear model of the FET as given in the datasheet. ADS and Microwave office models are more complex, and Microwave office uses vendor models which can be obtained from its xml libraries while ADS use some parameter entry models where the required model parameters can be found in the product datasheet.

#### 3.2.1 Simulation Models

##### *Antenna:*

According to Sainati and Fessenden, the Thevenin equivalent circuit of a monopole can be represented by Figure 3.4 that is, a resistance and a capacitance in series. The resistance value is given by  $25 \Omega$  and the capacitance was measured to be  $10 \text{ pF}$ . This equivalent circuit was used to theoretically determine the noise figure of the active

antenna, i.e., antenna with the high impedance amplifier. Some of the initial simulations also involved the equivalent circuit.

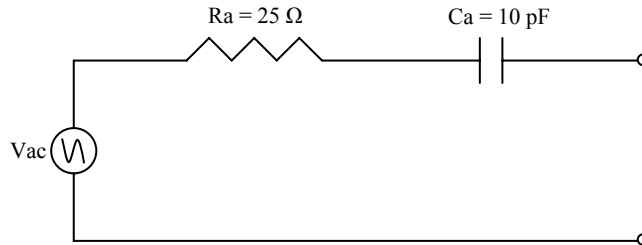


**Figure 3.4: Equivalent circuit of a monopole antenna**

*FET:*

Major part of the simulation was done in ADS and MWO. Due to the lack of a ready to use vendor model for the GaAs FET in Pspice an equivalent model NE325S01 was used, however the software does not have the provision to include transmission line models in simulation so ADS was used to simulate the circuit with and without the transmission lines to find the actual performance. ADS TOM – ‘Triquint scalable GaAsFET’ model with user-parameter entry was used to model the FET, as suggested by the vendor. The results obtained in ADS were cross-checked using the model in MWO. The FET models used in Pspice and ADS are shown in Figure 3.5.



### *Limiter diode:*

Limiter diode was modeled as its equivalent circuit obtained from the vendor, a resistance of  $1.5 \Omega$  in series with a  $0.8 \text{ pF}$  to ground.

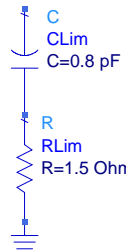


Figure 3.7: Equivalent model for DC path of the bias-tee.

### *Capacitors:*

Models for capacitors  $C_0$  and  $C_{p1}$  were obtained from the vendor libraries of ADS and MWO, but for simulation in PSpice all the capacitors were modeled as ideal. A capacitor value of  $950 \text{ pF}$  in the internal bias-tee was determined from the test measurement results. The  $0.1 \mu\text{F}$  capacitors did not have any specific vendor model, hence they were modeled as ideal.

Apart from these models the rest of the components were modeled as ideal components.

### 3.2.2 Amplifier Simulations

Using the above models, the amplifier circuit was simulated and analyzed to get a clearer picture of the gain, bandwidth, noise figure, stability, saturation, power consumption, etc. The initial simulations in Pspice were inconclusive as they did not include transmission line effects but are included in this section to show the

significance of including transmission line effects and non-ideal inductors and capacitors.

*DC analysis:*

The first simulation setup analyzed the circuit's DC state to see branch currents is being drawn and the voltages at each node especially FET's gate-to-source voltage ( $V_{gs}$ ) which is essential to see if the FET is being operated in reverse bias, close to saturation. Knowledge of the power dissipation at the resistors can prove useful while selecting appropriate sizes for implementation. Also the current drawn can tell the expected overall power consumption of the amplifier.

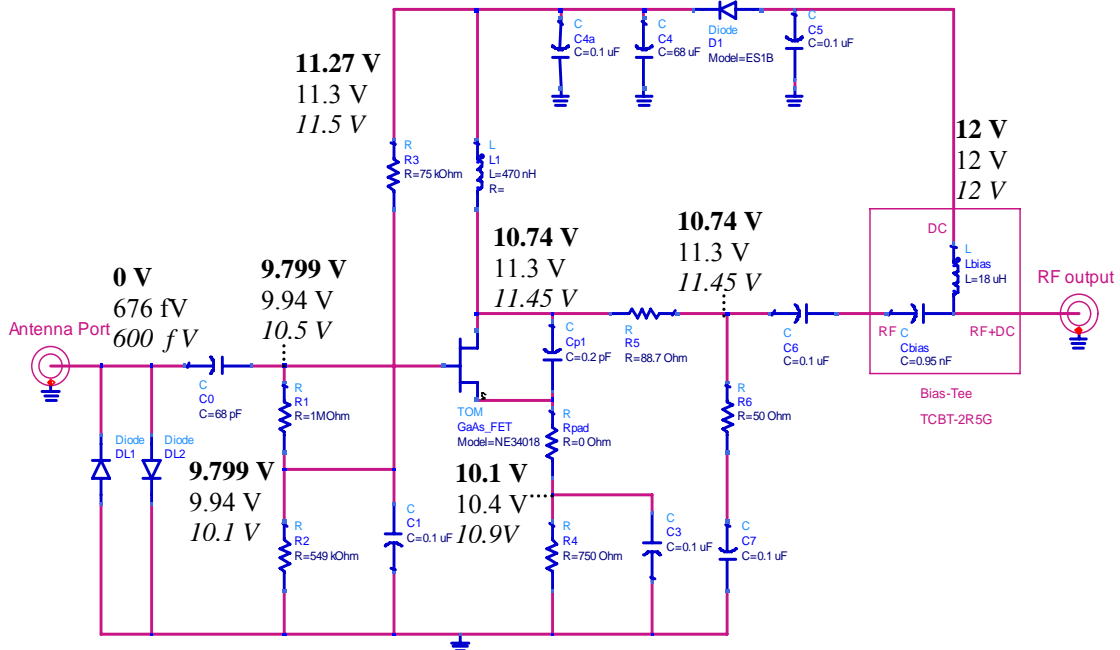


Figure 3.8: DC annotation of active antenna amplifier from all software packages  
 Legend: Pspice: **bold**, ADS: normal, MWO: *italicized*.

The parameters of interest are summarized in table 3.1. The results indicate that the FET is operating as expected close to saturation. The overall power is around 0.29 W

and the gate current is very low, which means that the FET is reverse biased as expected.

Table 3.1: Summary of results

Software	Vgs (V)	Current Drawn (mA)	Power Consumption (W)	Leakage from Gate (mA)
Pspice	-0.3	13.5	0.162	no leakage indicated
ADS	-0.36	13.8	0.165	no leakage indicated
MWO	-0.4	14.5	0.174	0.0004

*Gain and Bandwidth:*

As mentioned before, amplifier gain in addition to the antenna gain which is about 1.5 for a electrically small monopole, gives the gain of the active antenna. The bandwidth is dependent on two factors the mismatch between amplifier and antenna impedance, and the bandwidth of the amplifier itself. Hence the active antenna gain and bandwidth depend mostly on amplifier gain and bandwidth and input impedance.

Gain simulations were done using two simulation setups, AC simulation and S-parameter simulation. In AC setup the input section of the circuit is connected to an AC source with a fixed voltage level and the frequency is a variable parameter can be swept across the required range. The input and output voltages are recorded and then gain is calculated.

S-parameter setup works exactly like a network analyzer, the input and output sections are connected to ‘ports’. The circuit then is treated as a two port device and the setup allows the user to sweep the S-parameters across frequencies. The parameter  $S_{21}$  determines the gain of the amplifier. The added advantage with this setup is that along with gain, stability of the amplifier can be monitored too, and the circuit can include transmission lines used in the layout design.

Pspice is limited to AC analysis alone where as ADS can do both. MWO was used only for cross-checking the results from ADS so only S-parameter analysis was performed on it. The results from each of the software are presented below.

## Results

Pspice: AC simulation with input voltage of 1 nV.

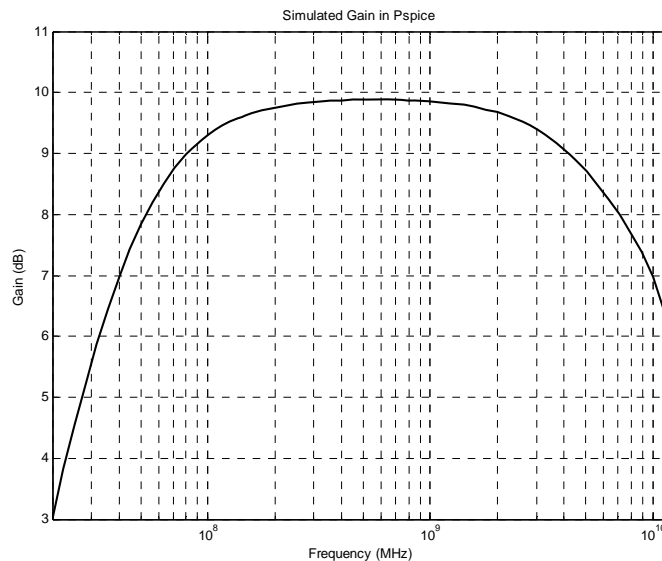


Figure: 3.9 Simulated Gain of active antenna amplifier from Pspice

ADS: AC simulation with input voltage 1 nV

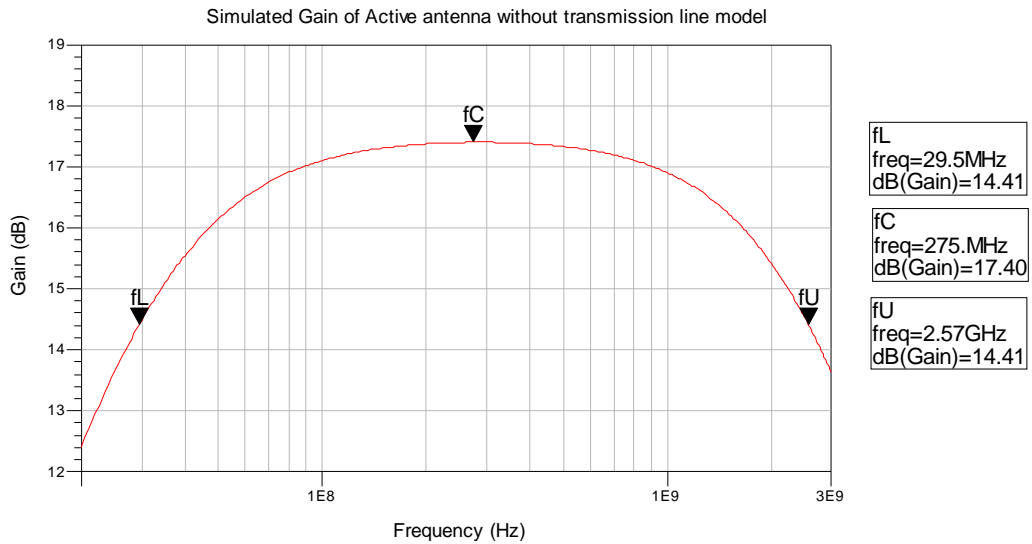


Figure: 3.10 Simulated gain of active antenna amplifier without transmission lines from ADS

ADS: S-parameter simulation with 50-ohm ports on input and output side.

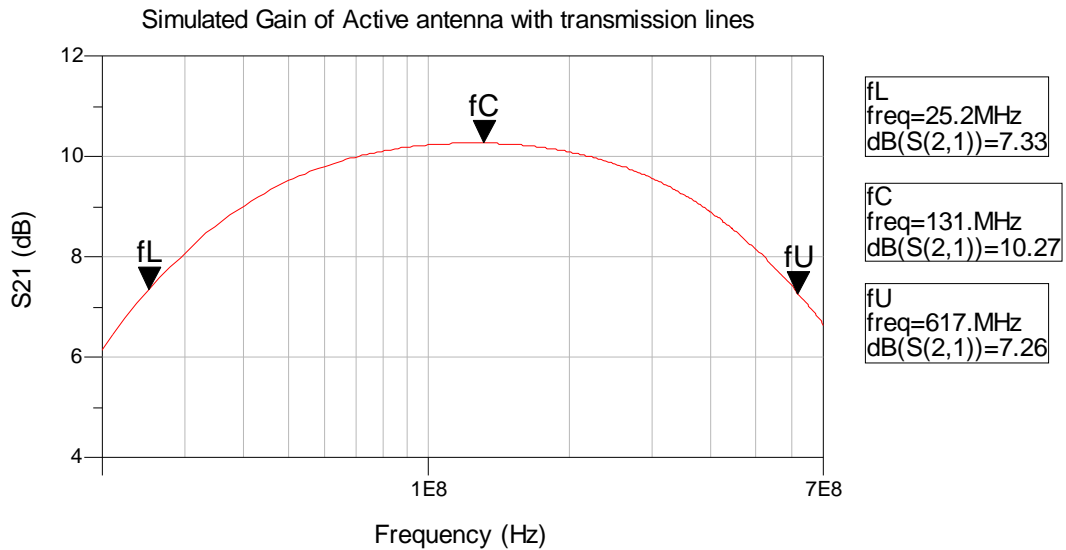


Figure 3.11: Simulated gain of active antenna amplifier with transmission lines from ADS

MWO: S-parameter simulation with -40 dBm input and 50 ohm ports on either side.

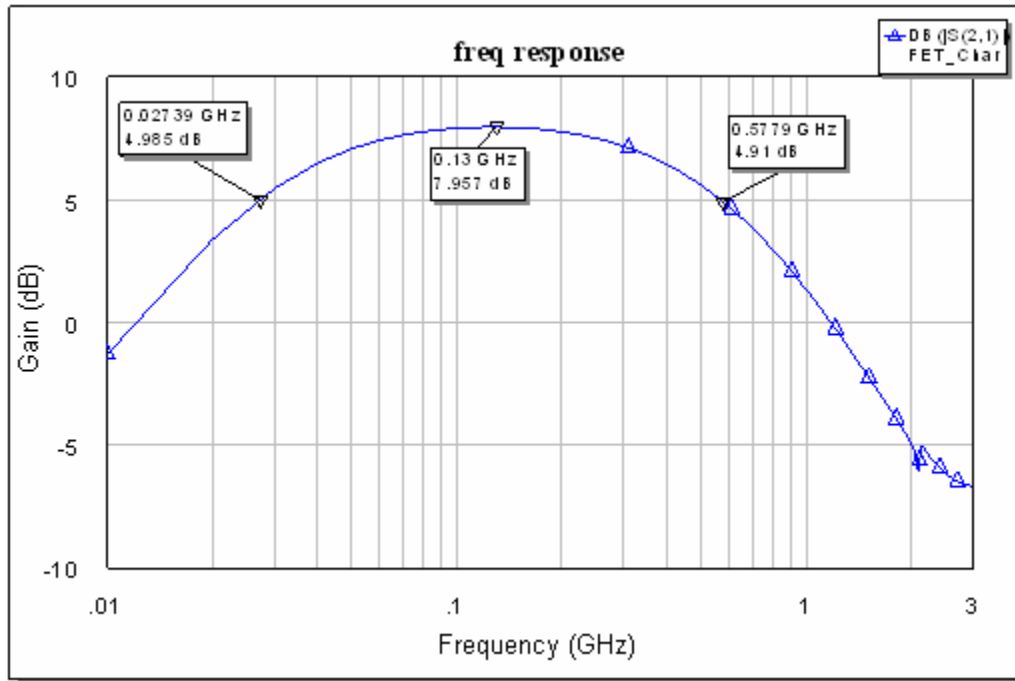


Figure 3.12: Simulated gain of active antenna amplifier with transmission lines from MWO

Table 3.2: Summary of results of gain simulation:

Software	Model	Peak gain (dB)	3-dB bandwidth (MHz)	Center frequency (MHz)	Cut off frequencies (MHz)	
					lower	upper
Pspice	without transmission lines	9.8	9980	400	20	1000
ADS	without transmission lines	17.4	2540.5	275	29.5	2570
	with transmission lines	10.27	591.8	131	25.2	617
MWO	with transmission lines	7.95	550.61	130	27.4	578

It can be seen from table 3.2 that there are two factors that affect the gain and bandwidth of the amplifier – the component model and the inclusion of transmission lines in the circuit model. Pspice uses ideal components and does not model transmission lines and hence the simulated gain and bandwidth are high. The ADS model without transmission lines also shows high gain and 2.5 GHz of bandwidth, but with the inclusion of non-ideal components and transmission lines, the bandwidth is reduced to 590 MHz. However ADS and MWO are within 40 MHz agreement in bandwidth and 3 dB in gain. Since the MWO model of the FET is direct vendor product, the bandwidth thus observed is assumed to be more precise.

*Input Impedance:*

The S-parameter simulation also gives the  $S_{11}$  parameter which can be converted to  $Z_{11}$  using  $Z_{11} = Z_0(1 + S_{11})/(1 - S_{11})$  the impedance plot of the amplifier is shown in figure 3.12. It can be seen that the amplifier impedance is around 366  $\Omega$  in magnitude, and the imaginary part which is representative of the reactive part of the impedance looks predominantly negative, means capacitive, also the corresponding capacitance at 150 MHz as indicated by the pointer in figure 3.12 is 2.8 pF and the magnitude of input impedance is 366  $\Omega$ . However it is not clearly known why the real part of the input impedance shows a low value of 21  $\Omega$  rather than 1 M  $\Omega$  according to theory.

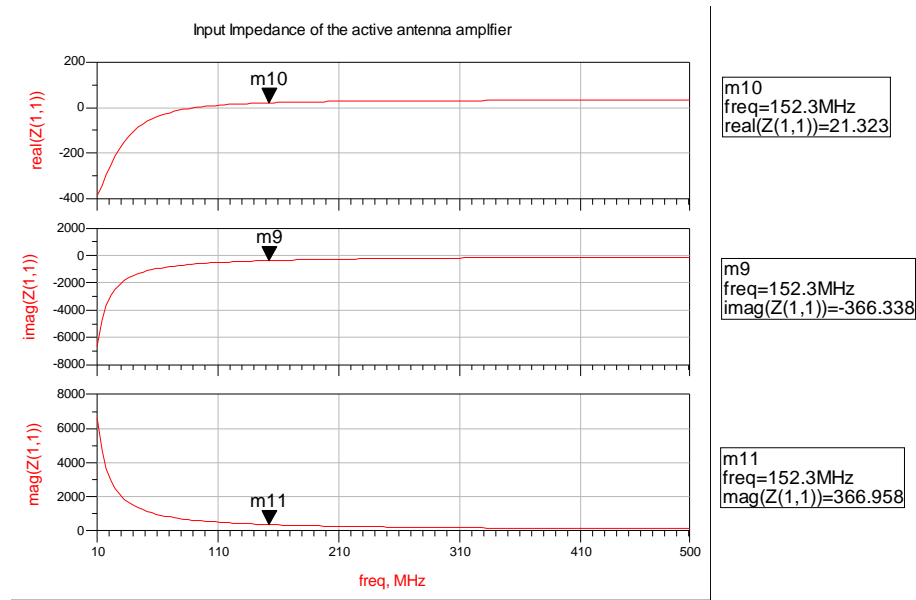


Figure 3.13: Input Impedance of active antenna amplifier from ADS

*Stability:*

Stability of an amplifier is important for any application. Stability can be determined from the S-parameters obtained from the previous S-parameter simulation setup using the following formula:

$$K = \frac{1 - |S_{11}|^2 - |S_{22}|^2 + |\Delta|^2}{2|S_{12}S_{21}|} \text{ where } \Delta = S_{11}S_{22} - S_{12}S_{21}$$

For an amplifier to be unconditionally stable, factor K should be >1 and |Δ| should be <1. These factors however show only whether or not the amplifier is ‘unconditionally’ stable, meaning that it does reflect that there could be oscillations at those frequencies, only under certain conditions, but the factors do not give the conditions under which the device is unstable . To know these load and source conditions, stability circles are plotted. The Input and Output stability circles can

show for what load conditions or source conditions the amplifier goes into oscillations. The following figures give both the stability factor and stability circles.

Results:

ADS:

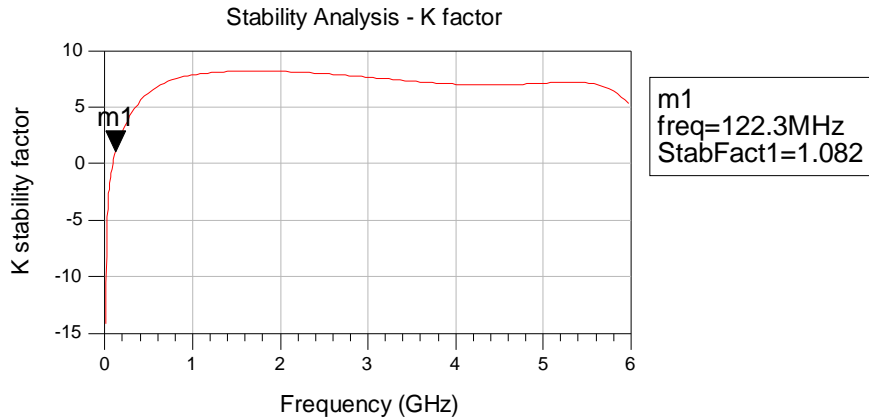


Figure 3.14: Stability factor K of active antenna amplifier from ADS

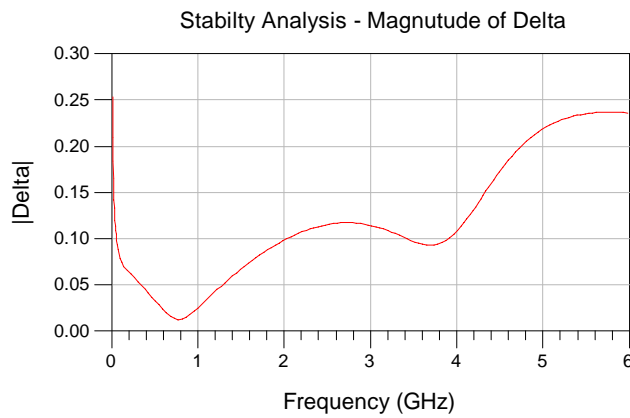
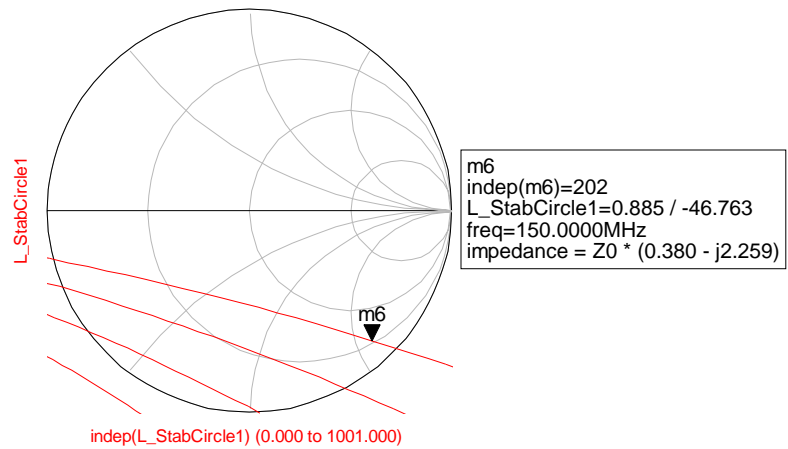
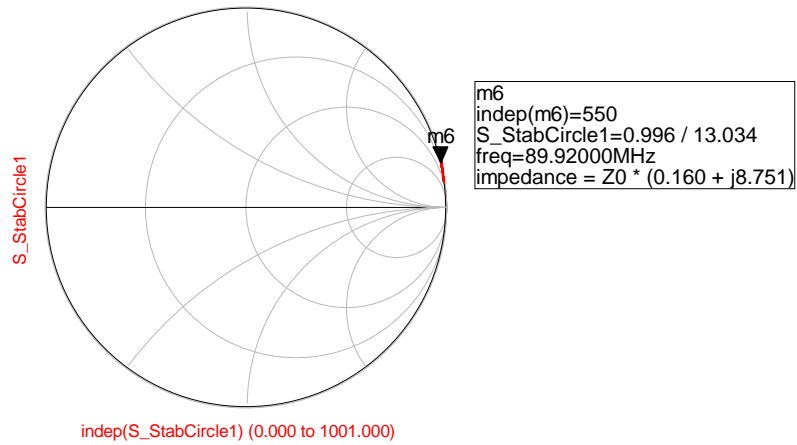


Figure 3.15: Stability factor  $|\Delta|$  of active antenna amplifier from ADS

It can be seen that the K factor is less than 1 for frequencies below 122 MHz. So the stability circles for those set of frequencies were plotted.



(a)



(b)

Figure 3.16 (a) Load stability circles for the active antenna amplifier for frequencies 10 to 150 MHz  
 (b) Source stability circles for the active antenna amplifier for frequencies 10 to 150 MHz

It can be seen from figures 3.15(a) and (b) that if the amplifier sees capacitive load, that can make the amplifier oscillate and sources that are near to open and inductive make the amplifier oscillate, but in our situation the source that the amplifier sees is the antenna element which is capacitive in nature which falls outside the stability circles and the impedance that is offered as load to the amplifier is nothing but the

input impedance of the radar system that follows it, which is  $50 \Omega$ . Hence we can be sure that the amplifier is oscillation free.

*Noise Figure:*

Even with no input, there is a small amount of voltage that can be measured at the output which can be distributed over the bandwidth, this is amplifier noise power. Noise Figure is a quantitative description of a noisy microwave amplifier and is given by the ratio of input signal to noise ratio to the output signal to noise ratio and most of the CAD tools that are used for circuit simulations use the same formula to calculate noise figure. Pspice does AC simulations to find out the input and output signal to noise ratios and then noise figure is calculated from that information. However in ADS and MWO the circuit is treated a noisy two port network [18] and have built in functions that calculate the noise figure and present it in dB. The following graphs show the simulated noise figure of the active antenna.

Pspice:

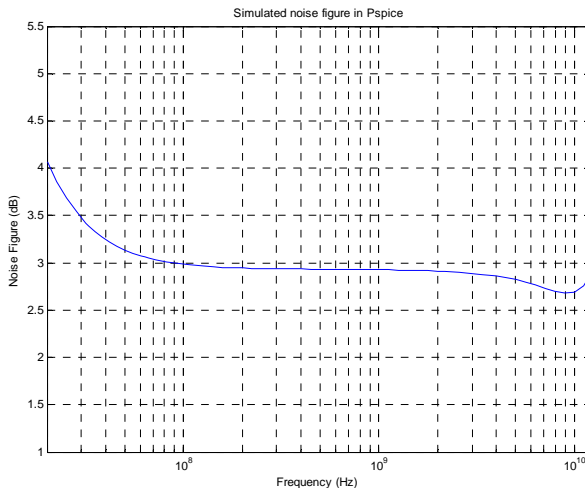


Figure 3.17: Simulated noise figure and SNR of active antenna amplifier from Pspice

ADS:

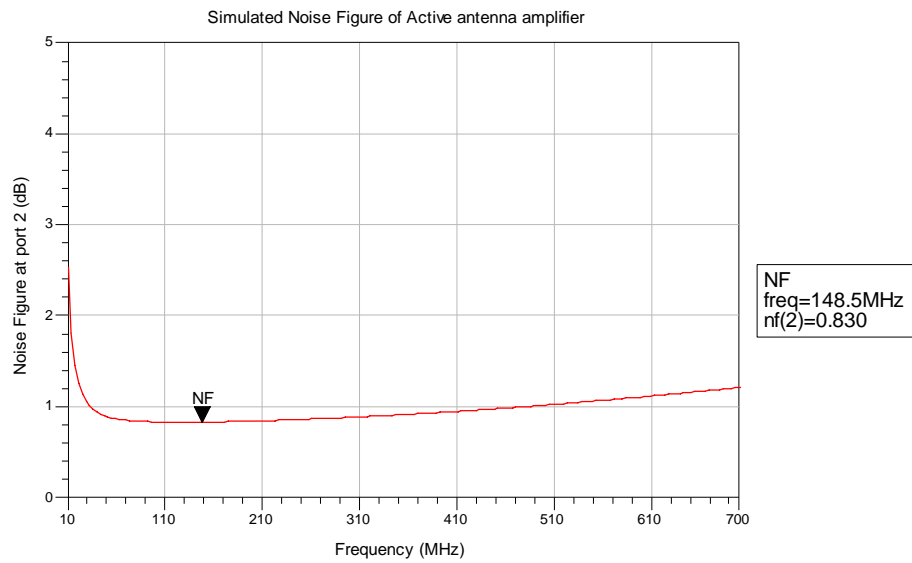


Figure 3.18: Simulated noise figure of active antenna amplifier from ADS

MWO:

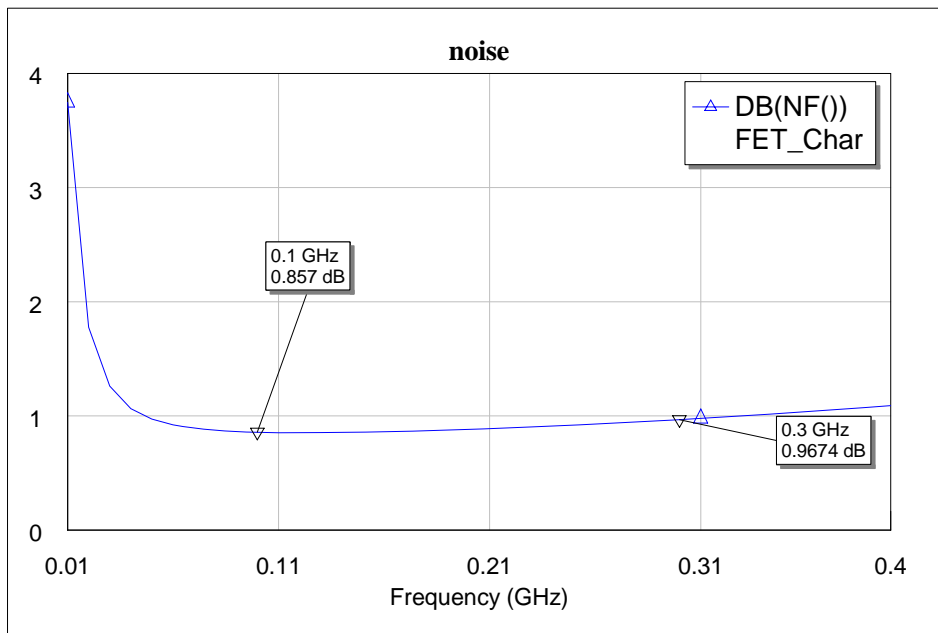


Figure 3.19: Simulated noise figure of active antenna amplifier from MWO

Table: 3.3 Summary of results

Software	Average Noise Figure (dB)	Range	
		Lower	upper
Pspice	2.9	2.7 dB	4 dB
ADS	0.9	0.83 dB	1.2 dB
MWO	0.85	0.85 dB	1.12 dB

GaAs FETs are generally very low noise devices; the typical noise figure is around 0.6 dB, thus making the overall amplifier noise low.

*Saturation:*

As mentioned before, the presence of strong signals in the same environment as that of the operation of the active antenna can saturate the amplifier and thus result in degradation of signal-to-noise ratio. This effect was simulated using transient simulation in ADS and Pspice with two sinusoids coupled into the input of the amplifier, one for strong interferer and one for desired signal, and the power level of interferer at which the amplifier shows significant harmonics with degradation in noise floor, was termed as the saturation point for the amplifier. In MWO harmonic balance simulation was performed to see the saturation and gain compression due to saturation. For simulations that involve a jammer signal, the amplitude of the interfering signal is progressively increased, and for each level, two types of simulations are done. One with decreasing desired signal amplitude, which gives an

estimate of the minimum detectable signal i.e. lowest signal amplitude that can be detected given the SNR degradation due to jammer presence. Typically, low levels of jammer do not affect the noise floor but as the jammer amplitude increases, the noise floor is also raised, thus decreasing the sensitivity of the amplifier. The second of the tests is increasing the desired signal amplitude in steps to a level that can saturate the amplifier. This way four scenarios can be studied: strong jammer–strong signal, strong jammer-weak signal, weak jammer – weak signal, weak jammer – strong signal. But before simulating circuit performance in presence of an interfering signal, the circuit was also simulated with a single input source to know what the dynamic range of the amplifier is.

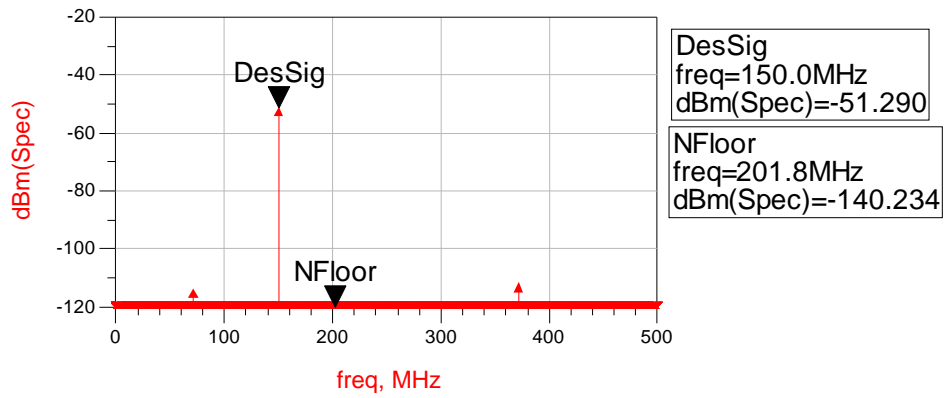
Table 3.4 gives a summary of results from ADS saturation simulation for amplifier performance without a jammer and Table 3.5 gives the results for simulation with a jammer. Also the figures that follow give an idea of the effect of high input power levels and high jammer power levels on the sensitivity of the amplifier.

Setup 1: Without Jammer:

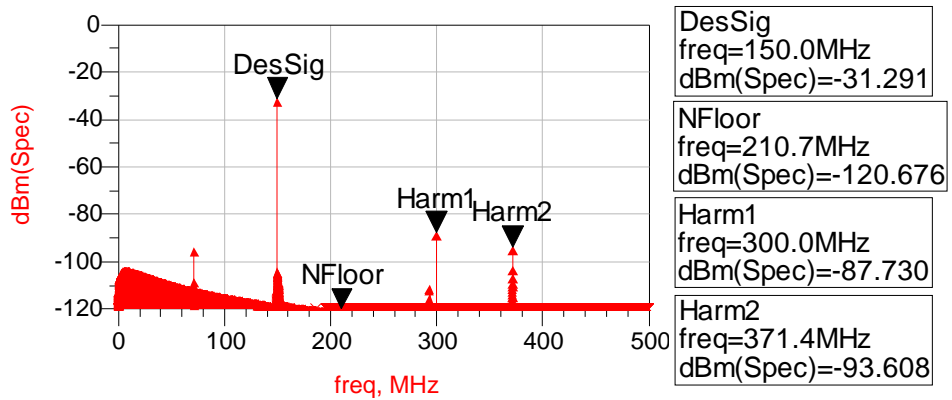
Input Signal frequency: 150 MHz

Input Signal power level: variable between -105 dBm to -10 dBm

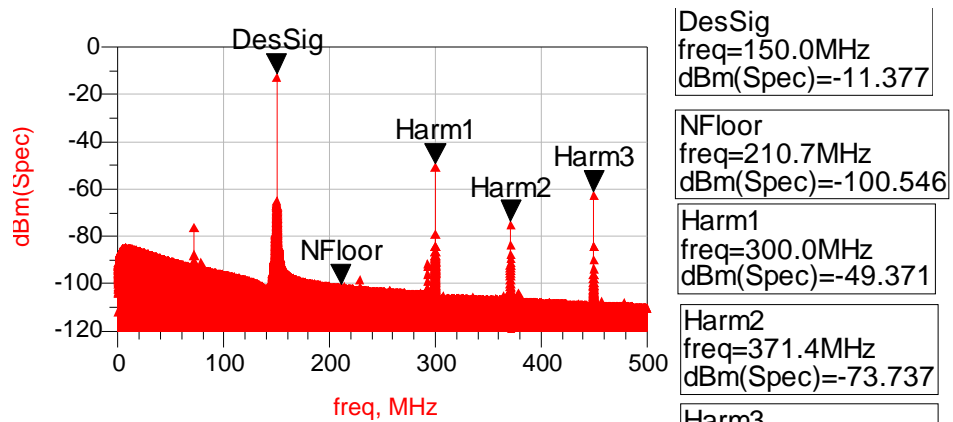
Noise BW: 1 kHz



(a)



(b)



(c)

Figure 3.20: ADS simulations (a) Input signal: -60 dBm (b) Input signal: -40 dBm (c) Input signal: -20 dBm

### 3.4: Saturation simulation summary of results for circuit performance without jammer

Desired signal level (dBm)		Noise Floor (dB)	SNR (dB)	Harmonic level (dBm)	Gain
input	output				
<b>Minimum Detectable Signal (MDS)</b>					
-70	-61.29	-140.7	79.41	-	8.71
-80	-71.29	-140.2	68.91	-	8.71
-90	-81.29	-142.97	61.68	-	8.71
-100	-90.25	-140.7	50.45	-	8.71
-120	-111	-140.7	29.7	-	9
-130	-121.29	-140.7	19.41		8.71
-140	-131.29	-140.7	9.41		8.71
<b>Saturation and Harmonics</b>					
-60	-51.29	-140.2	88.91	-118.2	8.71
-50	-41.29	-130.07	88.78	-108.1	8.71
-40	-31.29	-119.04	87.75	-87.7	8.71
-30	-21.3	-109.8	88.5	-67.64	8.7
-20	-11.37	-100.5	89.13	-49.09	8.63
-15	-7.3	-95.3	88.24	-31.32	7.7
-10	-6.12	-91.5	85.38	-20.73	3.88

It can be seen from both the figures and the table that as the input power increases, the signal to noise ratio decreases and the harmonic level increases, if saturation point can be defined as point when the harmonic level reaches up to 20 dB below the fundamental level and the gain drops by 1 dB, then looking at the table it can be said that saturation occurs at -15 dB.

Minimum Detectable Signal (MDS) is defined to be the lowest possible signal that can be detected before it gets submerged into the noise floor. To find the minimum detectable signal the input level is decreased till it can no longer be seen in the spectrum. MDS for the amplifier is -140 dBm.

By these results, we can say that the dynamic range of the amplifier is 125 dB i.e. from -15 dBm to -140 dBm.

Setup 2:

Interference signal frequency: 100 MHz ,

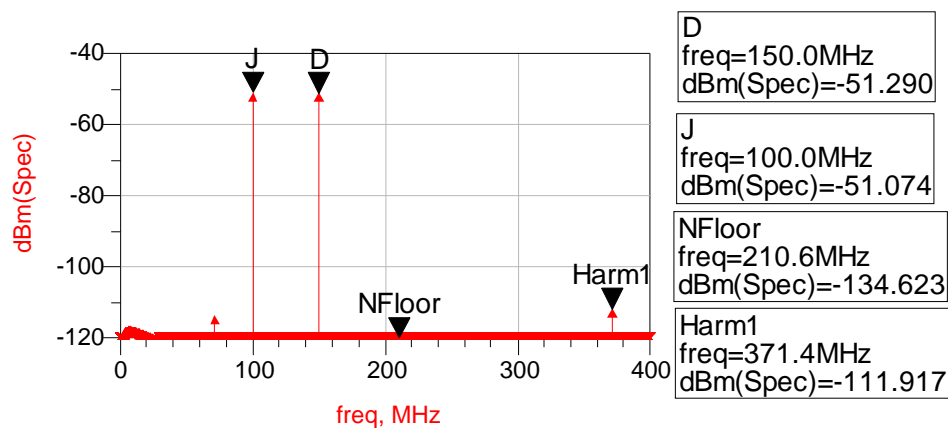
Interference signal power level: variable, in increasing steps

Desired signal frequency: 150 MHz

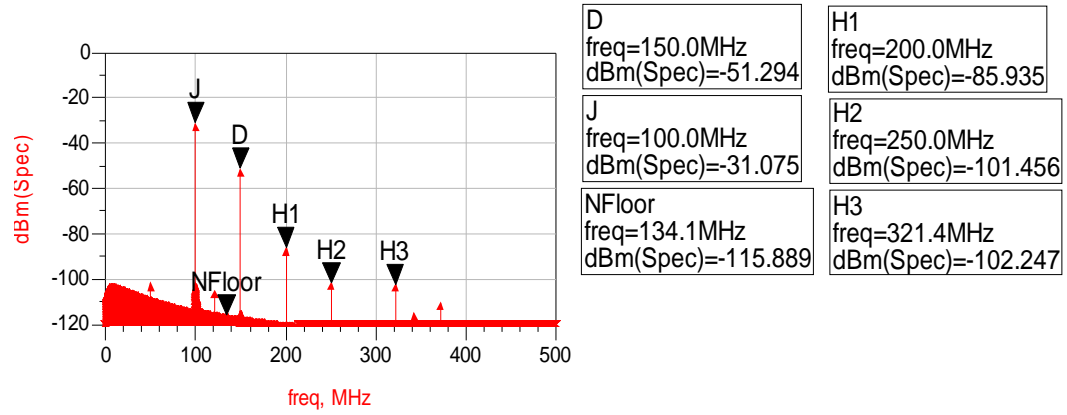
Desired signal power level: -60 dBm.

Noise BW: 1 kHz

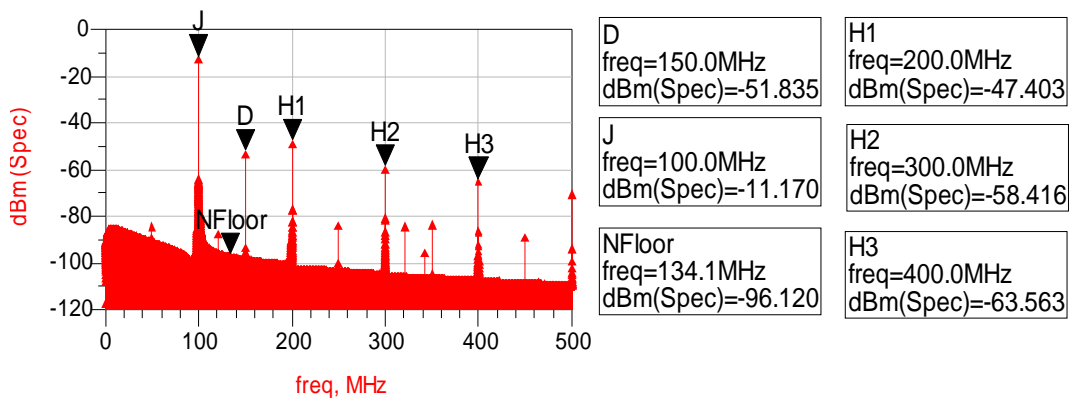
The plots that follow show the effect of various levels of interference signal on a -60 dBm desired signal.



(a)



(b)



(c)

Figure 3.21: ADS saturation simulation results (a) jammer at -60 dBm (b) jammer at -40 dBm (c) jammer at -20dbm

Table: 3.4(b): Saturation Simulation – Summary of results.

Jammer Level (dBm)		Desired signal level (dBm)		Noise floor (dB)	SNR (dB)	Harmonic level (dBm)	
Input	output	input	output			harm1	harm2
<b>Minimum Detectable Signal</b>							
-60	-51.07	-60	-51.29	-134.6	-83.31	-	-
		-80	-71.29	-134.6	-63.31	-	-
		-100	-91.29	-134.6	-43.31	-	-
		-120	-111.29	-134.6	-23.31	-	-
		-130	-121.29	-134.6	-13.31		
		-134	-125.29	-134.6	-9.31	-	-
<b>Saturation and Harmonics</b>							
-60	-49.8	-40	-31.29	-114	82.71	-93	-87.73
		-20	-11.8	-94	82.2	-73.31	-49.07
		-15	-7.49	-84	76.51	-64.71	-31.32
<b>Minimum Detectable Signal</b>							
-40	-31.07	-60	-51.29	-115	63.71	-85.4	-101.45
		-80	-71.29	-115	43.71	-87.01	-103.24
		-100	-91.29	-115	23.71	-87.01	-111.9
		-115	-106.29	-115	8.71	-87.01	-
<b>Saturation and Harmonics</b>							
-40	-31.07	-40	-31.29	-95.36	64.07	-80.44	-91.31
		-20	-11.86	-75.36	63.5	-58.28	-49.14
		-15	-7.45	-64.71	57.26	-48.36	-32.28
<b>Minimum Detectable Signal</b>							
-20	-11.17	-60	-51.8	-96.12	44.32	-47.4	-58.41
		-80	-71.8	-96.12	24.32	-47.4	-58.41
		-95	-86.8	-96.12	9.32	-47.4	-58.41
<b>Saturation and Harmonics</b>							
-20	-11.17	-40	-31.99	-76.32	44.33	-45.58	-57.07
		-20	-12.29	-56.32	44.03	-34	-38
		-15	-7.94	-46.32	-38.38	-27.4	-32.5

Note: there were other peaks at 50 MHz, 250 MHz and 350 MHz when the jammer level goes up to -20 dBm; they are at a lower level than the harmonics mentioned in the table hence were not included.

It can be seen from figures that as the jammer level is increased, the noise floor is also raised as a result, the signal to noise ratio is degraded and at -20 dBm of jammer level, the harmonics are huge, noise floor is raised quite a bit and also spurious peaks appear at 50, 250 and 350 MHz which are significantly above the noise floor but about 20 dB below the main harmonic. Thus -20 dB of jammer signal is the maximum that the amplifier can afford. Also dynamic range for each of the levels was computed and is shown below:

1. Dynamic range with jammer at -60 dB : 119 dB (-15 dBm to -134 dBm)
2. Dynamic range with jammer at -40 dB : 110 dB (-15 dBm to -115 dBm)
3. Dynamic range with jammer at -20 dB : 80 dB (-15 dBm to -95 dBm)

Any jammer above -20 dBm will saturate the amplifier and distorting the signals, thus degrading the performance of the active antenna. It should however be kept in mind that these results are raw results, i.e. no averaging or integration done on them, in reality however, the radar data is averaged and integrated to reduce the noise floor and increase the SNR, hence the MDS may actually be lower than what can be seen through these simulation results.

Through the above mentioned simulations, the active antenna amplifier has been completely characterized (theoretically).

### 3.2.3 Antenna Simulations

Although the design of the active part of the active antenna is more complex than the passive, both are equally responsible for the overall performance of the active antenna, therefore to ensure optimal performance over the range of frequency, the impedance of the radiating element of the active antenna should have impedance lesser than that of the amplifier and greater capacitance. These are the only two performance criteria for antenna design, apart from these, the antenna length should be lesser than  $\lambda/8$  for the highest frequency of operation.  $\lambda$  is 1 m at 300 MHz, so  $\lambda/8$  is 0.125 m or approximately 5". As mentioned before, the monopole is loaded capacitively using a rectangular copper patch this not just increases the capacitive reactance but makes the current distribution in the monopole uniform and thus increases the effective length of the antenna, while maintaining the physical size the same. Increase in the capacitive patch also increases the radiation resistance of the antenna. The antenna was simulated using Ansoft HFSS EM simulator. Increasing the area of the rectangular patch increases the capacitance, but the length of the element should be maintained at 5" so the variable parameters were the length and width of the trace, and length and width of patch. These parameters were optimized to obtain high input capacitance, impedance lower than that of the amplifier. The final design is shown in fig: 3.21 The impedance plots are shown in fig: 3.22

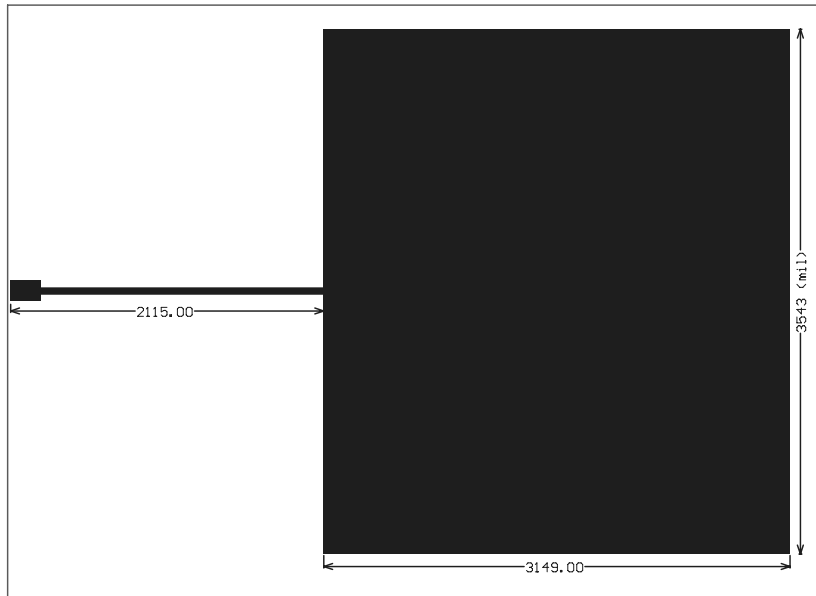


Figure 3.22: Dimensions of the monopole to be used with active antenna

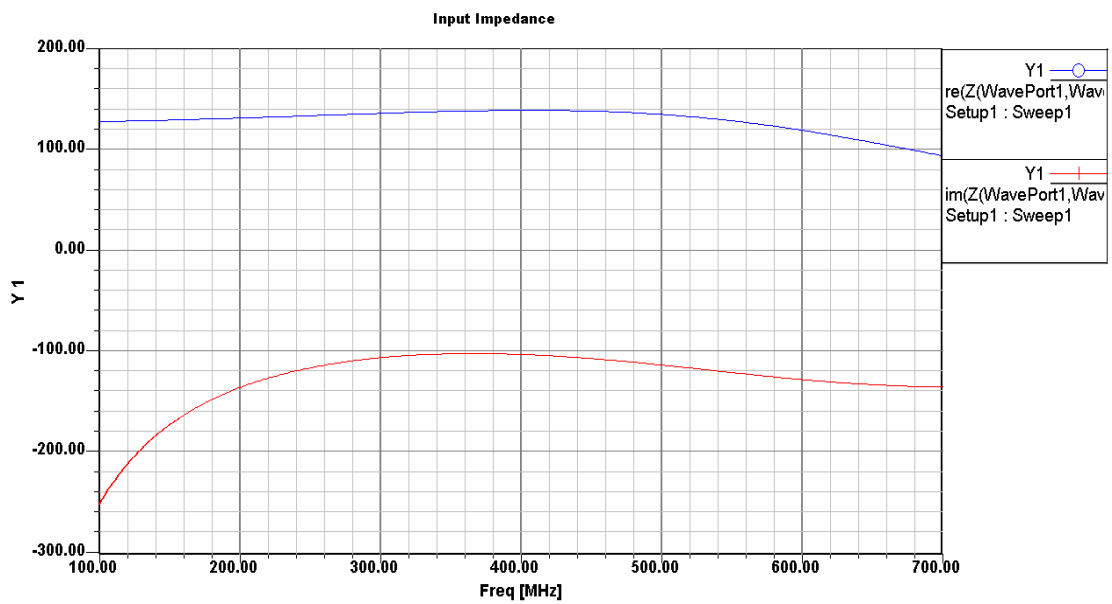


Figure 3.23 (a): Input Impedance (real, imaginary) of the monopole

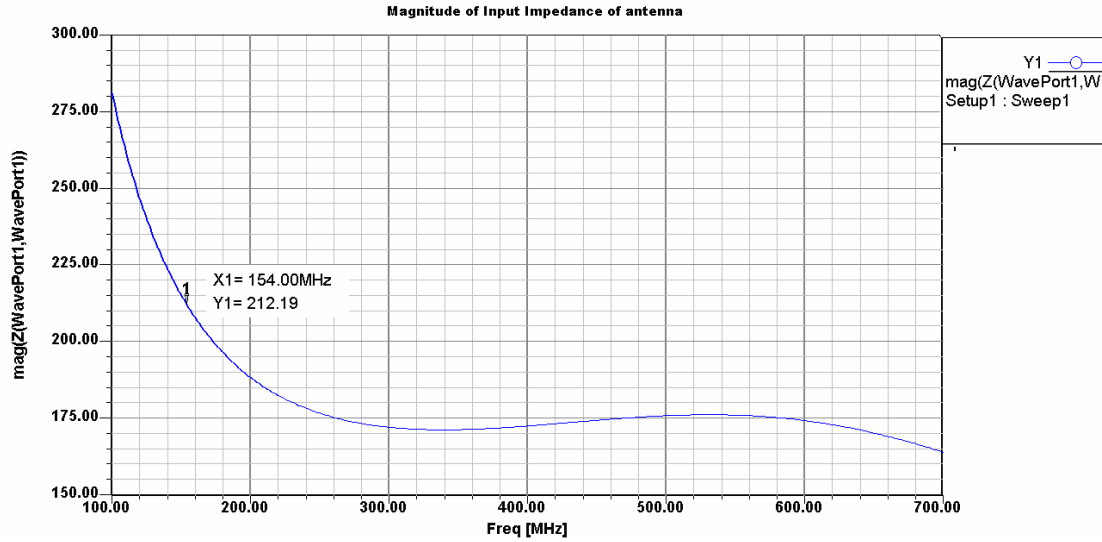


Figure 3.23 (b): Input Impedance (magnitude) of the monopole

The capacitance corresponding to 150 MHz as calculated from the imaginary part of the impedance plot is 6.24 pF, which is much more than the amplifier input impedance, thus the design constraint has been met. Also the monopole is electrically small up to 300 MHz hence acts as a Hertzian dipole, with gain and directivity of 1.5.

On completion of simulations for the active antenna, the amplifier board was fabricated and tested in the lab to completely characterize it. The next chapter deals with the implementation and measurement details of the antenna and the amplifier.

### **4.1 Implementation**

Implementation or realization of the circuit of the active antenna was done by first designing a Printed Circuit Board (PCB) layout for them using Altium Designer, the layout was then fabricated on an FR-4 **microstrip** board and then populated with components. The layout for radiating element section of the active antenna was also designed first in Altium Designer and then milled out on FR-4 substrate. The subsections that follow will describe in detail each step involved in implementation

#### 4.1.1 Implementation of active antenna amplifier

Altium Designer is software that enables the user to design a PCB layout given the schematic of the circuit and the footprints of each component. The component footprints were first placed and then connected using transmission lines of appropriate characteristic impedance. A two-layer FR4 substrate was used. The top layer has the components all of which are surface mount and the bottom layer is a ground plane.

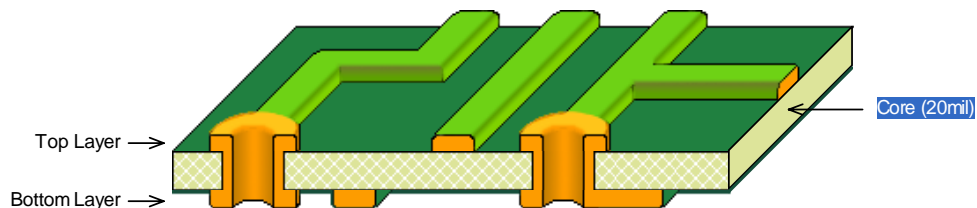


Fig 4.1: Layer stack up

The thickness of the substrate along with the dielectric of the substrate and width of the transmission line determines the characteristic impedance of the line. The formula for calculating the impedance is given by

$$Z_0 = \begin{cases} \frac{60}{\sqrt{\epsilon_r}} \ln\left(\frac{8d}{W} + \frac{W}{4d}\right) & \text{for } \frac{W}{d} \leq 1 \end{cases}$$

or

$$= \begin{cases} \frac{120\pi}{\sqrt{\epsilon_r} [W/d + 1.393 + 0.667 \ln(W/d + 1.444)]} & \text{for } W/d \geq 1 \end{cases}$$

Where W is the width of transmission line and d is the substrate thickness. Increase in substrate thickness increases the width of transmission line for certain characteristic impedance. The substrate thickness was thus chosen to be as thin as 20 mils so that the traces also can be thin.

The RF path, i.e. the path through which the RF signal passes shown highlighted in figure 4.2, is kept as straight as possible and the transmission lines were made as thin as possible (7 mils) to provide a high impedance. The DC chain and the lines connected to R<sub>6</sub> were 50 Ω hence had a greater width (34 mils).

Since the RF path had to be kept straight, it was necessary to run a trace beneath the diode D1. This however was safe as there was no metallization beneath the diode.

The lines connecting the inductor L1 had to be as thin as possible and short, to behave inductively.

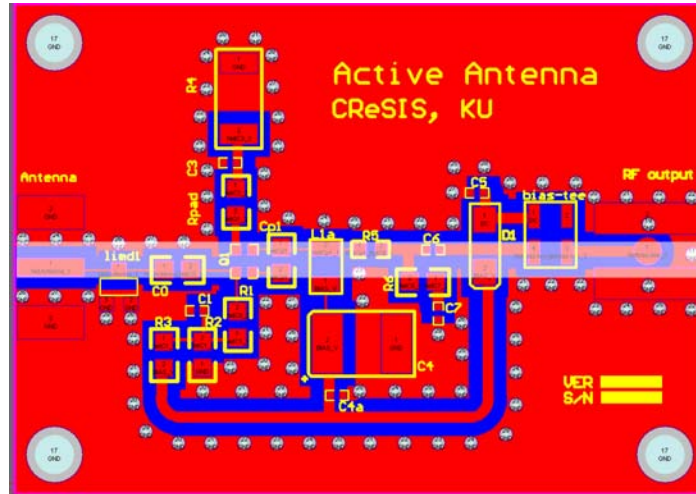


Figure 4.2: PCB layout for active antenna amplifier.

The top layer was filled with copper connected to ground with 75 mils clearance from the rest of the traces that carry signal. This provides shielding from Electromagnetic Interference (EMI). Also the ground fill was lined with ground vias to enable shortest path to ground for the signals, thus avoiding large ground loops. Holes on all four corners provide mechanical mounting support for the board. The final fabricated and populated board with silk screen and solder mask is shown and the populated board is shown in fig 4.3. The board dimensions are 2" x 1.5" x 0.02".

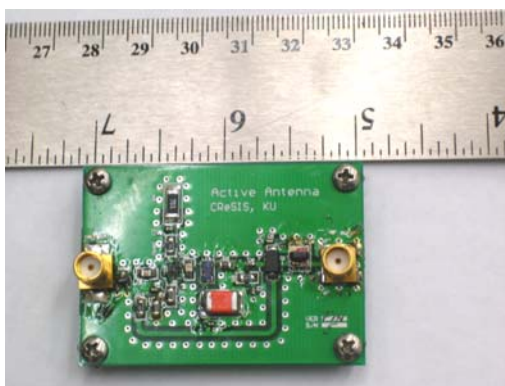
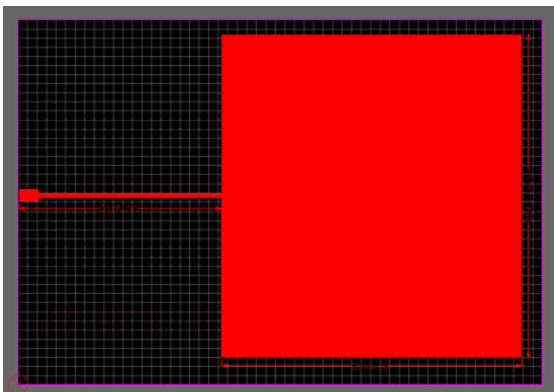


Figure 4.3: populated board of active antenna amplifier

#### 4.1.2 Implementation of monopole antenna

The layout design for the antenna element was also done using Altium Designer. The dimensions were extracted from Ansoft HFSS and the design was milled on a one sided copper coated, 64 mils thick FR4 substrate. The thickness does not matter much in this case as there is no ground plane on the bottom layer, hence the question of characteristic impedance of line does not come into picture. The dimensions of the board are 5.2"x 3.5" x 0.064". Figure 4.5(a) shows the layout and figure 4.5 (b) shows the milled out antenna. The trace width is 50 mils with 2" length and the capacitive patch is 3.2" x 3.5".



(a)



(b)

Figure 4.4: (a) Layout of monopole antenna with capacitive patch; (b) Final antenna after milling

## **4.2 Measurements**

After simulation and implementation, the next step in the design cycle of any device is testing. Simulations provide a virtual environment and equivalent models to evaluate the circuit. There are several methods to make it as ‘real’ as possible by adding transmission line models and also using vendor models rather than ideal ones, but it is possible to do that only to a certain extent, hence it is essential that the circuit be measured in the lab before it can be used in field. Even though the parameters of interest are the same, i.e. gain, bandwidth, impedance, stability, saturation etc. the method in which each parameter is measured is different. The following sections will deal with the measurement setup for each of the parameter measurements and the results obtained followed by an analysis that compares the measured and simulated results.

### **4.2.1 DC Probing:**

The setup for DC analysis was simple RF port was connected to the external bias-tee (Mini-Circuits ZNBT-60-1W), and the antenna port was left open. Each of the node voltages were measured using a multi-meter and were noted. The parameters of interest were  $V_{gs}$ , current drawn, gate leakage and power consumed. The measured results are given in table 4.1

Table 4.1 : DC analysis measurement results

$V_{gs}$	Gate leakage current	Current drawn	Power consumed
-1.58 V	0.76 $\mu$ A	14 mA	0.168 W @ 12V

Analysis:

The measured results show that the FET operates at -1.58 V of gate-to-source voltage, meaning that the FET is operating in reverse bias, but not as close to saturation as simulations show. However the other parameters almost match, the gate leakage is 0.76  $\mu$ A as compared to 0.4  $\mu$ A from simulation in MWO. The current drawn and the power consumed also match simulation results.

4.2.2 Stability

An amplifier is said to oscillate when there is an output signal output without any input. This can be verified by checking the amplifier output in the spectrum analyzer without any input on the antenna port. There are three conditions in which this can be done. One is to terminate the input with a 50- $\Omega$  load, then with the input port left open and finally with the antenna connected to the amplifier input. If the noise floor of the spectrum analyzer alone is seen, without any strong peaks then the amplifier is stable and oscillation free, else if there exist any peaks, that cannot be accounted for, i.e. when the antenna is connected to the amplifier and the output is observed, peaks at the lower frequency end can be observed which are either TV signals or other radio signals. Apart from these signals if there are peaks that cannot be accounted for then it means that he amplifier is oscillating.

### Test Setup:

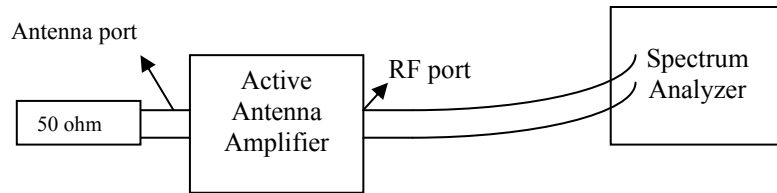


Figure 4.5: Setup for oscillation test

*Set up: (left to right) : 50 ohm load / open/ antenna → antenna port of active antenna → RF port → N-type male/ SMA male → bias-tee(ZNBT-60-1W) RF+DC port → RF port of bias-tee → N-type female/SMA male → Astrolab 24TC cable → Db block (MCC 15542) → Spectrum Analyzer Agilent E4407B. DC port of bias-tee → DC power supply (12V).*

### Results:

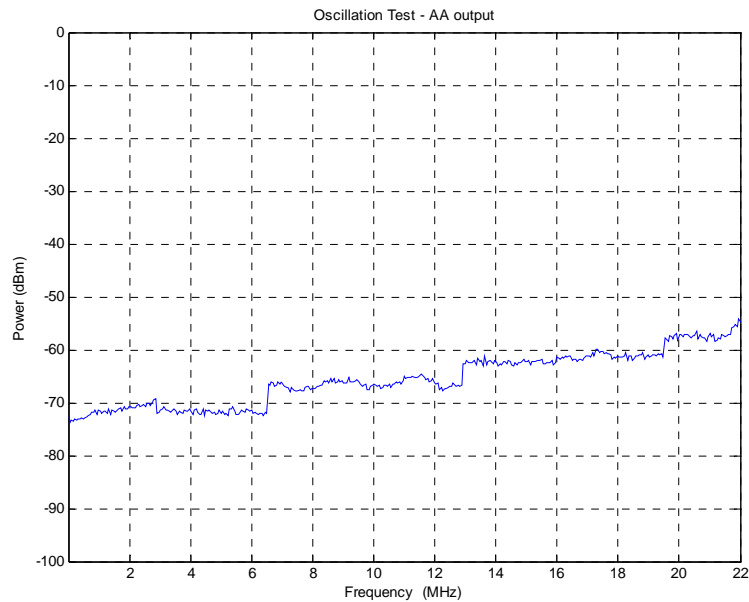


Figure 4.6: Measured spectral output from oscillation test

### Analysis:

The spectrum analyzer works from 9 kHz to 22 GHz and as seen from figure 4.6 only noise floor is visible and no other peaks for both open and terminated conditions

unlike the previous design versions of the active antenna amplifier that showed oscillations at 5.14 GHz and for the antenna attached to the amplifier only known signals are received and no spurious peaks. Hence the amplifier is stable throughout the spectrum.

#### 4.2.3 Gain and Bandwidth:

The gain and bandwidth of amplifier can be found from the  $S_{21}$  parameter measured versus frequency using a network analyzer. The measurement setup is given in figure 4.7.

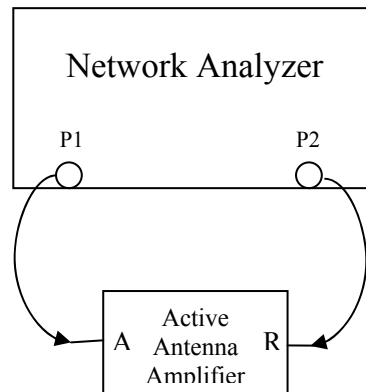


Figure: 4.7 Test setup for S-parameter measurements

*Set up: (left to right) : Network Analyzer port 1 → Astrolab 24TC cable → antenna port of active antenna → RF port → N-type male/ SMA male → bias-tee(ZNBT-60-1W) RF+DC port → RF port of bias-tee → type N female/SMA male → Astrolab 24TC cable → NA port 2. DC port of bias-tee → DC power supply (12V).*

The network analyzer was calibrated for the following settings:

Input power: -30 dBm

Start frequency: 10 MHz

Stop frequency: 500 MHz

Number of points: 1601

Number of averages: 5

Cable length: 24''

Results:

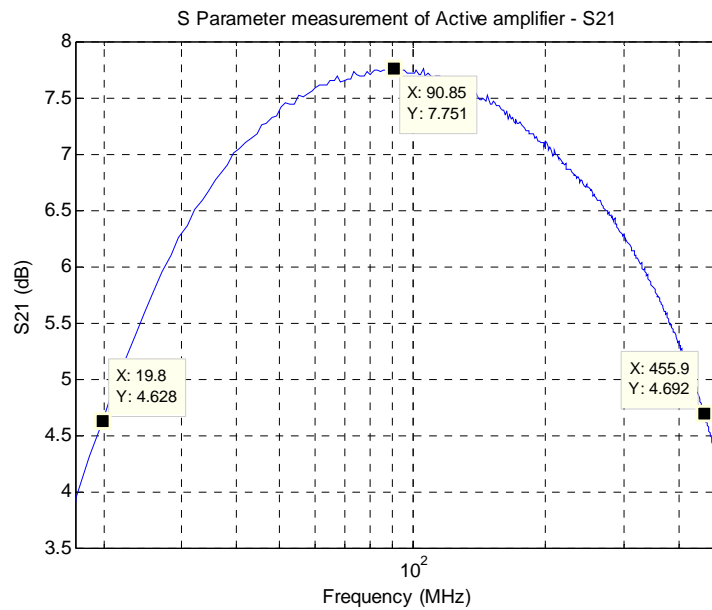


Figure 4.8: Measured gain of active antenna amplifier

Analysis:

Figure 4.8 shows the frequency response of the  $S_{21}$  parameter in dB scale. The peak gain of the amplifier is 7.75 dB at 90 MHz and the 3-dB cut off frequencies are nearly 20 MHz and 456 MHz. The difference of the two gives us the bandwidth of the amplifier which is 436 MHz and is within our frequency range (100 to 300 MHz) but it does not match the simulation results that predicted a 550-MHz bandwidth. The probable reason for the mismatch in the values obtained in simulation and measured

results is inaccuracy of the models used. The 0.1- $\mu$ F capacitors used extensively in the circuit are modeled as ideal as the vendor model was unavailable. This was also the case with the limiter diode which was modeled as an equivalent circuit based on the description given in the datasheet. Also in ADS the FET model was a user defined model again based on the parameters mentioned in the data sheet but the MWO model was a vendor model. It can be seen that the MWO results are a closer match to measured results.

#### 4.2.4 Input and output impedance:

The setup used for gain and bandwidth measurements can be used for  $S_{11}$  and  $S_{22}$  measurements. The  $S_{11}$  can be then converted to  $Z_{11}$  using  $Z_{11} = Z_0(1 + S_{11})/(1 - S_{11})$  to find out the input impedance. The graphs plotted below show the input impedance of the amplifier.

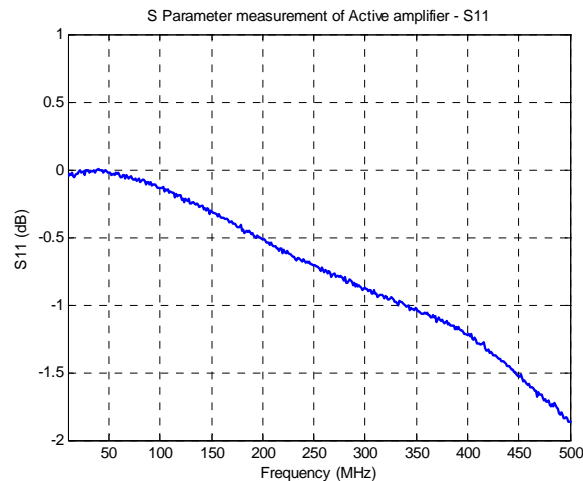


Figure 4.9:  $S_{11}$  measured from Network Analyzer

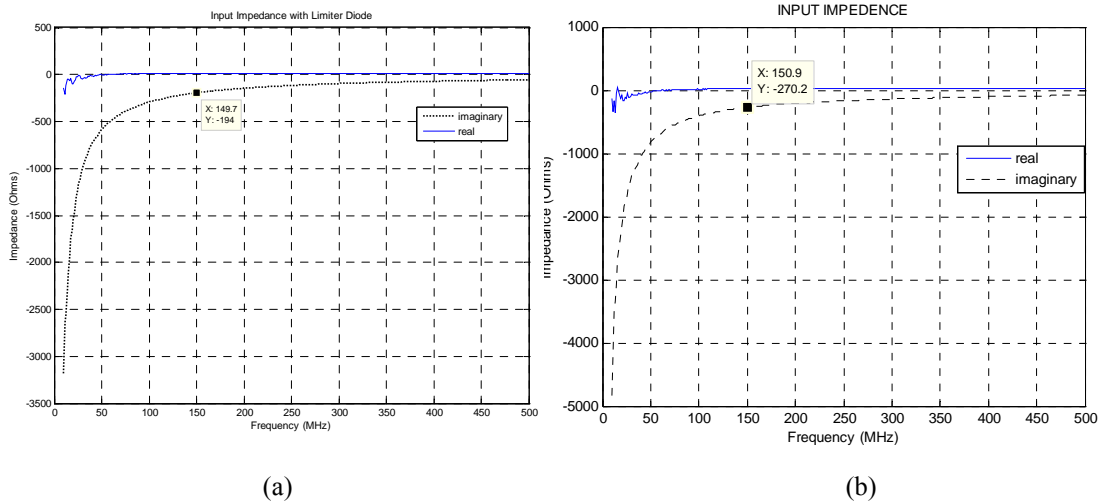


Figure 4.10: (a) Input impedance with limiter diode (b) Input impedance without limiter diode

### Analysis

As seen from figure 4.9 the input impedance is high, yielding an  $S_{11}$  value ranging from 0 to -2 dB as expected. The plots shown in figure 4.10 (a) show the input impedance calculated from the measured  $S_{11}$ . As predicted, the measured results show predominantly capacitive input impedance and the capacitance is nearly 5.5 pF with the limiter diode. This was higher than what was predicted in the simulations. The same test was repeated without the limiter diode and figure 4.10(b) shows the input impedance of the circuit without the limiter diode. The capacitance corresponding to this impedance was 3.92 pF thus showing a difference of 1.58 pF. It can be thus concluded that the limiter diode adds 1.58 pF of capacitance as opposed to 0.8 pF as mentioned in the datasheet. Also the board itself without any populated components was tested and was found to have nearly 2 pF of capacitance. Thus increasing the overall input capacitance of the amplifier, however this was less than the capacitance of the antenna which is 6.4 pF, thus not affecting the overall bandwidth of the active

antenna. The limiter diode can be removed in order to gain bandwidth, but this decrease in input capacitance was found to make the amplifier oscillate in some but not all of the prototypes hence that possibility was ruled out.

Output impedance of the amplifier can be calculated from the  $S_{22}$  parameter measured using the network analyzer. Figure 4.11 shows the  $S_{22}$  plotted versus frequency and it can be seen that it is less than -10 dB over the entire bandwidth. This translates to the return loss of the active antenna, which indicates a good match to a 50-ohm system.

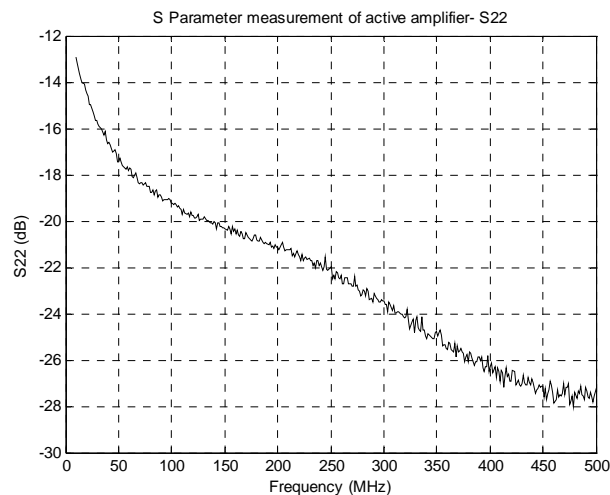
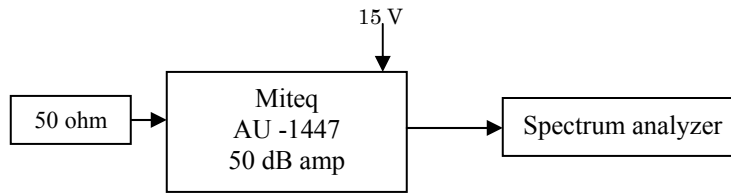


Figure: 4.11  $S_{22}$  measured in network analyzer.

#### 4.2.5 Noise Figure:

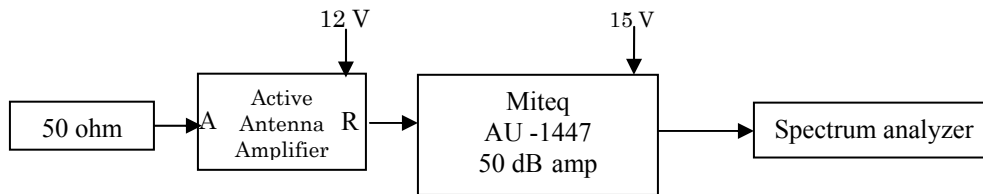
Noise figure measurement of the amplifier was done by observing the increase in noise floor when active amplifier is connected to the spectrum analyzer. However the noise figure of the spectrum analyzer is generally high and the rise in noise floor

cannot be seen. Hence it is necessary that the noise power offered by the active antenna amplifier be amplified above the noise floor of the spectrum analyzer to correctly estimate the noise figure. This can be done using a 50 dB, low noise amplifier that has sufficient gain to overcome the noise level of the spectrum analyzer. The test setups are shown in figures 4.12 (a) and 4.12 (b).



*Setup: left to right: 50 ohm load → Miteq amplifier (AU-1447) → Mini-bend cable → DC block (MCL 15542) → SA (Agilent E4407B). Also AU-1447 is connected to 15 V dc supply.*

Figure 4.12 (a): Setup 1: Noise floor measurement with 50-dB amplifier



*Setup: left to right: 50 ohm load → Antenna port of active antenna amplifier → RF port of active antenna amplifier → input of Miteq amplifier (AU-1447) → Mini-bend cable → DC block (MCL 15542) → SA (Agilent E4407B). Also AU-1447 is connected to 15 V dc supply and active antenna amplifier to 12 V supply*

Figure 4.12 (b): Setup 2: Noise floor measurement with the active antenna amplifier

The 50-dB amplifier used worked from 20 MHz to 200 MHz and has a noise figure of 1.2 dB. Results obtained from these setups are shown in figure 4.13.

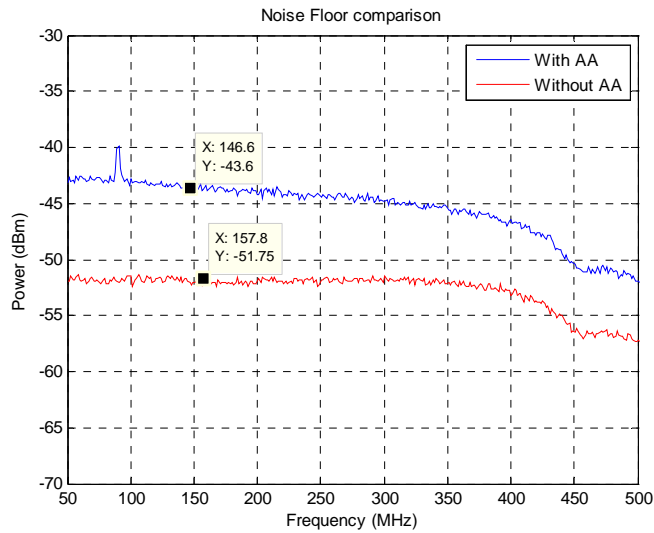


Figure 4.13: Noise floor measurement with setup 1 and setup 2.

Analysis:

It can be seen that the noise floor is raised after the addition of the active antenna amplifier. Treating this setup as a cascaded system, the noise figure of the active antenna amplifier is the only unknown quantity and can be found out using the following steps:

1. Divide noise floor level measured by the gains of both amplifiers to find out just noise power
2. Convert noise power to noise figure using  $P = k \times T \times B \times F$  where  $k$  is Boltzmann's constant,  $T$  is room temperature,  $B$  is the noise bandwidth used and  $F$  is the noise figure.

3. Find noise figure of the active antenna amplifier using

$$F = 1 + F_1 + \frac{F_2}{G_1} + \frac{F_3}{G_1 G_2}$$

where the first stage is the amplifier, the second stage

is the active antenna amplifier and the third is the spectrum analyzer.

The resultant noise figure is given in the figure 4.14

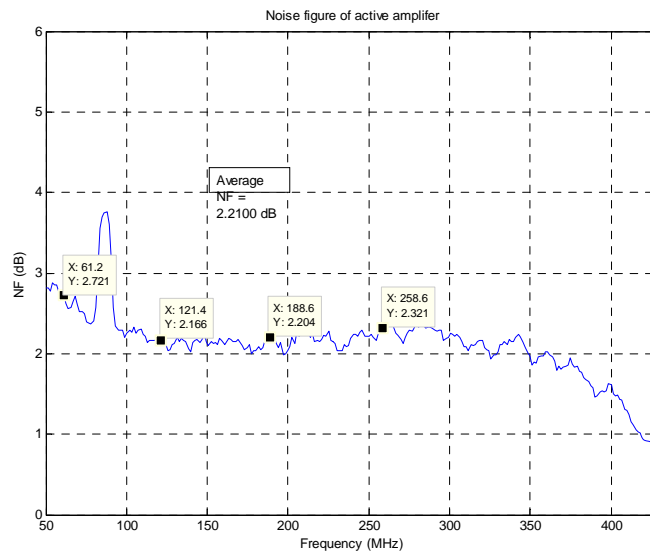


Figure 4.14 Noise figure of active antenna amplifier

Although the noise figure of the amplifier is less than 3 dB as per the requirements, it is not as low as 0.8 dB as predicted by the simulation tools. This again can be attributed to the inaccuracy in the models of components used.

#### 4.2.6 Saturation and Minimum Detectable Signal (MDS):

Saturation tests were done by inputting a signal of known level from function generator into the active antenna amplifier and testing the output signal on the spectrum analyzer. As the signal power increases at a certain level harmonics of the fundamental signal appear and the point the harmonic level is less than 20 dB below the fundamental, the noise floor also increases, thus indicating saturation point. On the other hand, when the signal level is decreased the point where the signal is submerged in the noise floor and is not retrievable by reducing the resolution bandwidth of the spectrum analyzer or by averaging, then this signal level is considered the output signal level. This test was repeated by coupling a jammer signal of high amplitude along with a desired signal whose amplitude can be varied, to find out the minimum detectable signal and saturation levels.

The setups for the saturation test is shown in figures 4.15 and 4.16

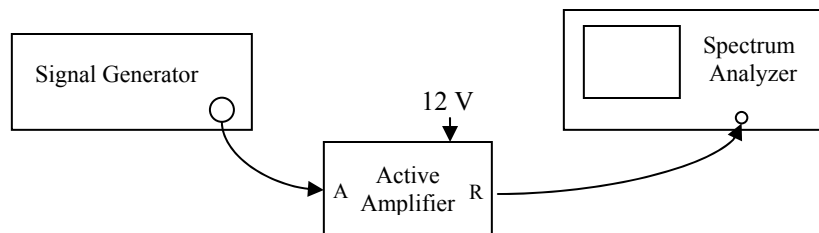


Figure 4.15: Setup 1 - MDS and Saturation without jammer signal

*Set up: (left to right) : Agilent 8648 D Signal Generator (9 kHz – 4000 MHz) → Minibend cable → active antenna amplifier Antenna Port → active antenna amplifier RF output port → Spectrum Analyzer (HP 8592L 9 kHz to 22 GHz).*

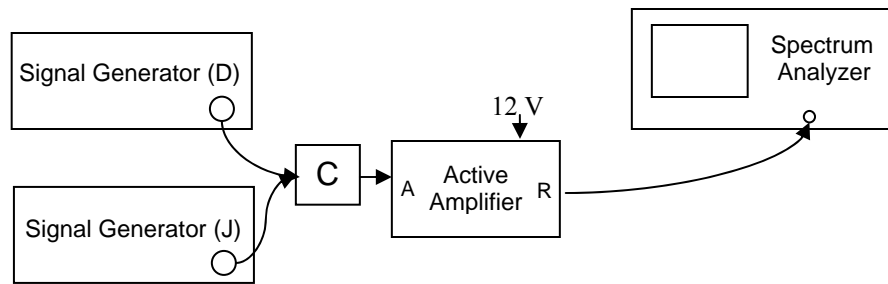


Figure 4.16: Setup 2 - MDS and Saturation with jammer signal

*Set up: (left to right): Agilent 8648 D Signal Generator (9 kHz – 4000 MHz) → Macom 3 dB coupler (20 – 200MHz) port A → Fluke Function generator → Macom 3 dB coupler (20 – 200MHz) port A → Macom 3 dB coupler port C → Minibend cable → active antenna amplifier Antenna Port → active antenna amplifier RF output port → Spectrum Analyzer (HP 8592L 9 kHz to 22 GHz).*

## Results

The results of setup 1 and setup 2 are shown in tables 4.2(a),(b) and 4.3(a),(b)

Table: 4.2(a) Minimum detectable signal for setup without jammer.

Reading Number	Input Frequency (MHz)	Input Power (dBm)	Output Power (dBm)	Harmonics Seen		Res.BW (kHz)	Video Avg.
				Frequency (MHz)	Level (dBm)		
1	125	-40	-32.9	250	-77	300	No
2	125	-60	-52.78	250	-80	300	No
3	125	-80	-72.5	-	-	300	No
4	125	-100	-92.1	-	-	30	No
5	125	-115	-100	-	-	1	2
6	125	-118	-110	-	-	1	2
7	125	-119	-	125.3 126.0	-100 -100.9	1	2

Table 4.2 (b): Saturation for setup without jammer

Reading Number	Input Frequency (MHz)	Input Power (dBm)	Output Power (dBm)	Harmonics Seen		Res.BW (MHz)	Video Avg.
				Frequency (MHz)	Level (dBm)		
1	125	-30	-22.9	250	-60		No
2	125	-25	-17.96	250	-60	1	No
3	125	-20	-13.1	250	-51	1	No
4	125	-15	-8.1	250	-35	3	No
				200	-78		
				115	-76		
5	125	-10	-6.1	250	-22	3	No
				200	-73		
				115	-70		

Analysis:

It can be thus seen from the above results that the minimum detectable signal is -118 dBm where the noise floor of the spectrum analyzer was at -116 dB with a 1-kHz resolution bandwidth. For a signal level of -20 dBm the gain starts to decrease and the harmonic level to increase, but the point where the harmonics are 20-dB beneath the fundamental is at -10 dBm of input power. Thus the dynamic range for the amplifier is 103 dB.

Setup 2 results: Dynamic range with jammer:

Jammer signal settings: Amplitude: -20 dBm

Frequency: 100 MHz.

Desired signal settings: Amplitude: variable

Frequency: 150 MHz.

Table 4.3(a) Minimum Detectable Signal in presence of a strong jammer

Reading Number	Desired signal's input power (dBm)	Output power (dBm)		Harmonics seen		Resolution BW	Video Avg.
		J	D	Frequency (MHz)	Level (dBm)		
1	-60	-16.4	-55.	200 250 300	-40 -68 -51	3 MHz	No
2	-80	-16.48	-77.8	92.7 200 300	-74 -41 -52	100 kHz	No
3	-90	-16.48	-87.90	92 200 300	-75 -41 -52	3 kHz	No
4	-100	-17	-93	92.3 200 300	-72 -40 -53	3 kHz	No
5	-112	-17	-104	200 300	-40 -51	1 kHz	2

Table 4.3(b) Saturation in presence of a strong jammer

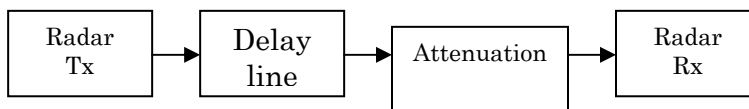
Reading Number	Desired signal's input power (dBm)	Output power (dBm)		Harmonics seen		Resolution BW	Video Avg.
		J	D	Frequency (MHz)	Level (dBm)		
1	-40	-16	-36.2	120 200 250 300	-60 -42 -53 -51	3 MHz	No
2	-30	-17.1	-26.2	200 250 300	-39.8 -44.3 -49.5	3 MHz	No
3	-20	-17.1	-17.4	200 250 300	-36 -34 -40	3 MHz	No
4	-15	-17.9	-13.5	200 250 300	-35 -29 -31	1 MHz	No

Analysis:

It was also seen that the noise floor with the presence of a strong jammer signal was -110 dBm at 1 kHz of resolution bandwidth. This shows that there is a significant increase in noise floor and thus a reduction in dynamic range is observed. Minimum detectable signal in presence of a strong jammer is -112 dBm and saturation occurs at -20 dBm hence the dynamic range is 92 dB.

These tests were done using a spectrum analyzer and sinusoidal signals, however in the actual application, the active antenna is to be used with a radar system (Multi Channel Radar Depth Sounder) that has its own noise floor determined by the electronics of the system and a chirp signal as the input unlike the sinusoid used in the previous setup. In order to find out how the amplifier affects the signal to noise ratio of the radar system , the saturation and minimum detectable signal tests were done by using setups shown in figure 4.17 (a) and (b) .

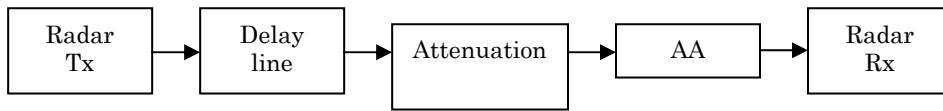
Setup without active antenna



*Setup: left to right: Radar transmitter → delay line → attenuator (50 dB) → power splitter (1:8) → attenuator (10 dB) on each channel → Radar LNAs.*

(a)

### Setup with active antenna



*Setup: left to right: Radar transmitter → delay line → attenuator (50 dB) → power splitter (1:8) → attenuator (10 dB) on each channel → active antenna amplifier on channel 5 with external attenuation → Radar LNAs.*

(b)

Figure: 4.17 (a) Radar test setup without active antenna (b) Radar test setup with active antenna.

### Setup details:

Radar transmitter is connected to a loop back signal generator that provides a -10 dBm signal and the delay line with the attenuator is to create a similar environment as seen in the field, i.e. delay accounts for the travel time of the signal from the radar to the ice sheet and back to the radar and the attenuator accounts for the signal attenuation by ice. Channels 1 to 5 present in the receiver each have an LNA to amplify the received signal, of which channel 5 had been connected to active antenna amplifier for comparison of SNR with the other channels that are similar. The minimum detectable signal test was done by adding attenuators to the 60 dB attenuator in series. Saturation test was not done with just the desired signal as the input signal was constantly generated at -10 dBm amplitude and attenuation of 60 dB was fixed.

In the Jammer test, the jammer was coupled in with the desired signal through one channel only and the SNR for increasing value of jammer signal was recorded after

which the setup was added with the active antenna amplifier and the test was repeated to find the SNR versus jammer signal. The results of which are plotted below.

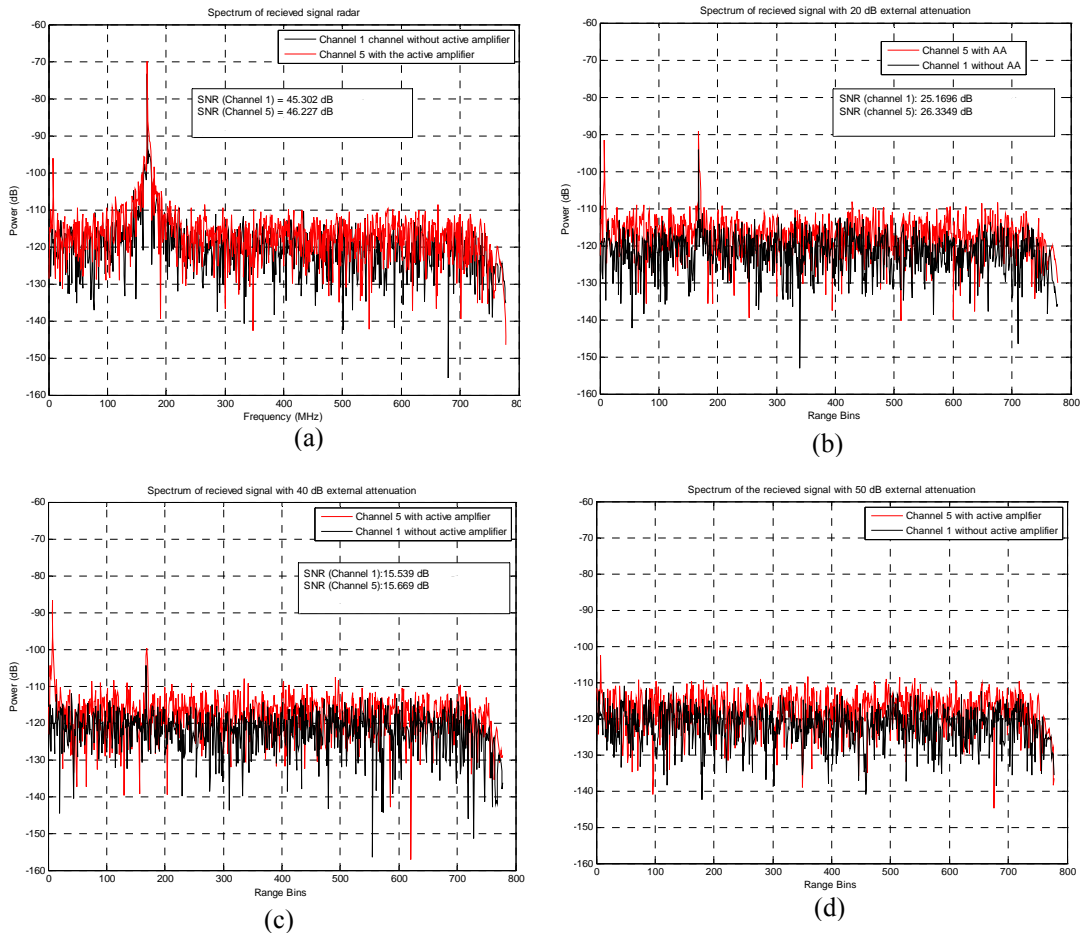


Figure 4.18: Radar setup for MDS (a) with 60 dB attenuation, (b) with 80 dB attenuation, (c) with 100 dB attenuation, (d) with 110 dB attenuation

*Note : The y-axis of the chart is plotted in Range bins, but is equivalent to number of samples per 4 m of depth of ice sheet.*

It can be inferred from the above plots the minimum detectable signal is between -110 and -120 dBm. The SNR plots show that the active antenna amplifier has 1 dB greater SNR than the Radar SNR.

With Jammer signal setup-1 details

Jammer signal at 100 MHz and variable amplitude

Desired signal 150 MHz (loop back signal) with 60 dB attenuation.

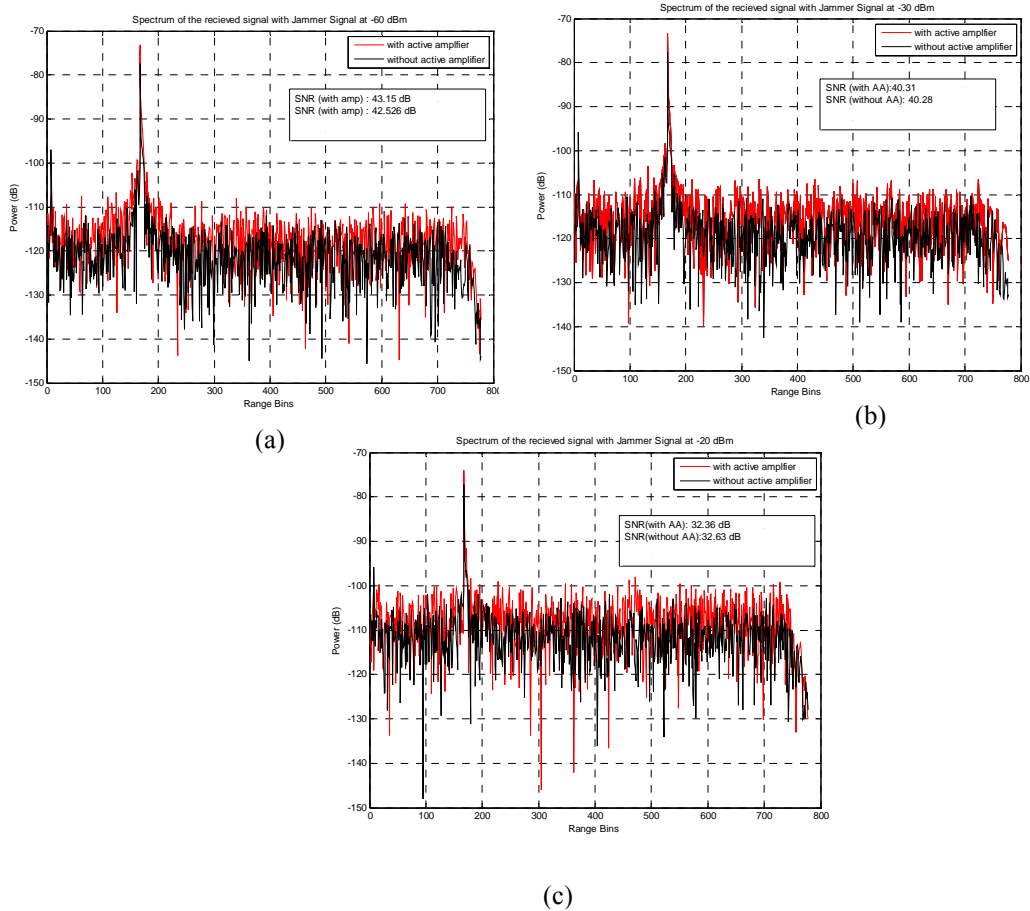


Figure 4.19: Radar setup-1 with jammer signal (a) jammer at -60 dB (b) jammer at -30 dBm (c) jammer at -20 dBm.

With Jammer signal setup-2 details

Jammer signal at 100 MHz and variable amplitude

Desired signal 150 MHz (loop back signal) with 80 dB attenuation.

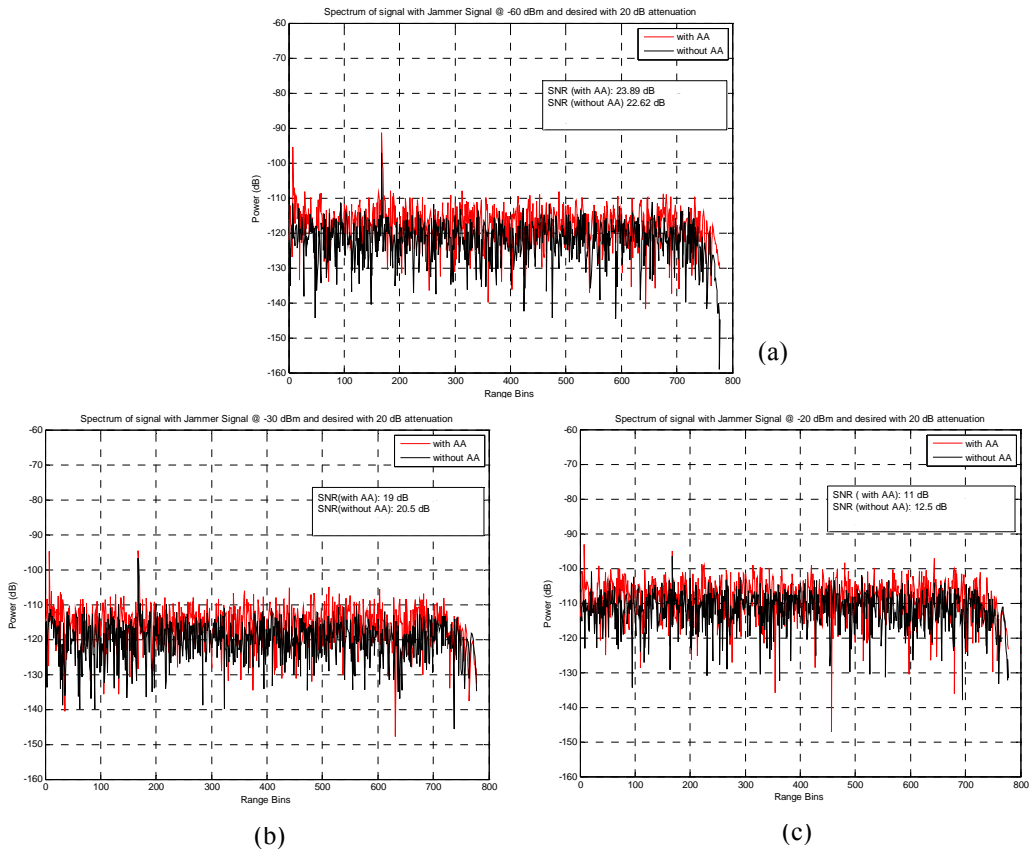


Figure 4.20: Radar setup-2 with jammer signal (a) jammer at -60 dB (b) jammer at -30 dBm (c) jammer at -20 dBm.

#### Analysis:

With just the desired signal, the signal-to-noise ratio of the channel with the active antenna amplifier was observed to be 1 dB better than the radar for strong signals but with a decrease in signal amplitude the SNR decreases and becomes equal to radar SNR, this can be seen from figure 4.21(a). It was observed that the noise floor increased as the jammer signal level was increased and at -20 dBm, both the setups showed a considerable increase in noise floor, thus degrading the SNR but this effect was not limited to the active antenna amplifier alone, the SNR of the radar

LNA also was degraded even though the jammer is an out of band signal for the radar that operates from 140 MHz to 160 MHz. However with strong jammer and weak signal the SNR degradation was greater with the active antenna amplifier. But the SNR of the active amplifier was within 2 dB difference of the radar SNR even in the strong jammer – weak signal scenario as is shown in the figures 4.21 (b) and (c)

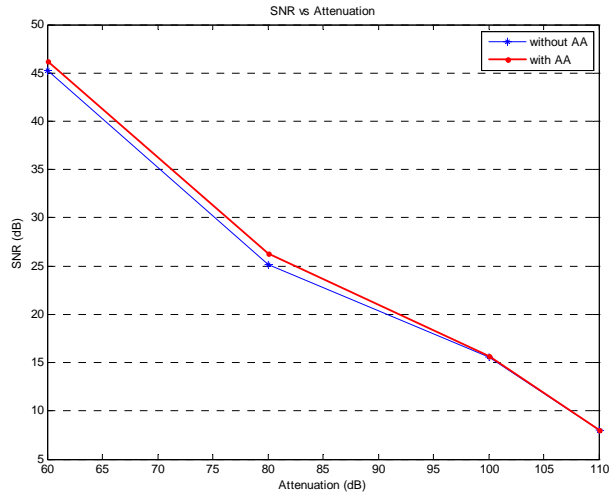
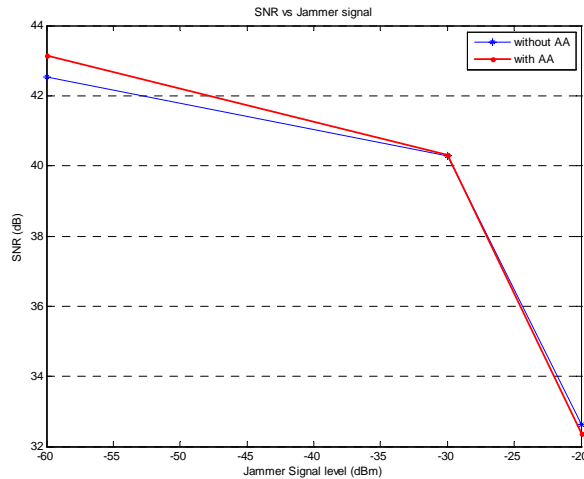
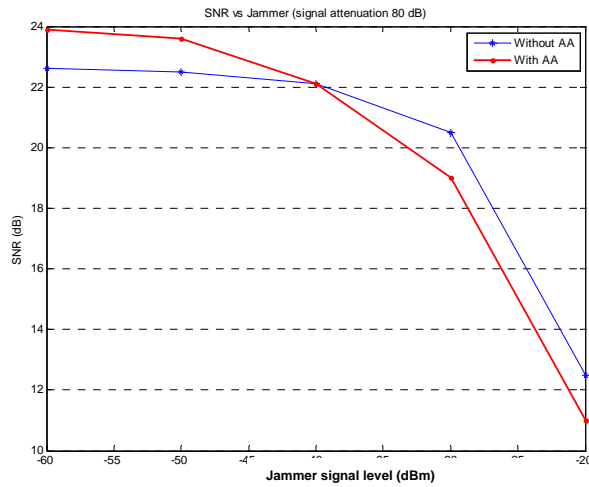


Figure 4.21(a) SNR versus attenuation comparison for setup without jammer



(b)



(c)

Figure 4.21 (b) SNR with desired signal with 60 dB attenuation (c) SNR with desired signal with 80 dB attenuation

From the above test it can be concluded that the SNR of the radar is not degraded with the addition of the active antenna amplifier, in fact with higher values of desired signal and lower values of jammer signal the SNR is better than the radar SNR. But even in presence of jammer the sensitivity of the radar is not affected much. Although this test can be repeated with antenna connected to the amplifier, the presence of other signals and mutipath etc. limit the accuracy of measurement. But the monopole contribution to the noise figure of active antenna is very low as electronic noise from the amplifier is dominant in the UHF/VHF frequencies.

#### 4.2.7 Free – Space Experiment:

The saturation test concludes the characterization of the amplifier alone. The next test involves combining the antenna and the amplifier together and testing the overall gain

of the active antenna. Active antenna designed in this thesis is a receive-only antenna hence the gain the active antenna can be found by comparing the received signal spectrum with a known reference antenna. The test not only gives us the gain but also provides us a yard stick to compare the efficiency of the active antenna with a passive antenna.

The free space experiment as the name suggests is done in an environment devoid of any reflective media. There are two steps involved in this experiment the first is to transmit a known signal through the transmit antenna and then receive it through a calibrated known antenna. The next step is to transmit through the same antenna, the same level of signal and receive using the active antenna while keeping all the cables, distances the same. By comparing the level of the received signal of the active antenna with the known reference antenna the gain of the active antenna can be found.

There are two ways to doing this experiment; the first method involves using a network analyzer. The network analyzer passes a known level of signal through the transmit antenna connected to its port 1 and the receive antenna senses this signal. The receive antenna should however be placed in the far field of the transmit antenna, which is  $R > 2d/\lambda$  where  $d$  is the largest dimension of the two antennas. The receive antenna is connected to port 2 and  $S_{21}$  is the measured. The parameter  $S_{21}$  indicates the ratio of power received to power transmitted. Figure 4.22 (a) shows the setup for

free space experiment with reference antenna, and figure 4.22 (b) shows the setup for active antenna. Once the  $S_{21}$  is recorded the gain of the antenna can be found using the Friss' transmission formula.

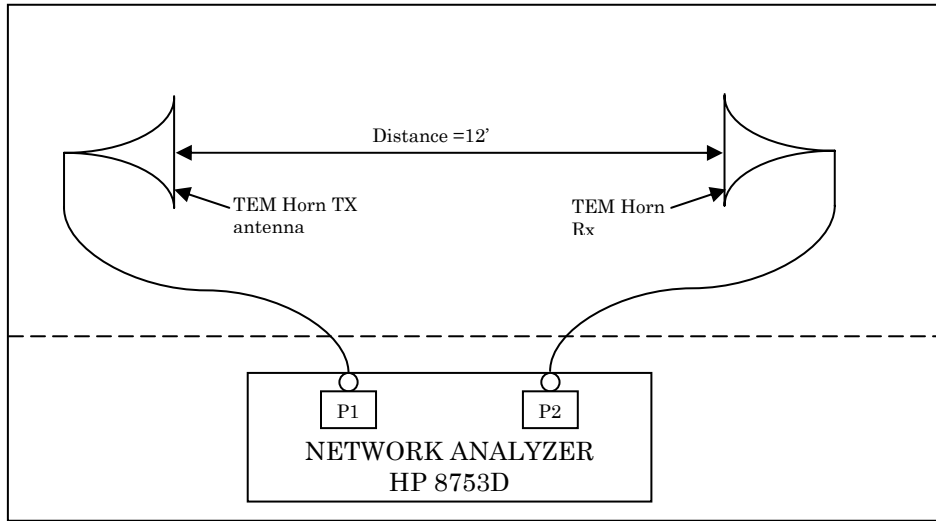


Figure 4.23 (a): Free space experiment setup for reference antenna

Setup: NA port 1 → TEM horn antenna → 11' Andrew Cinta cable → TEM horn Tx antenna → TEM horn Rx antenna → 11' Andrew cinta cable → 180 TC astrolabe cable → bias-tee w/o DC → Port 2 of NA.

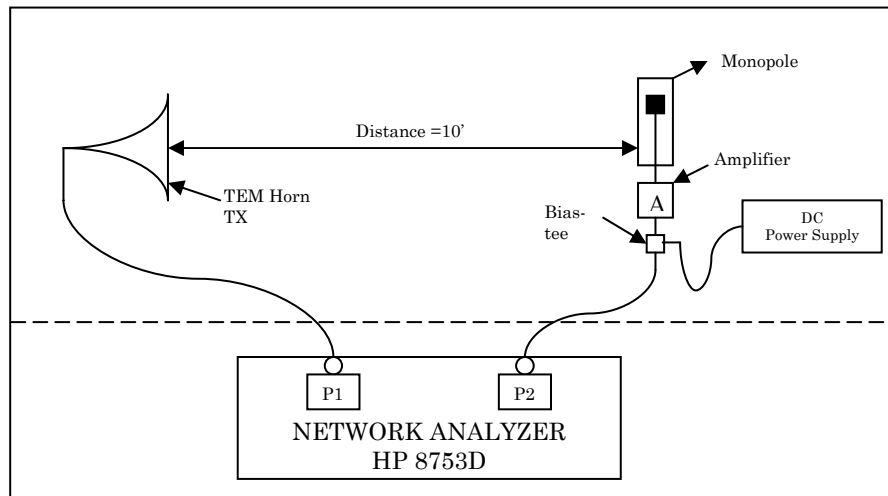


Figure 4.23 (b): Setup for free space experiment with active antenna

Setup: NA port 1 → TEM horn antenna → 11' Andrew Cinta cable → TEM horn Tx antenna → active antenna → 11' Andrew cinta cable → 180 TC astrolabe cable → bias-tee with DC → Port 2 of NA.

Setup details:

The antennas were mounted on plastic shelves that were 5.5 feet in height and the separation between the antennas was maintained at 12 feet. Both these settings allow for the ground reflected path arrival to be resolved from the direct line of sight path. For the test with the active antenna different monopoles were testing with the active antenna amplifier. The first being the 5.2" monopole given in figure 4.4 (b) followed by a smaller length monopole with a smaller capacitive patch and a larger monopole 9" with 1" x 1" capacitive patch. The results of which, in comparison with the horn gain are shown in figure 4.23.

Processing method:

As mentioned before the free space experiment is generally done in an environment free of reflections, however it is not always possible to obtain such environments for experimentation hence in order to resolve multipath, IFFT of the  $S_{21}$  is taken and using time domain filtering the reflected paths are removed, this process is known as time gating. The line of sight signal arrival time can be calculated the free space propagation velocity and distance of separation. Once this information is obtained, the first strong peak in the IFFT of the  $S_{21}$  is the line of sight signal and should match closely to the value obtained by calculation. The filter window is set such that only the line of sight signal is taken and the rest suppressed. After the time gating is completed the Friss transmission formula is used to find the gain of the antenna. If both transmit and receive antennas are identical then the formula used is

$G = 10 * \log_{10} \left( \sqrt{\left( \frac{(4\pi R)^2 \times |S_{21}|^2}{\lambda^2} \right)} \right)$  where R is the separation between the two

antennas. Else the formula  $G = 10 * \log_{10} \left( \frac{(4\pi R)^2 \times |S_{21}|^2}{\lambda^2 \times G_{ref}} \right)$  is used to find out the

gain of the uncalibrated antenna.

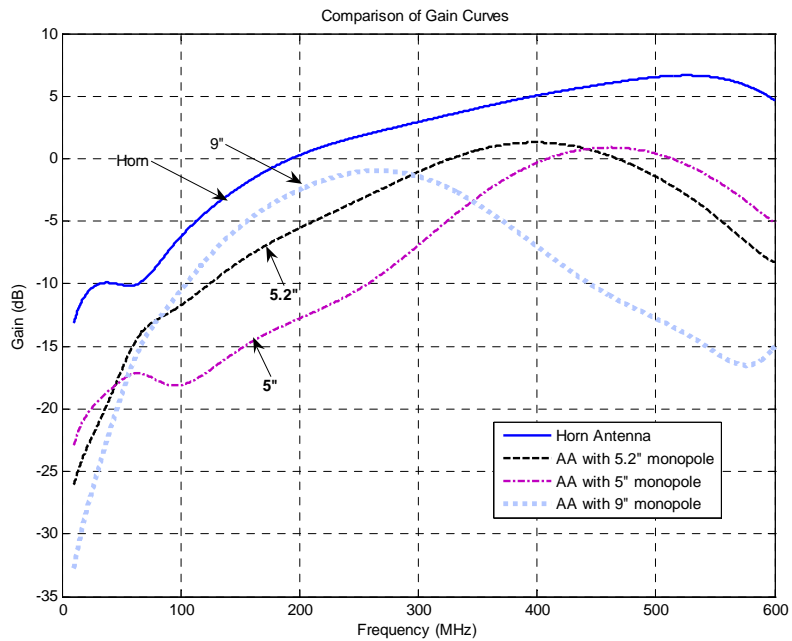


Figure 4.24: Gain curves comparison of active antennas with different monopoles with the horn antenna

Analysis:

It can be seen from figure that the gain of the horn antenna more than the gain of the active antenna. At 300 MHz horn has a gain of horn is 0 dB and that of 9" active antenna is -3 dB and 5.2" active antenna is -5 dB. However this does not match the readings with the amplifier alone that showed 7 dB of electronic gain and since the

antenna element of the active antenna is equivalent to Hertzian dipole, the antenna gain should be 1.7 dB and total gain of 8 dB. Possible reasons for this could be the following

1. The monopole does not have the predicted gain, due to its unmatched load.
2. The active antenna amplifier is getting saturated in presence of jammer signals present in the surroundings. For example KANU signal that measures -17 dBm can be considered as jammer and the amplifier showed a decrease in gain in presence of a jammer of as high amplitude as -20 dB when tested in the lab hence in presence of KANU the gain may be less than the actual gain of the active antenna.
3. There might be other irresolvable multipath or spectral content is lost while time-gating.

However something that can be inferred from the above experiment is the bandwidth. As seen from figure 4.23 the bandwidth of the 9" active antenna is lesser than the 5.2" active antenna as the 9" one no longer looks electrically small beyond 150 MHz hence the roll off is much quicker, where as the 5.2" is electrically small at 300 MHz and is nearly also half-wavelength at 600 MHz, hence has a broadband response.

In order to resolve some of the uncertainties encountered during the free space experiment using network analyzer, the same experiment was done indoors in relatively open space with the following setup.

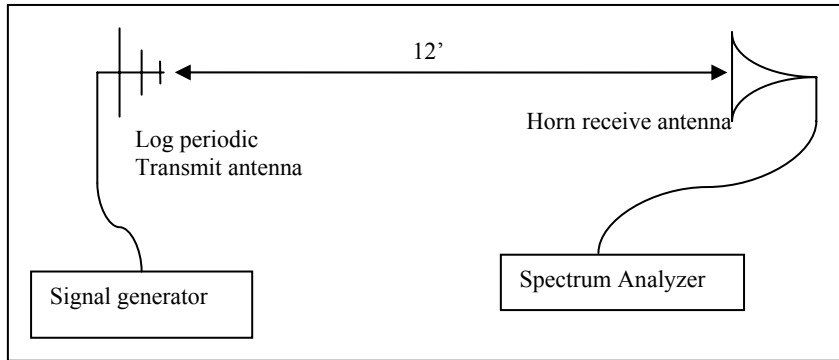


Figure 4.25(a): Free space experiment with spectrum analyzer (reference)

*Setup: left to right : Agilent signal generator → Astrolab 72 TC cable → log periodic antenna → Horn antenna → 180 TC cable → bias tee w/o DC → 120 TC cable → Spectrum analyzer (Agilent).*

A known signal level was passed through the log periodic antenna to the horn antenna place at a 12 feet distance, with no reflective objects within 2 m radius and both antennas were mounted at a height of 5.5 feet. The spectrum analyzer plot was captured and the test was repeated with the active receive antenna in place of the horn antenna. The setup for which is given by figure 4.23

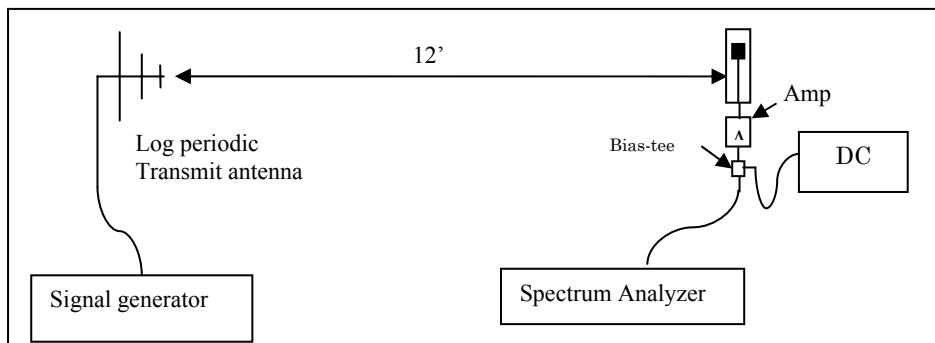


Figure 4.25(b): Free space experiment with spectrum analyzer (active antenna).

*Setup: left to right : Agilent signal generator → Astrolab 72 TC cable → log periodic antenna → Active antenna with 5.2" monopole → 180 TC cable → bias tee with DC → 120 TC cable → Spectrum analyzer (Agilent).*

A signal of -30 dBm at 150 MHz frequency was sent through the transmit antenna – the log periodic to the horn antenna which is the reference antenna for the experiment the signal received is recorded by the network analyzer. Along with the desired signal, the KANU signal and KJHK signal both of which are local radio channels are also received by the horn antenna as seen in figure 4.26. The horn antenna was then replaced by the active antenna with the same transmit signal and same distance and setup, the received signal spectrum was recorded.

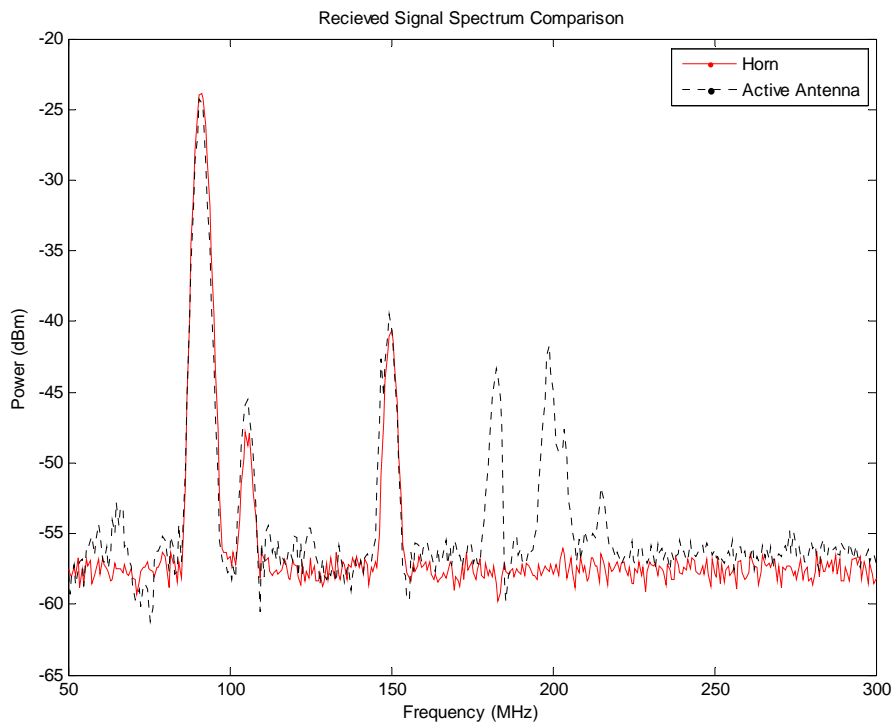


Figure 4.26: Received signal spectrum by horn antenna and active antenna

Analysis:

The above plot shows that the signal level received by the active antenna is a much as the horn antenna as the received signal spectrum almost overlaps the horn , in fact the

active antenna received signal level is more than the horn received signal level at 105 MHz and 150 MHz by a dB. Also the KANU signal at 91.5 MHz is at -24 dB which is lesser than what was offered outdoors. Hence there is no saturation of the amplifier. Looking at the actual gain curves of the horn antenna, at 150 MHz horn has a gain of -2 dB and active antenna according to figure 4.24 is 1 dB higher, so gain of active antenna can be inferred as -1 dB and in comparison with the horn antenna so the active antenna is as efficient as the horn. However this was done indoors, so there might be multipath, hence for an accurate measure of gain and efficiency the active antenna must be tested in truly reflection free environment like the anechoic chamber as was done with version 2 (*refer to the appendix*).

Although the measurement results don't match the simulated results, the active antenna characteristics were found to match the requirements of the radar system.

### **5.1 Conclusion**

A small, wideband antenna was designed for radar applications to be integrated with a lightweight, small aircraft like a UAV, using the concept of active antennas. The antenna can also be used in applications where there exists a space constraint. The active antenna characteristics are listed below:

1. Operating frequency range: 19 MHz to 455 MHz
2. Noise figure: 2.2 dB average without antenna noise.
3. Good stability all through the spectrum
4. Dynamic Range: 103 dBm without jammer signal  
97 dBm with a jammer signal power of -20 dBm.
5. Good amplifier performance, comparable to that of the MCRDS radar without jammer as well as with a -20 dBm jammer and weak desired signal, the signal-to-noise ratio is only 2 dB lesser than that of the MCRDS radar.
6. Good electronic gain of 7.75 dB and overall gain is comparable to that of the horn antenna.

The lab measurements of the active antenna show that it operates well within the range of the radar system that works from 100 MHz to 300 MHz and has almost the

same gain performance as the horn antenna while being 1/3 the height and almost negligible depth. This makes the active antenna a good solution for both the size problems faced by the UAV designers and the bandwidth issues faced by the radar designers.

However the gain measurements are not very conclusive, in terms of the efficiency, as the free space readings are inconsistent. If the antenna is tested in an anechoic chamber the actual efficiency as compared to the horn can be measured. If the efficiency of the active antenna is found to be less than that of the passive antenna then the transmit power required to sound the depth of the ice sheets needs to be increased as the reception is not optimal. This may pose a problem as power is also a premium on the UAV. If the free-space test results with the spectrum analyzer are taken to be close to reality then the antenna is 100% efficient (in comparison to the horn used regularly in field missions) hence there will not be a need for any increase in transmit power. If the gain of the antenna is less than the passive antenna then an additional low noise amplifier can be added to raise the gain and when added in series with the active antenna the noise figure is not raised as the gain of the active antenna amplifier compensates for it.

## ***5.2 Future Work***

As mentioned before, if the free space gain tests are done in an anechoic chamber which is reflection free, the correct estimates of gain can be obtained; also the some of the other test done only on the active antenna amplifier can be repeated for the active antenna using the anechoic chamber. For example the noise figure test for the active antenna amplifier was done using a  $50 \Omega$  termination on the input end as connecting an antenna would make it receive signals and no longer have RF quiet area. The same experiment if done in the anechoic chamber, which is a RF quiet area the noise figure of the amplifier and the antenna together, may be found. The same with the radar signal-to-noise ratio, the transmitter and receiver can be set up with reference antennas and then the receive end may be replaced with the active antenna to conclusive measure the effect of active antennas on the SNR of the radar. However as mentioned before the noise contributed by the monopole is very small compared to the amplifier and in any case the overall noise figure will not rise above 3 dB.

The next stage of development of the active antennas would be to increase their directivity and gain. This can be done by designing an array of active antennas. Also advanced digital signal processing like adaptive beam forming can also be implemented for issues related to clutter rejection to make the active antenna more efficient.

Recent studies have shown that, a new class of GaAs FETs, known as the Schottky GaAs FETs offer more stability at lower frequencies than the now available FETs; these devices were used in a commercially available active antenna called the DX500. But the Schottky GaAs FETs are not yet available for commercial use hence were not explored while designing the active antenna presented in this thesis, but the device is worth exploring for enhancing the performance of the active antenna.

## *References*

---

- [1] Balanis, C. "Antenna Theory – Analysis and Design", 2<sup>nd</sup> Edition, Wiley publications, 1996
  
- [2] Radio research laboratories, "VHF techniques volume 1", *Harvard University Publication*, 1947.
  
- [3] Sainati, R.A.; Fessenden, D.E.; "Performance of an electrically small antenna amplifier circuit," *IEEE Transactions on Aerospace and Electronic Systems*, 17(1), pp. 88-92, 1981.
  
- [4] Meinke, H.H.; Landstorfer, F.M.; "Noise and bandwidth limitations with transistorized antennas," *IEEE International Antenna and Propagation Symposium*, pp. 245-246, 1968.
  
- [5] Wong, W.C.; "Signal and noise analysis of a loop-monopole active antenna," *IEEE Transactions on Antennas and Propagation*, pp. 547-580, July 1974.
  
- [6] Nordholt, E.H.; Van Willigen, D.; "A new approach to active antenna design," *IEEE Transactions on Antennas and Propagation*, AP-28(6), pp. 904-910, November 1980.
  
- [7] Wu, X.D.; Chang, K.; "Integrated active slot dipole antenna amplifier," *Microwave and Optical Technology Letters*, 6(15), pp. 856-857. 1993.

- [8] An, H; Nauwelaers, B; Van de Capelle, A.; "Noise figure measurement of receiving active microstrip antennas," *Electronics Letters*, 29(18), pp. 1594-1596, 1993
- [9] Panton, W.R.; Beyer, J.B.; "The noise performance of an active, linear antenna array for reception," *IEEE MTT-S Digest*, pp. 317-320, 1994.
- [10] Duerr, W; "A low-noise active receiving antenna using a SiGe HBT," *IEEE Microwave and Guided Wave Letters*, 7(3), pp. 63-65, 1997
- [11] Skahill, G.; Rudish, R.M.; Piero, J.; "Electrically small, efficient, wide-band, low-noise antenna elements," *Proceedings of the 1998 Antenna Applications Symposium*; Univ. of Massachusetts, pp. 214-231, AFRL-SN-RS-TR-1999-86, 1999
- [12] Fredrick, JD; Itoh, T; "Recent developments in RF front ends based upon active antenna concepts," *TELSIKS 2001*, pp. 3-9, 2001
- [13] Al-Khateeb, B; Rabinovich, V; Oakley, B; "An active receiving antenna for short-range wireless communication," *Microwave and Optical Technology Letters*, 43(4), pp. 293-297, 2004.
- [14] Gonzales, V; Rodriguez, J.M.; Gonzalez, J.E.; Rueda, C.; Pascual, C.M.; ; "Design methodology for high efficiency active radiators," *Microwave Journal*, pp. 168-174, September 2001.
- [15] Segovia-Vargas, D; Gonzalez-Posadas, V; Castro-Galan, D; Vazquez, JL; Rojo, E, "Broad band active receiving microstrip antenna for DCS-UMTS," *IEEE Antennas and Propagation Society Symposium*, pp. 3935-3938, 2004.

- [16] Tan, G.H.; Rohner, C.; "The low frequency array active antenna system," *Proc. SPIE - Radio Telescopes*; Vol. 4015, Harvey R. Butcher; Ed., pp. 446-457, July 2000.
- [17] Grabherr, W; Menzel, W; "Broadband, low-noise active receiving microstrip antenna," *Proceedings of the 24th European Microwave Conference*, Part 2, pp. 1785-1790, 1994.
- [18] Agilent Advanced Design system user manual, noise analysis, <http://eesof.tm.agilent.com/docs/adsd2001/cktsim/index.html>, 2006
- [19] Mozaffer, S; "Multiband multistatic synthetic aperture radar for measuring ice sheet basal conditions", *Masters thesis*, Chapter 1, 2005.
- [20] Center for Remote Sensing of Ice Sheets (CReSIS) , official website [www.cresis.ku.edu](http://www.cresis.ku.edu) .
- [21] Allen, C. "Overview of Technology at CReSIS", [http://www.cresis.ku.edu/education/tutorial\\_2006/STC\\_Technology-Overview.pdf](http://www.cresis.ku.edu/education/tutorial_2006/STC_Technology-Overview.pdf)

Version 2 free space description and results:

Version 2 had JFET SST4416 instead of NE34018 and an op-amp stage as a voltage follower the schematic of which is given below

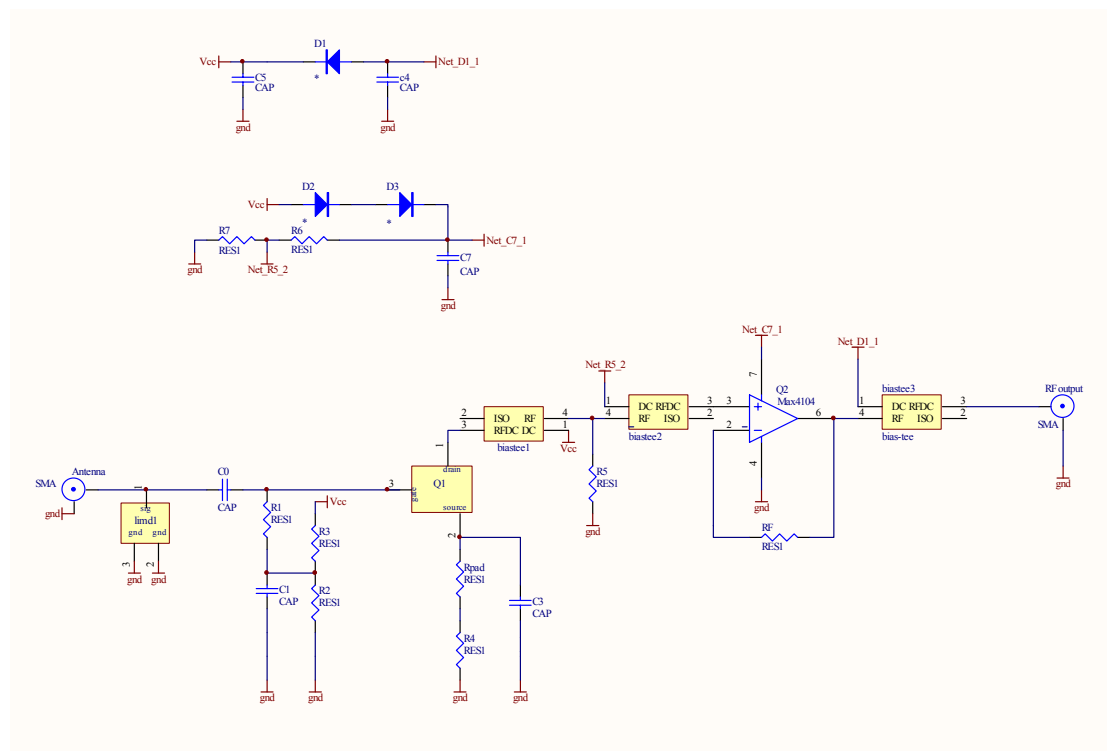


Figure A1: Circuit Schematic of version 2 from Protel

Description:

The TEM horn antenna was connected to port 1 of the Network Analyzer, and 0 dBm power was transmitted to the Active antenna placed at the same height and 12 feet away. The S21 measurements were noted on the HP 8753D Network Analyzer.

## Results:

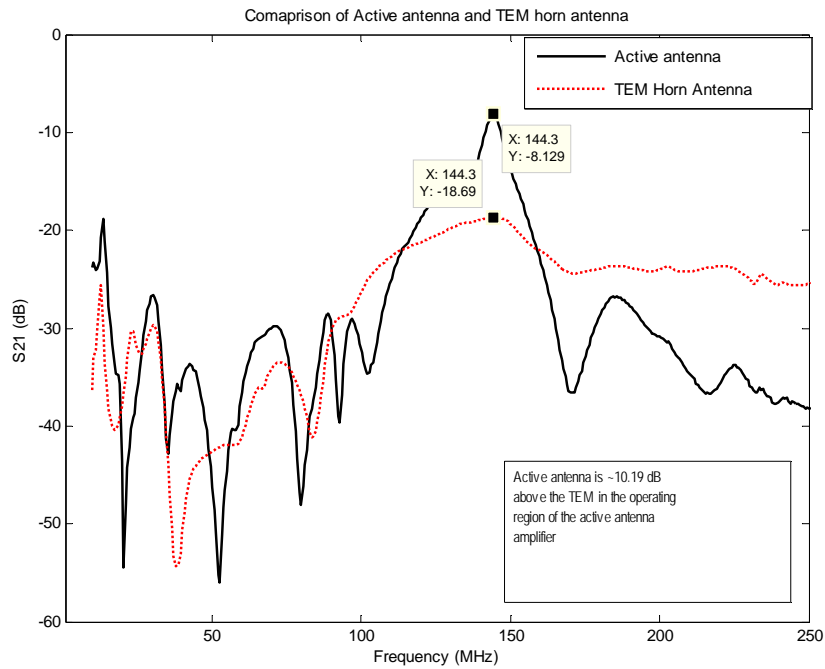


Figure A2: The S<sub>21</sub> measurements of TEM and Active antenna.

It can clearly be seen that the Active antenna is about 10.55 dB higher than the Horn antenna. The actual horn antenna gain 144 MHz is -0.3585 dB so the overall gain of active antenna is 10.19 dB this is however lesser than the electronic gain of the amplifier which was 14 dB this is probably due to saturation due to high incident power on the active antenna.

Bill of materials							
Component	Quantity	Size	Value	Unit price(\$)	Total Cost(\$)	Part Number	Vendor/Manufacturer
Resistors	1	0805	1 M ohm	0.048	0.048	-	Digikey
	1	0805	600 Kohm	0.038	0.038	-	Digikey
	1	0805	75 Kohm	0.038	0.038	-	Digikey
	1	0805	0 ohm	0.076	0.076	-	Digikey
	1	0805	50 ohm	0.038	0.038	-	Digikey
	1	0805	120 ohm	0.038	0.038	-	Digikey
	1	2010	750	0.4	0.4	P750WCT-ND	Digikey
Capacitors	4	0402	0.1uF	2.88	11.52	540L	ATCeramics
	1	-	47 uF	2.18	2.18	595D	Vishay/Mouser
	1	0805	0.2pF	2.88	2.88	-	ATCeramics
Inductor	1	-	470 nH	1	1	<a href="#">1206CS-471</a>	CoilCraft
Limiter Diode	1	-	-	2.88	2.88	HSMP-3822	Avago technologies
Diode	1	-	-	0.42	0.42	ES1B	Digikey
GaAs FET	1	-	-	1.43	2.86	NE34018-A	CEL (vendor:Mouser)
SMA connectors	2	-	50 ohm	3.98	7.96	530-142-0711-201	Mouser
Bias-tee	1	-	-	6.00	6.00	TCBT- 2R5G	Mini-Circuits
Total cost (per board)					38.376		
Board cost (Estimate)					20.00		
Grand Total					58.376		

## *Datasheets*



## GaAs HJ-FET L TO S BAND LOW NOISE AMPLIFIER (New Plastic Package)

**NE34018**

### FEATURES

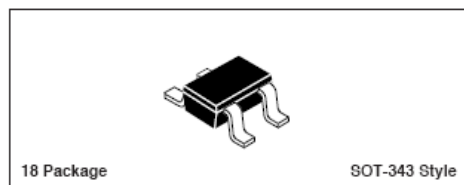
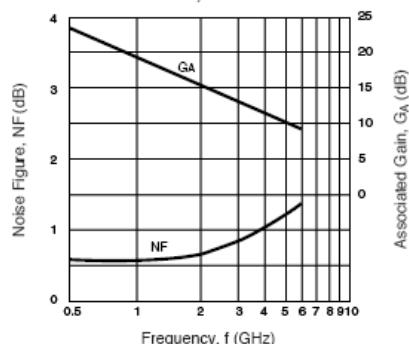
- **LOW COST MINIATURE PLASTIC PACKAGE** (SOT-343)
- **LOW NOISE FIGURE:**  
0.6 dB typical at 2 GHz
- **HIGH ASSOCIATED GAIN:**  
16.0 dB typical at 2 GHz
- **L<sub>G</sub> = 0.6 μm, W<sub>G</sub> = 400 μm**
- **TAPE & REEL PACKAGING**

### DESCRIPTION

NEC's NE34018 is a low cost gallium arsenide Hetero-Junction FET housed in a miniature (SOT-343) plastic surface mount package. The device is fabricated using ion implantation for improved RF and DC performance, reliability, and uniformity. Its low noise figure, high gain, small size and weight make it an ideal low noise amplifier transistor in the 1-3 GHz frequency range. The NE34018 is suitable for GPS, PCS, WLAN, MMDS, and other commercial applications.

NEC's stringent quality assurance and test procedures ensure the highest reliability and performance.

**NOISE FIGURE & ASSOCIATED GAIN vs. FREQUENCY**  
V<sub>DS</sub> = 3 V, I<sub>DS</sub> = 20 mA



### ELECTRICAL CHARACTERISTICS (T<sub>A</sub> = 25°C)

PART NUMBER PACKAGE OUTLINE			NE34018 18		
SYMBOL	PARAMETERS AND CONDITIONS	UNITS	MIN	TYP	MAX
NF	Noise Figure at V <sub>DS</sub> = 2 V, I <sub>b</sub> = 5 mA, f = 2 GHz	dB		0.6	1.0
GA	Associated Gain at V <sub>DS</sub> = 2 V, I <sub>b</sub> = 5 mA, f = 2 GHz	dB	14.0	16.0	
P <sub>1dB</sub>	Output Power at 1 dB Gain Compression Point, f = 2 GHz V <sub>DS</sub> = 2 V, I <sub>DS</sub> = 10 mA V <sub>DS</sub> = 3 V, I <sub>DS</sub> = 30 mA	dBm dBm		12 16.5	
G <sub>1dB</sub>	Gain at P <sub>1dB</sub> , f = 2 GHz V <sub>DS</sub> = 2 V, I <sub>DS</sub> = 10 mA V <sub>DS</sub> = 3 V, I <sub>DS</sub> = 30 mA	dB dB		17.0 17.5	
O/P I <sub>p3</sub>	Output I <sub>p3</sub> at f = 2 GHz, Δf = 1 MHz V <sub>DS</sub> = 2 V, I <sub>DS</sub> = 10 mA V <sub>DS</sub> = 2 V, I <sub>DS</sub> = 30 mA	dBm dBm		23 32	
I <sub>DS</sub>	Saturated Drain Current at V <sub>DS</sub> = 2 V, V <sub>GS</sub> = 0 V	mA	30	80	120
V <sub>P</sub>	Pinch Off Voltage at V <sub>DS</sub> = 2 V, I <sub>b</sub> = 100 μA	V	-2.0	-0.8	-0.2
g <sub>m</sub>	Transconductance at V <sub>DS</sub> = 2 V, I <sub>b</sub> = 5 mA	mS	30		
I <sub>GSO</sub>	Gate to Source Leakage Current at V <sub>GS</sub> = -3 V	μA		0.5	10
R <sub>TH(CH-A)</sub>	Thermal Resistance (Channel to Ambient)	°C/W		833	

Note:

1. Typical values of noise figures and associated gain are those obtained when 50% of the devices from a large number of lots were individually measured in a circuit with the input individually tuned to obtain the minimum value. Maximum values are criteria established on the production line as a "go-no-go" screening test with the fixture tuned for the "generic" type but not for each specimen.

California Eastern Laboratories

## NE34018

### ABSOLUTE MAXIMUM RATINGS<sup>1</sup> (T<sub>A</sub> = 25°C)

SYMBOLS	PARAMETERS	UNITS	RATINGS
V <sub>DS</sub>	Drain to Source Voltage	V	4
V <sub>GD0</sub>	Gate to Drain Voltage	V	-3
V <sub>GS0</sub>	Gate to Source Voltage	V	-3
I <sub>DS</sub>	Drain Current	mA	I <sub>DSS</sub>
T <sub>CH</sub>	Channel Temperature	°C	125
T <sub>STG</sub>	Storage Temperature	°C	-65 to +125
P <sub>T</sub>	Total Power Dissipation	mW	150

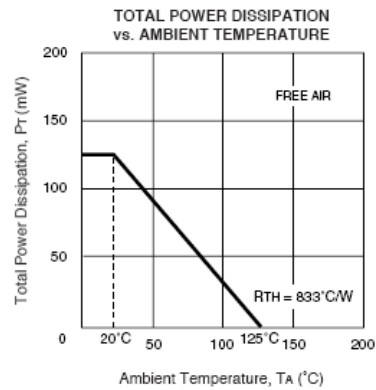
Note:

1. Operation in excess of any one of these parameters may result in permanent damage.

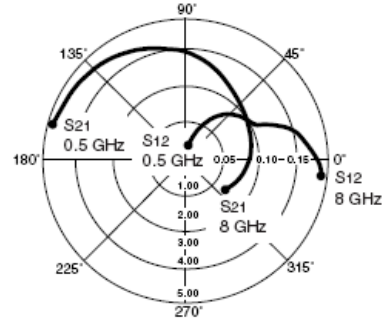
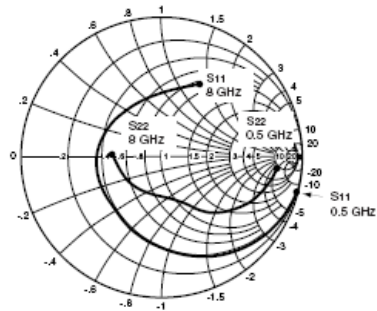
### TYPICAL NOISE PARAMETERS (T<sub>A</sub> = 25°C)

FREQ. (MHz)	NF <sub>OPT</sub> (dB)	G <sub>A</sub> (dB)	Γ <sub>OPT</sub>		R <sub>n</sub> /50
			MAG	ANG	
<b>V<sub>DS</sub> = 2 V, I<sub>DS</sub> = 10 mA</b>					
900	.56	20.5	.76	30	.45
2000	.63	16.3	.61	41	.28
2500	.68	14.1	.49	51	.18
3000	.70	13.6	.39	49	.16
3500	.76	12.3	.28	71	.12
4000	.82	11.6	.20	80	.10
<b>V<sub>DS</sub> = 2 V, I<sub>DS</sub> = 30 mA</b>					
2000	.60	17.0	.56	39	.23
2500	.70	15.3	.43	46	.15
3000	.76	14.2	.32	50	.26
<b>V<sub>DS</sub> = 3 V, I<sub>DS</sub> = 20 mA</b>					
900	.56	20.2	.74	26	1.54
2000	.62	16.8	.62	42	.43
2500	.66	14.9	.56	50	.31
3000	.70	14.0	.45	65	.24
3500	.80	13.2	.36	76	.14
4000	.84	12.8	.29	85	.10
4500	.90	11.0	.20	98	.08

### TYPICAL PERFORMANCE CURVES (T<sub>A</sub> = 25°C)



TYPICAL SCATTERING PARAMETERS (TA = 25°C)



V<sub>DS</sub> = 2 V, I<sub>DS</sub> = 5 mA

FREQUENCY (GHz)	S <sub>11</sub>		S <sub>21</sub>		S <sub>12</sub>		S <sub>22</sub>		K	MAG <sup>1</sup> (dB)
	MAG	ANG	MAG	ANG	MAG	ANG	MAG	ANG		
0.50	0.984	-15.1	4.945	165.0	0.020	80.6	0.807	-7.2	0.135	23.931
0.60	0.979	-18.0	4.908	162.3	0.023	78.9	0.803	-8.6	0.152	23.292
0.70	0.973	-21.0	4.899	159.4	0.027	77.0	0.798	-10.0	0.174	22.587
0.80	0.965	-23.9	4.871	156.7	0.031	75.3	0.793	-11.5	0.195	21.963
0.90	0.958	-26.8	4.843	153.9	0.034	73.7	0.788	-12.9	0.213	21.536
1.00	0.949	-29.8	4.825	151.1	0.038	72.1	0.781	-14.4	0.231	21.037
1.20	0.930	-35.7	4.783	145.6	0.045	68.7	0.767	-17.3	0.270	20.265
1.40	0.906	-41.5	4.723	140.2	0.052	65.4	0.751	-20.2	0.314	19.582
1.60	0.881	-47.5	4.660	134.7	0.058	62.2	0.734	-23.1	0.354	19.050
1.80	0.853	-53.6	4.605	129.3	0.064	59.1	0.715	-26.0	0.395	18.570
2.00	0.821	-59.8	4.531	123.8	0.070	56.0	0.696	-28.9	0.438	18.111
2.50	0.737	-76.3	4.332	110.5	0.082	48.2	0.648	-36.0	0.542	17.229
3.00	0.648	-94.2	4.092	97.6	0.092	41.4	0.600	-42.4	0.643	16.481
3.50	0.569	-113.6	3.805	85.3	0.098	35.3	0.556	-47.7	0.748	15.891
4.00	0.512	-133.0	3.516	73.9	0.102	30.5	0.518	-51.8	0.845	15.374
4.50	0.482	-150.9	3.248	63.8	0.105	27.2	0.480	-54.9	0.932	14.904
5.00	0.472	-165.2	3.025	54.7	0.108	25.3	0.444	-57.8	1.004	14.074
5.50	0.468	-175.7	2.846	46.4	0.112	24.5	0.405	-61.0	1.068	12.459
6.00	0.464	-176.0	2.714	38.4	0.118	23.7	0.367	-65.4	1.107	11.622
6.50	0.456	-167.9	2.601	30.5	0.126	22.4	0.331	-71.6	1.130	10.955
7.00	0.441	-158.2	2.505	22.1	0.134	20.2	0.302	-80.8	1.149	10.372
7.50	0.422	-144.3	2.417	13.3	0.142	18.0	0.283	-92.2	1.161	9.874
8.00	0.411	-127.5	2.321	4.0	0.151	15.0	0.281	-105.9	1.152	9.503

Note:

1. Gain Calculations:

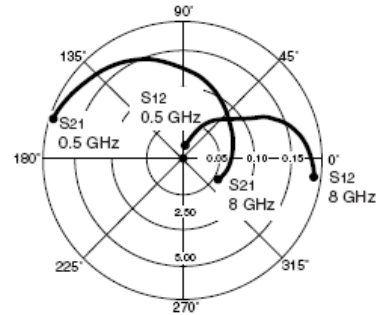
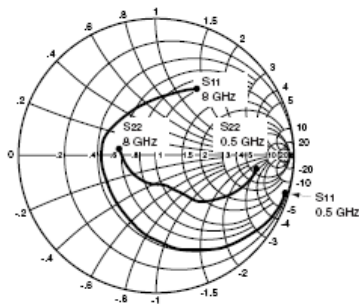
$$MAG = \frac{|S_{21}|}{|S_{12}|} \left( K = \sqrt{K^2 - 1} \right). \text{ When } K = 1, \text{ MAG is undefined and MSG values are used. } MSG = \frac{|S_{21}|}{|S_{12}|}, K = \frac{1 + |\Delta|^2 - |S_{11}|^2 - |S_{22}|^2}{2 |S_{12}| |S_{21}|}, \Delta = S_{11} S_{22} - S_{21} S_{12}$$

MAG = Maximum Available Gain

MSG = Maximum Stable Gain

NE34018

TYPICAL SCATTERING PARAMETERS (TA = 25°C)



V<sub>DS</sub> = 2 V, I<sub>DS</sub> = 10 mA

FREQUENCY (GHz)	S <sub>11</sub>		S <sub>21</sub>		S <sub>12</sub>		S <sub>22</sub>		K	MAG <sup>1</sup> (dB)
	MAG	ANG	MAG	ANG	MAG	ANG	MAG	ANG		
0.50	0.978	-17.0	6.806	162.8	0.018	80.1	0.723	-7.5	0.178	25.776
0.60	0.969	-20.3	6.731	159.7	0.022	78.7	0.719	-9.1	0.200	24.857
0.70	0.960	-23.6	6.691	156.5	0.025	77.3	0.712	-10.5	0.224	24.276
0.80	0.949	-26.9	6.624	153.4	0.028	75.5	0.706	-12.0	0.253	23.740
0.90	0.938	-30.1	6.559	150.3	0.032	73.6	0.698	-13.4	0.281	23.117
1.00	0.924	-33.3	6.502	147.2	0.035	72.4	0.690	-14.9	0.307	22.690
1.20	0.897	-39.8	6.371	141.2	0.041	69.2	0.673	-17.8	0.356	21.914
1.40	0.865	-46.0	6.217	135.3	0.047	66.3	0.655	-20.6	0.410	21.215
1.60	0.831	-52.4	6.065	129.5	0.053	63.4	0.635	-23.4	0.460	20.586
1.80	0.796	-58.7	5.912	123.9	0.058	60.7	0.614	-26.1	0.509	20.083
2.00	0.757	-65.1	5.750	118.3	0.063	58.1	0.594	-28.8	0.560	19.603
2.50	0.658	-81.9	5.336	105.0	0.074	51.7	0.546	-35.3	0.677	18.580
3.00	0.563	-100.1	4.909	92.4	0.083	46.5	0.501	-41.2	0.782	17.719
3.50	0.483	-119.7	4.478	80.8	0.091	41.8	0.463	-45.9	0.873	16.920
4.00	0.432	-139.4	4.080	70.2	0.097	38.1	0.429	-49.5	0.952	16.239
4.50	0.409	-157.2	3.733	60.8	0.103	35.1	0.388	-53.3	1.018	14.771
5.00	0.406	-171.0	3.448	52.3	0.109	33.2	0.363	-53.8	1.057	13.538
5.50	0.408	179.2	3.223	44.5	0.117	31.6	0.327	-55.6	1.085	12.618
6.00	0.411	171.4	3.050	37.0	0.126	29.9	0.293	-58.3	1.097	11.939
6.50	0.408	163.8	2.906	29.4	0.136	27.5	0.259	-62.8	1.106	11.320
7.00	0.397	154.5	2.782	21.5	0.145	24.1	0.232	-71.3	1.117	10.752
7.50	0.383	140.6	2.672	13.2	0.156	20.8	0.211	-83.2	1.112	10.298
8.00	0.376	123.6	2.560	4.4	0.166	16.5	0.204	-99.5	1.104	9.917

Note:

1. Gain Calculations:

$$MAG = \frac{|S_{21}|}{|S_{12}|} (K = \sqrt{K^2 - 1}). \text{ When } K = 1, \text{ MAG is undefined and MSG values are used. } MSG = \frac{|S_{21}|}{|S_{12}|}, K = \frac{1 + |\Delta|^2 - |S_{11}|^2 - |S_{22}|^2}{2 |S_{12} S_{21}|}, \Delta = S_{11} S_{22} - S_{21} S_{12}$$

MAG = Maximum Available Gain  
MSG = Maximum Stable Gain

## TYPICAL SCATTERING PARAMETERS (TA = 25°C)

VDS = 2 V, IDS = 20 mA

FREQUENCY (GHz)	S11		S21		S12		S22		K	MAG <sup>1</sup> (dB)
	MAG	ANG	MAG	ANG	MAG	ANG	MAG	ANG		
0.50	0.969	-18.6	8.533	160.8	0.017	81.2	0.635	-7.3	0.221	27.007
0.60	0.958	-22.1	8.416	157.3	0.020	79.4	0.631	-8.8	0.256	26.241
0.70	0.946	-25.7	8.331	153.8	0.023	77.8	0.624	-10.2	0.289	25.590
0.80	0.931	-29.2	8.211	150.4	0.026	76.4	0.617	-11.6	0.324	24.994
0.90	0.916	-32.7	8.092	147.1	0.029	75.1	0.610	-12.9	0.354	24.457
1.00	0.899	-36.1	7.982	143.7	0.032	73.8	0.601	-14.3	0.387	23.970
1.20	0.864	-42.9	7.737	137.3	0.037	71.1	0.584	-16.9	0.451	23.204
1.40	0.825	-49.3	7.469	131.1	0.043	68.5	0.566	-19.4	0.512	22.398
1.60	0.785	-55.8	7.205	125.2	0.048	66.1	0.547	-21.8	0.570	21.764
1.80	0.745	-62.1	6.948	119.5	0.053	63.8	0.527	-24.2	0.623	21.176
2.00	0.701	-68.6	6.692	113.9	0.058	61.7	0.509	-26.5	0.675	20.621
2.50	0.596	-85.3	6.075	100.9	0.069	56.6	0.467	-32.4	0.786	19.447
3.00	0.499	-103.3	5.495	88.9	0.079	52.0	0.428	-37.8	0.879	18.423
3.50	0.422	-123.1	4.953	77.8	0.088	47.9	0.397	-42.4	0.952	17.504
4.00	0.374	-142.9	4.477	67.8	0.096	44.3	0.369	-45.8	1.009	16.118
4.50	0.357	-160.6	4.073	58.9	0.104	41.1	0.340	-47.7	1.047	14.596
5.00	0.359	-174.1	3.745	50.9	0.112	38.6	0.310	-48.8	1.073	13.589
5.50	0.366	176.6	3.487	43.4	0.122	36.2	0.278	-49.1	1.084	12.796
6.00	0.372	169.3	3.285	36.2	0.133	33.6	0.248	-50.0	1.084	12.160
6.50	0.372	162.1	3.118	29.0	0.144	30.4	0.219	-52.7	1.086	11.571
7.00	0.365	153.0	2.975	21.4	0.154	26.4	0.193	-60.2	1.090	11.031
7.50	0.353	139.1	2.852	13.4	0.165	22.2	0.169	-72.2	1.088	10.569
8.00	0.348	122.0	2.729	5.0	0.176	17.4	0.156	-91.3	1.079	10.189

Note:

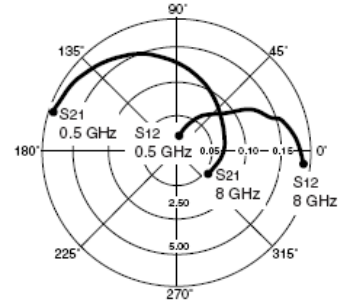
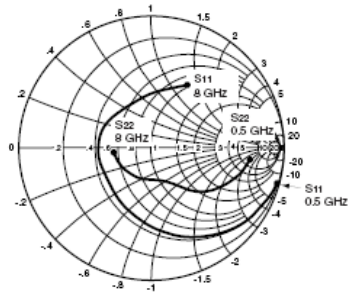
1. Gain Calculations:

$$MAG = \frac{|S_{21}|}{|S_{12}|} \left( K \pm \sqrt{K^2 - 1} \right). \text{ When } K \leq 1, \text{ MAG is undefined and MSG values are used. } MSG = \frac{|S_{21}|}{|S_{12}|}, K = \frac{1 + |\Delta|^2 - |S_{11}|^2 - |S_{22}|^2}{2 |S_{12} S_{21}|}, \Delta = S_{11} S_{22} - S_{21} S_{12}$$

MAG = Maximum Available Gain

MSG = Maximum Stable Gain

TYPICAL SCATTERING PARAMETERS (TA = 25 °C)



VDS = 3 V, IDS = 10 mA

FREQUENCY (GHz)	S11		S21		S12		S22		K	MAG <sup>1</sup> (dB)
	MAG	ANG	MAG	ANG	MAG	ANG	MAG	ANG		
0.50	0.977	-17.0	6.912	162.9	0.018	80.5	0.744	-7.5	0.170	25.843
0.60	0.969	-20.2	6.836	159.7	0.021	79.0	0.740	-9.0	0.194	25.126
0.70	0.959	-23.5	6.795	156.5	0.024	77.1	0.733	-10.4	0.226	24.520
0.80	0.948	-26.8	6.728	153.4	0.027	75.4	0.727	-11.9	0.252	23.965
0.90	0.937	-30.0	6.659	150.3	0.031	73.7	0.719	-13.3	0.278	23.320
1.00	0.923	-33.2	6.602	147.2	0.034	72.4	0.712	-14.8	0.302	22.882
1.20	0.895	-39.6	6.467	141.2	0.040	69.1	0.695	-17.6	0.355	22.086
1.40	0.863	-45.8	6.310	135.3	0.045	66.2	0.676	-20.3	0.410	21.468
1.60	0.829	-52.1	6.152	129.5	0.051	63.5	0.656	-23.0	0.459	20.814
1.80	0.793	-58.4	5.996	123.9	0.056	60.8	0.636	-25.7	0.508	20.297
2.00	0.754	-64.8	5.830	118.3	0.061	58.0	0.616	-28.3	0.559	19.803
2.50	0.656	-81.4	5.407	105.1	0.071	52.1	0.568	-34.6	0.674	18.817
3.00	0.559	-99.2	4.973	92.7	0.080	46.7	0.524	-40.1	0.781	17.935
3.50	0.479	-118.5	4.538	81.1	0.087	42.3	0.486	-44.7	0.876	17.173
4.00	0.426	-138.0	4.138	70.6	0.093	38.9	0.454	-48.2	0.953	16.483
4.50	0.402	-155.8	3.788	61.2	0.099	36.4	0.422	-50.6	1.011	15.173
5.00	0.397	-169.6	3.500	52.8	0.105	34.6	0.389	-52.6	1.058	13.757
5.50	0.399	-179.6	3.274	45.0	0.112	33.3	0.355	-54.6	1.090	12.833
6.00	0.401	172.6	3.101	37.6	0.121	31.8	0.322	-57.5	1.100	12.163
6.50	0.399	165.2	2.956	30.1	0.131	29.6	0.290	-62.2	1.104	11.573
7.00	0.389	156.1	2.832	22.3	0.140	26.6	0.264	-70.4	1.112	11.026
7.50	0.387	144.7	2.798	15.4	0.153	20.4	0.245	-81.6	1.063	11.085
8.00	0.365	125.8	2.614	5.4	0.161	19.3	0.240	-96.5	1.094	10.240

Note:

1. Gain Calculations:

$$MAG = \frac{|S_{21}|}{|S_{12}|} \left( K \pm \sqrt{K^2 - 1} \right). \text{ When } K \leq 1, \text{ MAG is undefined and MSG values are used. } MSG = \frac{|S_{21}|}{|S_{12}|}, K = \frac{1 + |\Delta|^2 - |S_{11}|^2 - |S_{22}|^2}{2 |S_{12} S_{21}|}, \Delta = S_{11} S_{22} - S_{21} S_{12}$$

MAG = Maximum Available Gain

MSG = Maximum Stable Gain

### TYPICAL SCATTERING PARAMETERS (T<sub>A</sub> = 25 °C)

V<sub>DS</sub> = 3 V, I<sub>DS</sub> = 20 mA

FREQUENCY (GHz)	S <sub>11</sub>		S <sub>21</sub>		S <sub>12</sub>		S <sub>22</sub>		K	MAG <sup>1</sup> (dB)
	MAG	ANG	MAG	ANG	MAG	ANG	MAG	ANG		
0.500	0.969	-18.7	8.662	160.8	0.016	81.1	0.667	-7.3	0.215	27.335
0.600	0.957	-22.2	8.541	157.3	0.019	79.1	0.663	-8.8	0.255	26.528
0.700	0.945	-25.8	8.454	153.7	0.022	78.0	0.655	-10.2	0.282	25.846
0.800	0.930	-29.3	8.332	150.3	0.025	76.3	0.649	-11.6	0.318	25.228
0.900	0.915	-32.7	8.209	147.0	0.028	74.8	0.641	-12.9	0.350	24.671
1.000	0.898	-36.1	8.096	143.6	0.031	73.3	0.632	-14.3	0.384	24.169
1.200	0.862	-42.8	7.844	137.2	0.036	70.6	0.615	-16.9	0.447	23.382
1.400	0.823	-49.3	7.571	131.1	0.041	68.1	0.596	-19.3	0.509	22.664
1.600	0.781	-55.7	7.299	125.1	0.046	65.7	0.577	-21.7	0.569	22.005
1.800	0.741	-62.0	7.036	119.4	0.051	63.5	0.557	-24.0	0.621	21.398
2.000	0.697	-68.4	6.775	113.9	0.056	61.4	0.539	-26.4	0.670	20.827
2.250	0.644	-76.6	6.458	107.2	0.061	58.7	0.517	-29.3	0.731	20.248
2.500	0.591	-84.9	6.144	100.9	0.066	56.5	0.496	-32.0	0.786	19.689
2.750	0.541	-93.7	5.848	94.8	0.071	54.3	0.476	-34.7	0.833	19.157
3.000	0.493	-102.7	5.553	88.9	0.075	52.1	0.458	-37.1	0.884	18.695
3.500	0.415	-122.2	5.007	78.0	0.084	48.2	0.426	-41.5	0.956	17.753
4.000	0.368	-141.9	4.526	68.0	0.091	44.9	0.399	-44.7	1.016	16.188
4.500	0.349	-159.7	4.119	59.2	0.099	42.2	0.372	-46.8	1.052	14.798
5.000	0.349	-173.2	3.790	51.2	0.107	39.9	0.343	-48.1	1.077	13.794
5.500	0.357	177.4	3.532	43.8	0.116	37.9	0.313	-49.1	1.089	13.021
6.000	0.362	170.2	3.332	36.7	0.127	35.6	0.284	-50.8	1.086	12.405
6.500	0.363	163.3	3.166	29.5	0.138	32.7	0.255	-54.2	1.084	11.836
7.000	0.356	154.4	3.024	22.0	0.148	28.8	0.230	-61.8	1.087	11.307
7.500	0.343	140.7	2.902	14.1	0.160	25.0	0.208	-73.1	1.079	10.876
8.000	0.336	123.7	2.782	5.7	0.171	20.3	0.199	-89.6	1.067	10.531

Note:

1. Gain Calculations:

$$\text{MAG} = \frac{|S_{21}|}{|S_{12}|} \left( K = \sqrt{K^2 - 1} \right). \text{ When } K \approx 1, \text{ MAG is undefined and MSG values are used. } \text{MSG} = \frac{|S_{21}|}{|S_{12}|}, K = \frac{1 + |\Delta|^2 - |S_{11}|^2 - |S_{22}|^2}{2 |S_{12} S_{21}|}, \Delta = S_{11} S_{22} - S_{21} S_{12}$$

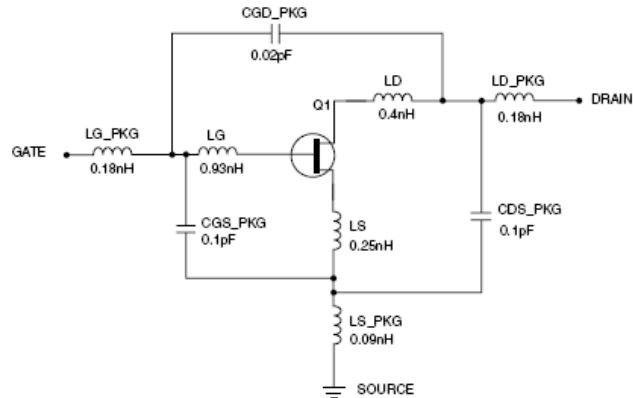
MAG = Maximum Available Gain

MSG = Maximum Stable Gain

## NE34018

### NE34018 NONLINEAR MODEL

#### SCHEMATIC



#### FET NONLINEAR MODEL PARAMETERS <sup>(1)</sup>

Parameters	Q1	Parameters	Q1
VTO	-0.6885	RG	4
VTOSC	0	RD	1.5
ALPHA	5	RS	2
BETA	0.1838	RGMET	0
GAMMA	0.038	KF	0
GAMMADC	0.03	AF	1
Q	1.8	TNOM	27
DELTA	0.25	XTI	3
VBI	0.7	EG	1.43
IS	3e-13	VTOTC	0
N	1	BETATCE	0
RIS	0	FFE	1
RID	0		
TAU	4e-12		
CDS	0.1e-12		
RDB	5000		
CBS	1e-11		
CGSO	0.95e-12		
CGDO	0.04e-12		
DELTA1	0.3		
DELTA2	0.05		
FC	0.5		
VBR	Infinity		

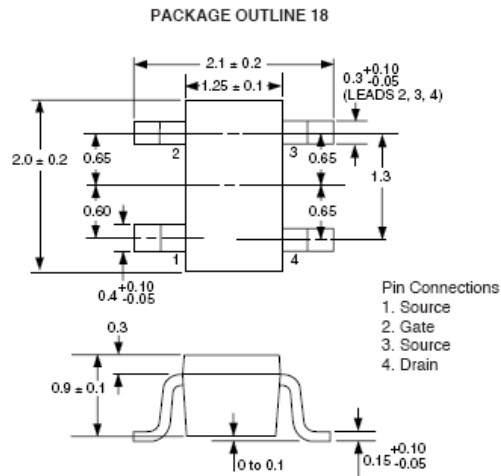
(1) Series IV Libra TOM Model

#### UNITS

Parameter	Units
time	seconds
capacitance	farads
inductance	henries
resistance	ohms
voltage	volts
current	amps

#### MODEL RANGE

Frequency: 0.5 to 6 GHz  
 Bias:  $V_{DS} = 1\text{ V to }3\text{ V}$ ,  $I_D = 5\text{ mA to }40\text{ mA}$   
 Date: 6/97

**OUTLINE DIMENSIONS** (Units in mm)

**ORDERING INFORMATION**

PART NUMBER	QTY	I <sub>DRSS</sub> RANGE (mA)	MARKING
NE34018-A	Bulk up to 3 K	30-120	V63 or V64
NE34018-TI-63-A	3 K/Reel	30-65	V63
NE34018-TI-64-A	3 K/Reel	60-120	V64

**Life Support Applications**

These NEC products are not intended for use in life support devices, appliances, or systems where the malfunction of these products can reasonably be expected to result in personal injury. The customers of CEL using or selling these products for use in such applications do so at their own risk and agree to fully indemnify CEL for all damages resulting from such improper use or sale.

EXCLUSIVE NORTH AMERICAN AGENT FOR **NEC** RF, MICROWAVE & OPTOELECTRONIC SEMICONDUCTORS

**CEL** CALIFORNIA EASTERN LABORATORIES • Headquarters • 4590 Patrick Henry Drive • Santa Clara, CA 95054-1817 • (408) 988-3500 • Telex 34-6993 • FAX (408) 988-0279

24-Hour Fax-On-Demand: 800-390-9232 (U.S. and Canada only) • Internet: <http://WWW.CEL.COM>

DATA SUBJECT TO CHANGE WITHOUT NOTICE

PRINTED IN USA ON RECYCLED PAPER -12/99

Subject: Compliance with EU Directives

CEL certifies, to its knowledge, that semiconductor and laser products detailed below are compliant with the requirements of European Union (EU) Directive 2002/95/EC Restriction on Use of Hazardous Substances in electrical and electronic equipment (RoHS) and the requirements of EU Directive 2003/11/EC Restriction on Penta and Octa BDE.

CEL Pb-free products have the same base part number with a suffix added. The suffix –A indicates that the device is Pb-free. The –AZ suffix is used to designate devices containing Pb which are exempted from the requirement of RoHS directive (\*). In all cases the devices have Pb-free terminals. All devices with these suffixes meet the requirements of the RoHS directive.

This status is based on CEL's understanding of the EU Directives and knowledge of the materials that go into its products as of the date of disclosure of this information.

Restricted Substance per RoHS	Concentration Limit per RoHS (values are not yet fixed)	Concentration contained in CEL devices	
		-A	-AZ
Lead (Pb)	< 1000 PPM	Not Detected	(*)
Mercury	< 1000 PPM	Not Detected	
Cadmium	< 100 PPM	Not Detected	
Hexavalent Chromium	< 1000 PPM	Not Detected	
PBB	< 1000 PPM	Not Detected	
PBDE	< 1000 PPM	Not Detected	

If you should have any additional questions regarding our devices and compliance to environmental standards, please do not hesitate to contact your local representative.

**Important Information and Disclaimer:** Information provided by CEL on its website or in other communications concerning the substance content of its products represents knowledge and belief as of the date that it is provided. CEL bases its knowledge and belief on information provided by third parties and makes no representation or warranty as to the accuracy of such information. Efforts are underway to better integrate information from third parties. CEL has taken and continues to take reasonable steps to provide representative and accurate information but may not have conducted destructive testing or chemical analysis on incoming materials and chemicals. CEL and CEL suppliers consider certain information to be proprietary, and thus CAS numbers and other limited information may not be available for release.

In no event shall CEL's liability arising out of such information exceed the total purchase price of the CEL part(s) at issue sold by CEL to customer on an annual basis.

See CEL Terms and Conditions for additional clarification of warranties and liability.

# BIAS-TEES

50Ω Surface Mount □

High CURRENT 100 kHz to 6000 MHz



JEBT



TCBT

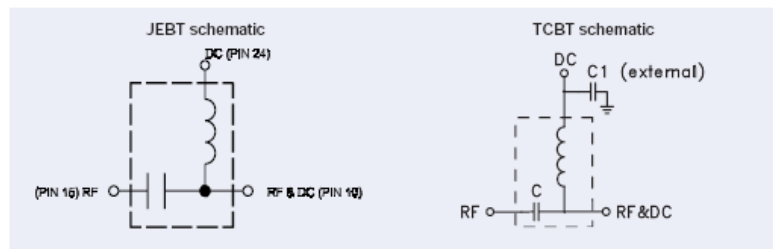
MODEL NO.	FREQ. RANGE (MHz) $f_L$ - $f_U$	INSERTION LOSS* (dB)						ISOLATION* (dB) (RF port to DC port) (RF&DC port to DC port)						VSWR** (:1)						CASE STYLE Note B	CONNECTION	PRICE \$ ea. Qty. (1-9)
		L		M		U		L		M		U		L		M		U				
		Typ.	Max.	Typ.	Max.	Typ.	Max.	Typ.	Min.	Typ.	Min.	Typ.	Min.	Typ.	Max.	Typ.	Max.	Typ.	Max.			
JEBT-4R2G	10-4200	0.15	0.6	0.6	1.2	0.6	1.6	32	20	40	20	40	20	—	—	—	—	—	—	BL301	hr	39.95
JEBT-4R2GW	0.1-4200	0.15	0.8	0.6	1.2	0.6	1.6	25	15	40	20	40	20	—	—	—	—	—	—	BL301	hr	59.95
NEW TCBT-2R5G	20-2500	0.2	0.8	0.35	0.8	0.7	1.2	65	40	44	25	25	20	1.05	1.5	1.05	1.2	1.1	1.2	GU1041	pr	(10-49) 6.95
NEW TCBT-6G	50-6000	0.2	0.8	0.7	1.8	1.1	2.5	52	38	28	18	19	17	1.05	1.5	1.1	1.3	1.2	2.2	GU1041	pr	9.95

L = low range [ $f_L$  to  $10 f_L$ ]    M = mid range [ $10 f_L$  to  $f_U/2$ ]    U = upper range [ $f_U/2$  to  $f_U$ ]

see suggested PCB layout (PL-146) for TCBT models

### features

- wide band coverage 0.1 to 6000 MHz
- low insertion loss 0.4 dB typ.
- miniature surface mount 0.15"X0.15" (TCBT models)
- patent pending



### NOTES:

- Non-hermetic
- \* Insertion loss and isolation are guaranteed up to 20 dBm-RF power and 200 mA DC current for PBTC, JEBT, and ZFBT Series; for TCBT, up to 25 dBm RF & 100mA current. (tested with C external=0.01 μF) for ZNBT, up to 30 dBm RF power and 500mA DC current.
- \*\* VSWR measured with open and short at DC port. For TCBT tested with C external=0.01 μF
- ◆ Insertion loss 1 dB Max. and isolation 7 dB Min. 0.1 to 0.3 MHz.
- ▼ Connectors: SMA-F at "RF", and SMA-M at "RF & DC" port.  
For DC port, ZFBT available with SMA-F and for ZFBT-FT available with feedthrough terminal.  
For ZNBT-60-1W, N-M at "RF", N-F at "RF+DC", BNC-F at DC.
- A. General Quality Control Procedures, Environmental Specifications, Hi-Rel and MIL description are given in General Information (Section 0).
- B. Case mounted options, case finishes are given in section 0, see "Case styles & Outline Drawings".
- C. Prices and specifications subject to change without notice.
- 1. Absolute maximum power, voltage and current ratings:
  - 1a. max. input current: 500 mA, except TCBT models, 200 mA.
  - 1b. max. RF power: 30 dBm
  - 1c. max. voltage at DC port: 30V; JEBT series, 25V.
- 2. DC resistance from DC to RF & DC port: 4.5 ohm typical.



INTERNET <http://www.minicircuits.com>

P.O. Box 350166, Brooklyn, New York 11235-0003 (718) 934-4500 Fax (718) 332-4661  
Distribution Centers NORTH AMERICA 800-664-7949 • 417-335-5935 • Fax 417-335-5945 • EUROPE 44-1252-832600 • Fax 44-1252-837104

Mini-Circuits ISO 9001 & ISO 14001 Certified

## Plug-In & Coaxial

### WIDEBAND 0.1 to 6000 MHz

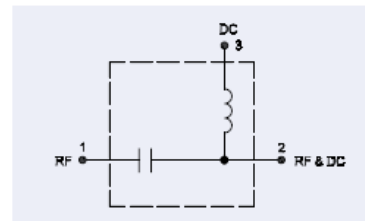


MODEL NO.	FREQ. RANGE (MHz) $f_l$ - $f_u$	INSERTION LOSS* (dB)						ISOLATION* (dB) (RF port to DC port) (RF&DC port to DC port)						VSWR** (:1)						CASE STYLE ▼ Note B	CONNECTION	PRICE \$ ea. Qty. (1-9)
		L		M		U		L		M		U		L		M		U				
		Typ.	Max.	Typ.	Max.	Typ.	Max.	Typ.	Min.	Typ.	Min.	Typ.	Min.	Typ.	Max.	Typ.	Max.	Typ.	Max.			
PBTC-1G	10-1000	0.15	0.7	0.3	0.7	0.3	1.0	27	20	33	20	30	20	1.06	1.2	1.06	1.2	1.1	1.39	CO7	hh	28.20
PBTC-3G	10-3000	0.15	0.7	0.3	1.5	1.0	2.5	27	20	30	20	35	20	1.06	1.2	1.13	1.66	1.6	1.7	CO7	hh	38.20
✦ PBTC-1GW	0.1-1000	0.15	0.8	0.3	0.7	0.3	1.0	25	15	33	20	30	20	1.06	1.6	1.06	1.2	1.1	1.39	CO7	hh	38.20
✦ PBTC-3GW	0.1-3000	0.15	0.8	0.3	1.5	1.0	2.5	25	15	30	20	35	20	1.06	1.6	1.13	1.66	1.6	1.7	CO7	hh	49.20
<b>NEW</b> ZNBT-60-1W	2.5-6000	0.2	0.9	0.6	2.0	1.6	2.2	75	45	45	25	35	20	1.1	1.5	1.1	1.3	1.35	1.6	K559	gf	82.95
ZFBT-4R2G	10-4200	0.15	0.6	0.6	1.2	0.6	1.6	32	20	40	20	50	20	1.06	1.2	1.13	1.3	1.13	1.3	K18	gf	59.95
ZFBT-4R2G-FT	10-4200	0.15	0.6	0.6	1.2	0.6	1.6							1.06	1.2	1.13	1.3	1.13	1.3	Y460	nr	59.95
ZFBT-6G	10-6000	0.15	0.6	0.6	1.4	1.0	2.2	32	20	40	20	30	17	1.06	1.2	1.13	1.3	1.13	1.5	K18	gf	79.95
ZFBT-6G-FT	10-6000	0.15	0.6	0.6	1.4	1.0	2.2							1.06	1.2	1.13	1.3	1.13	1.5	Y460	nr	79.95
✦ ZFBT-4R2GW	0.1-4200	0.15	0.8	0.6	1.2	0.6	1.6	25	15	40	20	50	20	1.06	1.6	1.13	1.3	1.13	1.3	K18	gf	79.95
✦ ZFBT-4R2GW-FT	0.1-4200	0.15	0.8	0.6	1.2	0.6	1.6							1.06	1.6	1.13	1.3	1.13	1.3	Y460	nr	79.95
✦ ZFBT-6GW	0.1-6000	0.15	0.8	0.6	1.4	1.0	2.2	25	15	40	20	30	17	1.06	1.6	1.13	1.3	1.13	1.5	K18	gf	89.95
✦ ZFBT-6GW-FT	0.1-6000	0.15	0.8	0.6	1.4	1.0	2.2							1.06	1.6	1.13	1.3	1.13	1.5	Y460	nr	89.95

L = low range [ $f_l$  to  $10 f_l$ ]      M = mid range [ $10 f_l$  to  $f_u/2$ ]      U = upper range [ $f_u/2$  to  $f_u$ ]

#### applications

- biasing amplifiers
- biasing of laser diodes
- DC return
- DC blocking
- good for digital & analog applications



#### pin & coaxial connections

PORT	gf	hf	hh	hr	pf
RF	1	in	9	15	4
RF & DC	2	out	12	10	3
DC	3	+15	3	24	1
GND	—	—	all other pins	all other pins	—
ISOLATED	—	—	—	—	2
DEMO BOARD	—	—	—	—	18-268

#### NSN GUIDE

MCL NO.	NSN
ZFBT-4R2G	5895-01-481-4754
ZFBT-4R2GW-FT	5895-01-495-8905
ZPBT-4R2GW	5895-01-514-2948

The Design Engineers Search Engine  
Provides Actual Data Instantly  
At: <http://www.minicircuits.com>

In Stock... Immediate Delivery  
For Custom Versions Of Standard Models  
Consult Our Applications Dept.



# Chip Inductors – 1206CS Series (3216)

The 1206CS features high SRF and excellent Q values. Their ceramic cores make 1% tolerances practical and economical and ensure the utmost in thermal stability, predictability and consistency.

Coilcraft **Designer's Kit C320** contains samples of all 5% inductance tolerance parts. To order, contact Coilcraft or visit <http://order.coilcraft.com> to purchase on-line.

Part number <sup>1</sup>	Inductance <sup>2</sup> (nH)	Percent tolerance <sup>3</sup>	Q min <sup>4</sup>	SRF min <sup>5</sup> (MHz)	DCR max <sup>6</sup> (Ohms)	I <sub>rms</sub> <sup>7</sup> (mA)
1206CS-030X_L	3.3 @ 100 MHz	<b>5</b>	30 @ 300 MHz	6200	0.050	1000
1206CS-060X_L	6.8 @ 100 MHz	<b>5</b>	30 @ 300 MHz	5500	0.070	1000
1206CS-100X_L	10 @ 100 MHz	<b>5</b>	40 @ 300 MHz	4000	0.080	1000
1206CS-120X_L	12 @ 100 MHz	<b>5,2</b>	40 @ 300 MHz	3200	0.080	1000
1206CS-150X_L	15 @ 100 MHz	<b>5,2</b>	40 @ 300 MHz	3200	0.100	1000
1206CS-180X_L	18 @ 100 MHz	<b>5,2</b>	50 @ 300 MHz	2800	0.100	1000
1206CS-220X_L	22 @ 100 MHz	<b>5,2</b>	50 @ 300 MHz	2200	0.100	1000
1206CS-270X_L	27 @ 100 MHz	<b>5,2</b>	50 @ 300 MHz	1800	0.110	1000
1206CS-330X_L	33 @ 100 MHz	<b>5,2</b>	55 @ 300 MHz	1800	0.110	1000
1206CS-390X_L	39 @ 100 MHz	<b>5,2</b>	55 @ 300 MHz	1800	0.120	1000
1206CS-470X_L	47 @ 100 MHz	<b>5,2</b>	55 @ 300 MHz	1500	0.130	1000
1206CS-560X_L	56 @ 100 MHz	<b>5,2,1</b>	55 @ 300 MHz	1450	0.140	1000
1206CS-680X_L	68 @ 100 MHz	<b>5,2,1</b>	55 @ 300 MHz	1200	0.260	900
1206CS-820X_L	82 @ 100 MHz	<b>5,2,1</b>	55 @ 300 MHz	1200	0.210	900
1206CS-101X_L	100 @ 100 MHz	<b>5,2,1</b>	55 @ 300 MHz	1100	0.260	850
1206CS-121X_L	120 @ 100 MHz	<b>5,2,1</b>	60 @ 300 MHz	1100	0.260	800
1206CS-151X_L	150 @ 100 MHz	<b>5,2,1</b>	60 @ 300 MHz	950	0.310	750
1206CS-181X_L	180 @ 50 MHz	<b>5,2,1</b>	60 @ 300 MHz	900	0.430	700
1206CS-221X_L	220 @ 50 MHz	<b>5,2,1</b>	60 @ 300 MHz	760	0.500	670
1206CS-271X_L	270 @ 50 MHz	<b>5,2,1</b>	55 @ 300 MHz	730	0.560	630
1206CS-331X_L	330 @ 50 MHz	<b>5,2,1</b>	45 @ 150 MHz	650	0.620	590
1206CS-391X_L	390 @ 50 MHz	<b>5,2,1</b>	45 @ 150 MHz	600	0.750	530
1206CS-471X_L	470 @ 50 MHz	<b>5,2,1</b>	45 @ 150 MHz	550	1.30	490
1206CS-561X_L	560 @ 35 MHz	<b>5,2,1</b>	45 @ 150 MHz	470	1.34	460
1206CS-621X_L	620 @ 35 MHz	<b>5,2,1</b>	45 @ 150 MHz	470	1.58	460
1206CS-681X_L	680 @ 35 MHz	<b>5,2,1</b>	45 @ 150 MHz	450	1.58	430
1206CS-751X_L	750 @ 35 MHz	<b>5,2,1</b>	45 @ 150 MHz	440	2.25	320
1206CS-821X_L	820 @ 35 MHz	<b>5,2,1</b>	45 @ 150 MHz	420	1.82	400
1206CS-911X_L	910 @ 35 MHz	<b>5,2,1</b>	45 @ 150 MHz	410	2.95	310
1206CS-102X_L	1000 @ 35 MHz	<b>5,2,1</b>	45 @ 150 MHz	400	2.80	320
1206CS-122X_L	1200 @ 35 MHz	<b>5,2,1</b>	45 @ 150 MHz	380	3.20	300

1. When ordering, specify tolerance, termination and packaging codes:

1206CS-122XJLC

- Tolerance:** F = 1% G = 2% J = 5%  
(Table shows stock tolerances in bold.)
- Termination:** L = RoHS compliant silver-palladium-platinum-glass frit.  
Special order: T = RoHS tin-silver-copper (95.5/4/0.5) or  
S = non-RoHS tin-lead (63/37).
- Packaging:** C = 7" machine-ready reel, EIA-481 embossed plastic tape (2000 parts per full reel).  
B = Less than full reel, in tape, but not machine ready.  
To have a leader and trailer added (\$25 charge), use code letter C instead.  
D = 13" machine-ready reel, EIA-481 embossed plastic tape. Factory order only, not stocked (7500 parts per full reel).

2. Inductance measured using a Coilcraft SMD-A fixture in an Agilent/HP 4286A impedance analyzer with Coilcraft-provided correlation pieces.

3. Tolerances in bold are stocked for immediate shipment.
4. Q measured using an Agilent/HP 4291A with an Agilent/HP 16193 test fixture.
5. SRF measured using an Agilent/HP 8720D network analyzer and a Coilcraft SMD-D test fixture.
6. DCR measured on a Cambridge Technology Micro-ohmmeter and a Coilcraft CCF840 fixture.
7. Average current for a 15°C rise above 25°C ambient.
8. Operating temperature range -40°C to +125°C.
9. Electrical specifications at 25°C.  
See Qualification Standards section for environmental and test data.  
See Color Coding section for part marking data.

**COILCRAFT** ACCURATE  
**PRECISION** REPEATABLE  
MEASUREMENTS  
SEE INDEX **TEST FIXTURES**

**Coilcraft**<sup>®</sup>

Specifications subject to change without notice.  
Please check our website for latest information.

Document 104-1 Revised 03/23/06

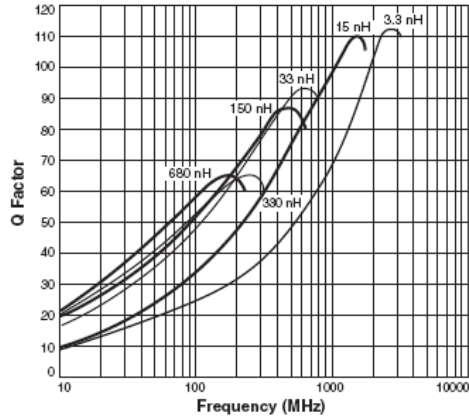
1102 Silver Lake Road Cary, Illinois 60013 Phone 847/639-6400 Fax 847/639-1469  
E-mail [info@coilcraft.com](mailto:info@coilcraft.com) Web <http://www.coilcraft.com>

© Coilcraft, Inc. 2006



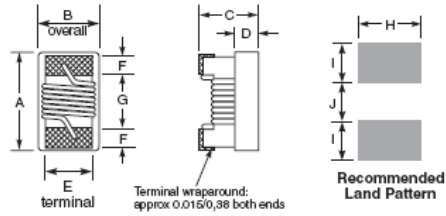
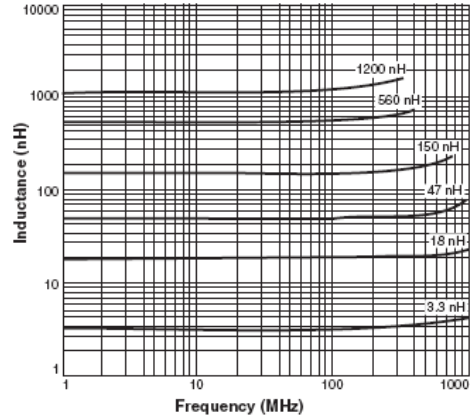
# 1206CS Series (3216)

## Typical Q vs Frequency



**S-Parameter files**  
ON OUR WEB SITE OR CD  
**SPICE models**  
ON OUR WEB SITE OR CD

## Typical L vs Frequency



A max	B max	C max	D ref	E	F	G	H	I	J
0.140	0.085	0.060	0.020	0.056	0.020	0.080	0.076	0.040	0.070
3,56	2,16	1,52	0,51	1,42	0,51	2,03	1,93	1,02	1,78

Weight: 19.5 – 23.0 mg  
Tape and reel: 2000/7" reel; 7500/13" reel 8 mm tape width  
For packaging data see Tape and Reel Specifications section.



Specifications subject to change without notice.  
Please check our website for latest information. Document 104-2 Revised 01/18/05

1102 Silver Lake Road Cary, Illinois 60013 Phone 847/639-6400 Fax 847/639-1469  
E-mail info@coilcraft.com Web http://www.coilcraft.com

© Coilcraft, Inc. 2006